

INVESTIGATING THE EFFECT OF QUINCE SEED POWDER ON ALGINATE  
HYDROGELS BY MAGNETIC RESONANCE

A THESIS SUBMITTED TO  
THE GRADUATE SCHOOL OF NATURAL AND APPLIED SCIENCES  
OF  
MIDDLE EAST TECHNICAL UNIVERSITY

BY

İREM ALAÇIK DEVELİOĞLU

IN PARTIAL FULFILLMENT OF THE REQUIREMENTS  
FOR  
THE DEGREE OF MASTER OF SCIENCE  
IN  
FOOD ENGINEERING

SEPTEMBER 2019



Approval of the thesis:

**INVESTIGATING THE EFFECT OF QUINCE SEED POWDER ON  
ALGINATE HYDROGELS BY MAGNETIC RESONANCE**

submitted by **İREM ALAÇIK DEVELİOĞLU** in partial fulfillment of the requirements for the degree of **Master of Science in Food Engineering Department, Middle East Technical University** by,

Prof. Dr. Halil Kalıpçılar  
Dean, Graduate School of **Natural and Applied Sciences**

\_\_\_\_\_

Prof. Dr. Serpil Şahin  
Head of Department, **Food Engineering**

\_\_\_\_\_

Assoc. Prof. Dr. Mecit Halil Öztop  
Supervisor, **Food Engineering, METU**

\_\_\_\_\_

Prof. Dr. Serpil Şahin  
Co-Supervisor, **Food Engineering Department, METU**

\_\_\_\_\_

**Examining Committee Members:**

Prof. Dr. Servet Gülüm Şumnu  
Food Engineering Department, METU

\_\_\_\_\_

Assoc. Prof. Dr. Mecit Halil Öztop  
Food Engineering, METU

\_\_\_\_\_

Prof. Dr. Hami Alpas  
Food Engineering Department, METU

\_\_\_\_\_

Prof. Dr. Behiç Mert  
Food Engineering Department, METU

\_\_\_\_\_

Assist. Prof. Dr. Emin Burçin Özvural  
Food Engineering Department, Çankırı Karatekin University

\_\_\_\_\_

Date: 06.09.2019

**I hereby declare that all information in this document has been obtained and presented in accordance with academic rules and ethical conduct. I also declare that, as required by these rules and conduct, I have fully cited and referenced all material and results that are not original to this work.**

Name, Surname: İrem Alaçık Develiođlu

Signature:

## ABSTRACT

### INVESTIGATING THE EFFECT OF QUINCE SEED POWDER ON ALGINATE HYDROGELS BY MAGNETIC RESONANCE

Alaçık Develiođlu, İrem  
Master of Science, Food Engineering  
Supervisor: Assoc. Prof. Dr. Mecit Halil Öztop  
Co-Supervisor: Prof. Dr. Serpil Şahin

September 2019, 98 pages

Quince seed powder (QSP) and xanthan gum (XG) based oil in water emulsions were prepared with different formulations. Whey protein isolate (WPI) and sodium alginate (AL) were also combined with QSP and XG to explore possible synergistic effects. Sunflower oil was used as the dispersed phase. Emulsions were analyzed through rheology, particle size and low field  $^1\text{H}$  NMR measurements. Emulsions containing QSP or XG, WPI and AL were gelled via crosslinking with calcium ( $\text{Ca}^{2+}$ ) ions. Gels were characterized mainly by longitudinal ( $T_1$ ), transverse ( $T_2$ ) relaxation times and scanning electron microscope (SEM) images. A detailed relaxation spectrum analysis was performed to investigate the ability of different emulsion formulations on dispersing the oil phase. QSP having emulsions generally attained longer  $T_2$  values than XG samples ( $p < 0.05$ ). Addition of either QSP or XG produced a more pseudoplastic flow behavior ( $p < 0.05$ ). Both QSP and XG provided sufficient emulsification with different characteristics. For the hydrogels, NMR relaxometry measurements were performed using a  $0.5\text{ T}$  system and Magnetic Resonance Imaging (MRI) experiments were performed on a  $3\text{ T}$  system. The longest  $T_1$  and  $T_2$  results of XG emulsion gels observed at the low field agreed with the lower particle size distribution of respective XG emulsions ( $p < 0.05$ ).  $T_1$  and  $T_2$  decreasing effect of oil

lumps were compensated by smaller and more homogenous oil droplet distribution within the XG gels. MR images provided better insight on the relaxation times. A multi slice multi echo sequence was used and  $T_2$  relaxation maps were obtained. Relaxation decay curves showed the presence of two compartments; *protons associated with the polymer matrix* and *protons interacting with the oil phase*. Exchange between 2 compartments was also detected when the relaxation times were investigated. The contribution of 1<sup>st</sup> component was the largest in QSP hydrogels confirmed by the lowest standard deviation in the  $T_2$  maps obtained from multi echo images. This behavior was explained by the emulsification ability of QSP as also seen in the emulsions. Results showed that QSP would be a good alternative hydrocolloid that can be used in emulsion and emulsion gel formulations.

Keywords: Hydrogel, Emulsion, NMR Relaxometry, Magnetic Resonance Imaging (MRI), Quince Seed Powder (QSP), Xanthan Gum (XG), Alginate

## ÖZ

### AYVA ÇEKİRDEĞİ TOZUNUN ALJİNAT HİDROJELLERİ ÜZERİNDEKİ ETKİSİNİN MANYETİK REZONANS İLE İNCELENMESİ

Alaçık Develioğlu, İrem  
Yüksek Lisans, Gıda Mühendisliği  
Tez Danışmanı: Doç. Dr. Mecit Halil Öztop  
Ortak Tez Danışmanı: Prof. Dr. Serpil Şahin

Eylül 2019, 98 sayfa

Ayva çekirdeği tozu ve ksantan zamkı içeren su içinde yağ emülsiyonları farklı formülasyonlarda hazırlanmıştır. Ayva çekirdeği tozu ve ksantanın olası sinerjistik etkilerini araştırmak adına izole peynir altı suyu proteini ve sodyum aljinat ile birleştirilip, dağılan faz olarak ayçiçek yağı kullanılmıştır. Hazırlanan emülsiyonlar reoloji, parçacık boyutu ve düşük alanlı NMR relaksometre ile analiz edilmiştir. Ayva çekirdeği tozu veya ksantan içeren, izole peynir altı suyu proteini ve aljinat ile hazırlanan emülsiyonlar, kalsiyum ( $Ca^{2+}$ ) iyonları ile çapraz bağlanma yoluyla jelleştirilmiştir. Jeller öncelikli olarak boylamsal ( $T_1$ ) ve enlemsel ( $T_2$ ) relaksometre zamanları ile daha sonra ise taramalı elektron mikroskobu (TEM) görüntüleri ile karakterize edilmiştir. Farklı emülsiyon formülasyonlarının yağ fazını dağıtma kabiliyetini araştırmak için detaylı bir relaksometre spektrum analizi yapılmıştır. Ayva çekirdeği tozu içeren emülsiyonlar, genellikle ksantan içeren örneklerden daha uzun  $T_2$  relaksometre değerlerine ulaşmıştır ( $p < 0.05$ ). Ayva çekirdeği tozu veya ksantan eklenmesi emülsiyonların psödoplastik akış davranışını artırmıştır ( $p < 0.05$ ). Hem ayva çekirdeği tozu hem de ksantan, emülsiyonlar üzerinde farklı özelliklerde emülsifikasyon sağlamıştır. Hidrojellerin NMR relaksometre ölçümleri 0.5 T'lık bir sistemi kullanarak, Manyetik Rezonans Görüntüleme (MRG) deneyleri ise 3 T'lık bir

sistemi kullanarak gerçekleştirilmiştir. NMR relaksometre sonuçlarına göre en uzun  $T_1$  ve  $T_2$  değerlerini gösteren ksantan içeren emülsiyon jelleri ve düşük parçacık boyutuna sahip ksantan emülsiyonları sonuçları bağdaşmaktadır ( $p < 0.05$ ). Yağ topaklarının  $T_1$  ve  $T_2$  değerleri üzerindeki azaltıcı etkisi, ksantan hidrojelleri içindeki daha küçük ve daha homojen yağ damlacıkları dağılımı ile telafi edilmiştir. MR görüntüleri relaksometre zamanlarını yorumlamada fayda sağlamıştır. Görüntülemeye MSME sekansı kullanılmış ve  $T_2$  relaksometre haritaları elde edilmiştir. Relaksometre eğrileri polimer matrisi ile ilişkili protonlar ve yağ fazı ile etkileşime giren protonlar olmak üzere iki farklı alanın olduğunu göstermiştir. Relaksometre süreleri incelendiğinde bu iki alan arasındaki değişim tespit edilmiştir. MSME datalarından elde edilen  $T_2$  haritalarında, birinci bileşenin katkısı, ayva çekirdeği tozu içeren hidrojellerde en küçük standart sapma ile en yüksek değeri göstermiştir. Bu davranış, emülsiyonlarda da görüldüğü gibi ayva çekirdeği tozunun emülsifikasyon yeteneği ile açıklanmıştır. Sonuçlar ayva çekirdeği tozunun emülsiyon ve emülsiyon jel formülasyonlarında kullanılabilir bir hidrokolloit alternatifi olacağını göstermiştir.

Anahtar Kelimeler: Hidrojel, Emülsiyon, NMR relaksometre, Manyetik rezonans görüntüleme (MRG), Ayva çekirdeği tozu, Ksantan zıncığı, Aljinat

To my beloved mom and dad,

## ACKNOWLEDGEMENTS

I would like to state my appreciation to my advisor Assoc. Prof. Mecit Halil Öztop for his continuous support, guidance, and encouragement throughout this study. He always tried to help me, and it would be very hard to complete the research without his support and knowledge. Also, I am grateful to my co-advisor Prof. Serpil Şahin for her valuable advices throughout this study.

I also would like to thank all Öztop Laboratory members since 2012; Elif Akbaş who is a secret power in my life, Şirvan S. Uğuz who always makes me smile, and replaces my frustrations with funny details, Emrah Kırtıl that I started to work in this way together, Simge Tutku Yıldırım, Damla Dağ, Helin Karaçam, Selen Güner, Pelin Poçan, Betül Tatar, Sevil Çıkrıkçı, Serap Namlı and especially because of his helps during writing period Barış Özel, and all other members. Your helps, smiles, gossips during tea breaks... were very precious for me. And dear Betül Söyler, maybe we couldn't share too much time but your wonderful heart, your lovely words have always encouraged me. Thanks for touching my heart.

My special thanks go to my sister from another mother, Gül (Toruk) Uzun. We shared lots of things together during our college life, and now, we share everything about our lives. She has always been with me and always listened both my all problems and my all happiness since 2008. You can be sure that you are my luck in this troubled life.

And as all people know, everyone has a destiny. No matter how much you plan, you live whatever your destiny. I worked too much and planned lots of things about my academic career and future. Then, I learned that my destiny had already made a plan for me without my dreams and plans, and it taught me one more time that the most important priority of my life is my family, and the biggest plans of my life are about my family. By the way, I would like to express my deepest appreciation to my parents Aysel Alaçık (she is the originator of my thesis title) and Necmi Alaçık. They taught me the goodness in my heart, and they are my only reasons for happiness. Knowing

that my family exists is the biggest and the most meaningful chance in my life. During my life, whatever my decision is, they have been always on side of me and they have respected all my decisions through my life, and they made me feel so lucky to have such a family. Thank you very much for all the things that you have made for me. Any word cannot express my gratitude and love to them. On the other hand, I would like to thank my left side, my secret guide behind my achievements, my parents' greatest gift, my brother Onur, and his gifts to me, my sister Sevim and my little heart Burak Yağız. And finally, I would like to thank my husband, and my life friend Alper Develioğlu for being with me on all my stressful days and for supporting me with a great patience. So, as it should to be, this thesis is dedicated to my beloved family.

And I hope that everything about my dreams starts now...

## TABLE OF CONTENTS

ABSTRACT .....	v
ÖZ .....	vii
ACKNOWLEDGEMENTS.....	x
TABLE OF CONTENTS .....	xii
LIST OF TABLES.....	xv
LIST OF FIGURES .....	xvi
LIST OF ABBREVIATIONS.....	xix
CHAPTERS	
1. INTRODUCTION.....	1
1.1. Emulsions.....	1
1.2. Emulsion Stability.....	1
1.3. Stabilizing Agents Used for Emulsions .....	4
1.3.1. Natural Emulsifiers.....	6
1.3.1.1. Phospholipids.....	6
1.3.2. Protein Based Stabilizing Agents .....	7
1.3.2.1. Whey Protein .....	8
1.3.2.2. Casein .....	9
1.3.3. Synthetic Surfactans .....	9
1.3.3.1. Tween 80 .....	9
1.3.4. Polysaccharide Based Stabilizing Agents .....	10
1.3.4.1. Alginate.....	11
1.3.4.2. Xanthan.....	12

1.3.5. Quince Seed Powder: As a New Source of Stabilizing Agent .....	14
1.4. Food Gels .....	15
1.4.1. Gel types .....	16
1.4.1.1. Polysaccharide Gels .....	16
1.4.1.2. Protein Gels .....	19
1.4.1.3. Binary, Mixed, or Composite Gels .....	22
1.4.2. Gelation Mechanism .....	23
1.4.2.1. Heat Gelation .....	23
1.4.2.2. Cold Gelation .....	24
1.5. Nuclear Magnetic Resonance Relaxometry .....	26
1.6. Magnetic Resonance Imaging .....	30
1.7. Objectives of Study .....	32
2. MATERIALS AND METHODS.....	33
2.1. Materials .....	33
2.2. Methods .....	33
2.2.1. Preparation of Quince Seed Powder .....	33
2.2.2. Emulsion Capacity Determination.....	34
2.2.3. Emulsion Preparation.....	34
2.2.4. Cold Set Gel Preparation .....	36
2.2.5. Emulsion and Hydrogel Characterization.....	37
2.2.5.1. Mean Particle Size Measurements .....	37
2.2.5.2. Scanning Electron Microscopy .....	37
2.2.5.3. Determination of Rheological Properties.....	38
2.2.5.4. Nuclear Magnetic Resonance (NMR) Relaxometry .....	38

2.2.5.5. Magnetic Resonance Imaging Experiments for Hydrogels .....	41
2.3. Statistical Analysis .....	45
3. RESULTS AND DISCUSSION .....	47
3.1. Gelation Time Determination .....	47
3.2. Determination of Emulsion Capacity .....	48
3.3. Particle Size Measurements .....	48
3.4. Rheological Measurements .....	51
3.4.1. Polysaccharide Solution Rheology .....	51
3.4.2. Emulsion Rheology .....	53
3.5. NMR Relaxometry Measurements .....	55
3.5.1. Transverse Relaxation Times ( $T_2$ ) of Solutions and Emulsions .....	55
3.5.2. NMR Relaxometry for Hydrogels .....	61
3.5.3. NMR Relaxometry for the Hydrogels Using MR Imaging .....	65
3.6. Scanning Electron Microscopy (SEM) Experiments .....	69
4. CONCLUSION .....	71
REFERENCES .....	73
APPENDICES	
A. ANOVA TABLES .....	87
B. SPIN ECHO MR IMAGES .....	97
C. CROSS-SECTIONAL VISUAL OF HYDROGEL SAMPLES .....	98

## LIST OF TABLES

### TABLES

Table 3.1. Rheological constants of polysaccharide solutions prepared by distilled water and 0.25 M calcium chloride solution. Different letters in each column mean solution type differed significantly ( $p < 0.05$ ). Errors are represented as standard deviations. ....	51
Table 3.2. Rheological constants of emulsions. Control, QSP and XG emulsions represent the formulations; AL-WPI-Oil-Water, QSP-AL-WPI-Oil-Water, XG-AL-WPI-Oil-Water, respectively. Different letters in each column mean emulsion type differed significantly ( $p < 0.05$ ). Errors are represented as standard deviations. ....	54
Table 3.3. Transverse relaxation spectrum analysis of all emulsion formulations. Different letters in each column mean emulsion type differed significantly ( $p < 0.05$ ). Errors are represented as standard deviations. ....	58
Table 3.4. XPFit $T_2$ results obtained from the MR images. ....	66

## LIST OF FIGURES

### FIGURES

Figure 1.1. Oil-in-water emulsions may become physically unstable because of different physicochemical processes known as gravitation separation, flocculation, coalescence, and phase separation (McClements & Gumus, 2016). .....	2
Figure 1.2. Emulsions can be either water-in-oil (W/O) or oil-in-water (O/W) form, and their stabilization is provided using emulsifier (Mohamed et al., 2018). .....	3
Figure 1.3. Stabilizing agents have two important key roles during commercial emulsion-based product formation: (a) they ease emulsion formation and (b) they enhance emulsion stability (McClements & Gumus, 2016).....	5
Figure 1.4. Chemical structure of phosphatidylcholine (lecithin). .....	6
Figure 1.5. Composition of whey protein (Oztop, 2012). .....	8
Figure 1.6. Chemical structure of Tween 80. ....	10
Figure 1.7. Chemical structure of alginate.....	12
Figure 1.8. Chemical structure of xanthan gum. ....	13
Figure 1.9. Gelation effect of quince seed mucilage when seeds are put into water. ....	15
Figure 1.10. Idealized junction zones in polysaccharide gels. (a) Point crosslink, (b) extended block-like junction zone, (c) egg-box model for the junction zones in alginate and pectin gels [the calcium ions (eggs) link the blocks of the polysaccharide chains (egg-boxes) together], (d) double- helical junction zone, and (e) junction zone formed by aggregation of helical segments of the polysaccharide chains (Morris, 2007).....	17
Figure 1.11. Schematic illustration of thermal denaturation of proteins (Noritomi, 2013). .....	24
Figure 1.12. Schematic of magnetization occurred by placing a sample into an external magnetic field in z direction, $B_0$ . .....	26

Figure 1.13. Schematic showing the direction the protons are facing in samples (a) without the presence of an external magnetic field. (b) under the influence of an external magnetic field of $B_0$ .....	27
Figure 1.14. Relaxation of transverse ( $M_{xy}$ ), and longitudinal ( $M_z$ ) magnetization after application of a $90^\circ$ RF pulse (Hashemi, Bradley, & Lisanti, 2010). ....	28
Figure 1.15. Representative curves of longitudinal magnetization, $T_1$ , and transverse magnetization, $T_2$ . ....	29
Figure 1.16. Tomato and corn images obtained using MRI.....	30
Figure 1.17. Gel system images obtained using MRI that are prepared with using different emulsifiers. ....	31
Figure 2.1. Flow chart of emulsion preparation. ....	35
Figure 2.2. Plastic mesh baskets used during gelation.....	36
Figure 2.3. (a) A hydrogel sample in the $0.25M$ $CaCl_2 \cdot 2H_2O$ solution at the end of gelation period, (b) A cross-sectional view of a hydrogel sample prepared without any hydrocolloid. ....	37
Figure 2.4. (a) Fitted decay curve of transverse relaxation, $T_2$ , (b) Longitudinal relaxation, $T_1$ , data fitted curve, (c) Multi-exponential distribution of the $T_2$ decay curve.....	40
Figure 2.5. Representative Spin Echo MR images of the hydrogels containing quince seed gum acquired using an echo time 12ms, TR of 3s. ....	42
Figure 2.6. Multi-echo images of the quince seed containing hydrogels for Slice # 4 .....	43
Figure 2.7. Representative CPMG decay of the hydrogels containing quince seed gum from the selected region of interest using an echo time 13.8 ms, TR of 3,150 ms. ....	44
Figure 2.8. $T_2$ Maps of hydrogels. Each voxel corresponds to a different relaxation time.....	45
Figure 3.1. Image of thickness change of gels with respect to time for 30 min time periods for 5 h. ....	47
Figure 3.2. Thickness change (mm) of hydrogels with respect to time (h) for 24 h. ....	48

Figure 3.3. Mean particle size [D (4, 3)] values of emulsions ( $p < 0.05$ ). Control, QSP and XG emulsions represent the formulations; AL-WPI-Oil-Water, QSP-AL-WPI-Oil-Water, XG-AL-WPI-Oil-Water, respectively. Error bars are represented as standard errors. .... 50

Figure 3.4. Shear stress vs shear rate measurements and power law fitting curves of Control, QSP and XG emulsions. .... 53

Figure 3.5. Transverse relaxation profiles of all formulations ( $p < 0.05$ ). Gums represent either XG or QSP. Error bars are represented as standard errors. .... 55

Figure 3.6. Longitudinal relaxation profiles of gels ( $p < 0.05$ ). Control, XG and QSP gels represent the formulations; AL-WPI-Oil-Water, XG-AL-WPI-Oil-Water, QSP-AL-WPI-Oil-Water, respectively. Error bars are represented as standard errors. .... 61

Figure 3.7. Transverse relaxation profiles of gels ( $p < 0.05$ ). Control, XG and QSP gels represent the formulations; AL-WPI-Oil-Water, XG-AL-WPI-Oil-Water, QSP-AL-WPI-Oil-Water, respectively. Error bars are represented as standard errors. .... 63

Figure 3.8. (a) CPMG decay curve of samples, (b)  $T_2$  compartments obtained using XPFit from the MR images (Control, QSP, and XG). .... 66

Figure 3.9. (a) Oil accumulation presentation,  $T_2$  maps of taken MR images (b)  $T_2$  profile of samples. .... 68

Figure 3.10. SEM images of gels: A, Control; B, QSP; C, XG. Control, QSP and XG gels represent the formulations; AL-WPI-Oil-Water, QSP-AL-WPI-Oil-Water, XG-AL-WPI-Oil-Water, respectively. .... 69

## **LIST OF ABBREVIATIONS**

AL: Alginate

MRI: Magnetic resonance imaging

NMR: Nuclear magnetic resonance

T<sub>1</sub>: Longitudinal relaxation time

T<sub>2</sub>: Transverse relaxation time

QSP: Quince seed powder

WPI: Whey protein isolate

XG: Xanthan gum



## CHAPTER 1

### INTRODUCTION

#### 1.1. Emulsions

A natural emulsion system contains two immiscible liquids, which are oil and water (McClements, 1999). Forming an emulsion by homogenizing these liquids together is possible. An emulsion can be either oil-in-water (O/W) emulsion in which oil droplets are dispersed in an aqueous phase such as mayonnaise, sauces, milk, and cream, or a water-in-oil (W/O) emulsion in which water droplets are dispersed in an oil phase such as margarine, butter, and spreads (Tatar, Sumnu, & Sahin, 2017). On the other hand, these emulsion phases rapidly separate into two layers due to the layer of oil having lower density and oil floats on the top. In an emulsion, because of the oil and water molecules' interaction is energetically unfavorable, they are known as thermodynamically unstable (McClements, 1999).

#### 1.2. Emulsion Stability

The emulsion ability for resisting to the changes in properties of emulsion over time refers to the term of emulsion stability. An emulsion may become unstable because of various physical and chemical processes. Physical instability problems are related about the change in spatial distribution and/or structural organization of molecules such as, sedimentation, gravitational separation, flocculation, coalescence, creaming, phase inversion as shown in Figure 1.1 (Tcholakova et al., 2006; McClements, 1999). The term of creaming process occurs when droplets move upwards because of smaller droplet density than continuous phase density. When the density of continuous phase is smaller than the density of droplets, droplets move downwards, and it is called as sedimentation.

Flocculation is another process in which two or more droplets merge together to form an aggregate and droplets still retain their individual integrity. And during coalescence process, two or more droplets stick each other to form a single larger droplet. On the other hand, chemical instability is directly related with chemical structure change of the molecules such as, oxidation, hydrolysis (Fennema, 1996a).

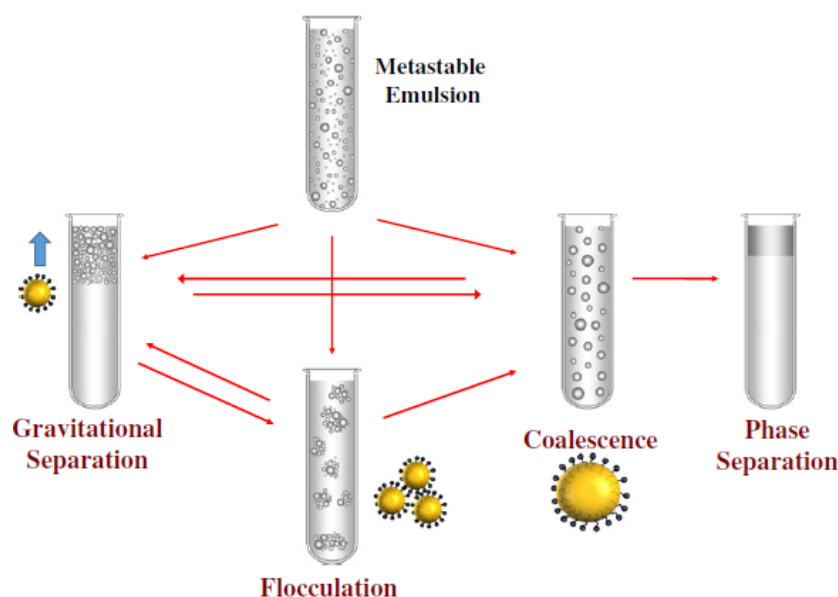


*Figure 1.1.* Oil-in-water emulsions may become physically unstable because of different physicochemical processes known as gravitation separation, flocculation, coalescence, and phase separation (McClements & Gumus, 2016).

Oil-in-water emulsions can be obtained using high and/or low energy approaches. High-energy approaches are based on the mechanical devices called homogenizers that depend on mixing the oil and water phases in order to produce fine lipid droplets. And the most commonly used mechanical devices for homogenizing the emulsions in the food industry are high speed mixers, high shear mixers, colloid mills, microfluidizers, high-pressure valve homogenizers, and sonicators (Santana et al., 2013; McClements, 2015).

The stability and rheology of oil-in-water emulsions depends on the interaction between droplets. In order to form kinetically stable emulsions for a limited time period with resistances to the environmental stresses, sometimes homogenizers cannot be sufficient. Therefore, it is necessary to use substances known as stabilizers, such as emulsifiers, thickening agents, weighting agents, gelling agents or ripening inhibitors (McClements & Gumus, 2016)

Emulsifiers are very important materials required to obtain stable emulsions with suitable shelf life and functional attributes (Chen 2015; Tan 2016). An emulsifier is an amphiphilic molecule containing a hydrophilic head known as water-loving, polar group, and a hydrophobic tail known as oil/fat loving, non-polar group as shown in Figure 1.2. And it provides emulsion stabilization by positioning itself between oil and water phases with the help of hydrophilic head and water phase interaction, and hydrophobic tail and oil phase interaction.

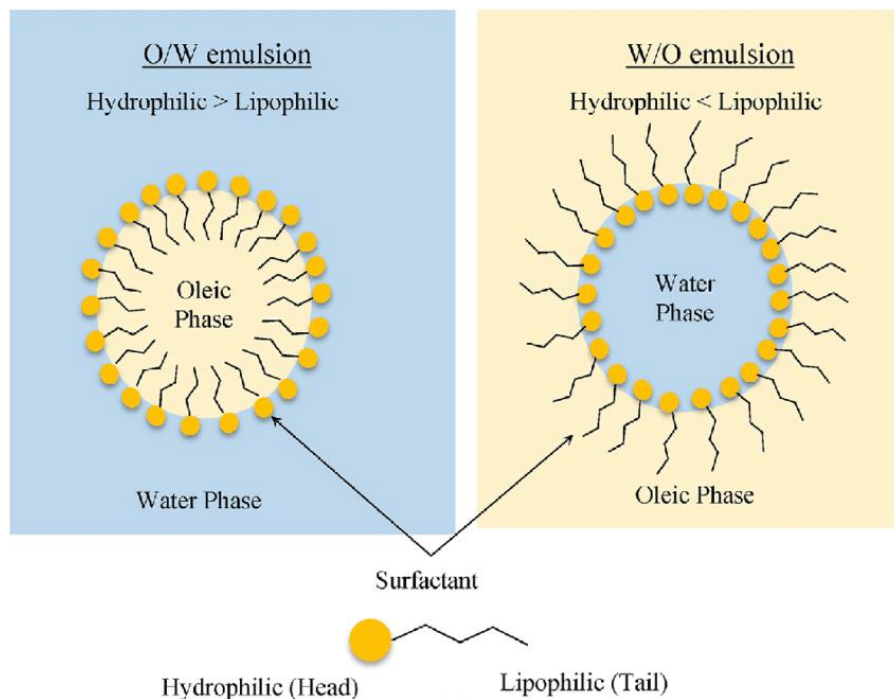


Figure 1.2. Emulsions can be either water-in-oil (W/O) or oil-in-water (O/W) form, and their stabilization is provided using emulsifier (Mohamed et al., 2018).

During these interactions, emulsifier eases the formation of small oil droplets by absorbing at the surface of the disrupted droplets, and then reduces the interfacial tension between the water and oil phases and forms a stable emulsion (Tan, 2016). The emulsifiers that commonly used in the food industry are amphiphilic proteins, small-molecule surfactants, and phospholipids (McClements, 1999). To sum up, emulsifiers are known as surface-active molecules/proteins which are adsorbed on the droplet surfaces in order to prevent them to come close enough together, and the aggregation by lowering surface tension.

Thickening agents are mainly polysaccharides and they are also used to stabilize emulsion. They increase viscosity of emulsion's continuous phase and enhance the stability of emulsions by delaying the movement of the droplets. And protein and polysaccharide combinations provide high surface activity and high viscosity to the emulsions. On the other hand, these types of combinations form gel-like adsorbed layers. By the way it delivers physicochemical stability, storage stability and texture properties to emulsions (Sun et al., 2006). Subsequently, the stability of emulsions is directly related with repulsion effect of emulsion droplets and effect of stabilizer layer on the droplets.

### **1.3. Stabilizing Agents Used for Emulsions**

An effective stabilizing agents have two important basic roles in the formation of a successfully stabilized emulsion based products as shown in Figure 1.3: (i) they ease the initial formation of small lipid droplets at the time of homogenization; (ii) they improve the stability of the lipid droplets once they have been formed by reducing the interfacial tension by an perceivable amount to facilitate droplet disruption and providing a coat as a protective which prevents the aggregation of droplets with their neighbors ( Walstra, 2003; McClements, 2004; Mcclements & Gumus, 2016).

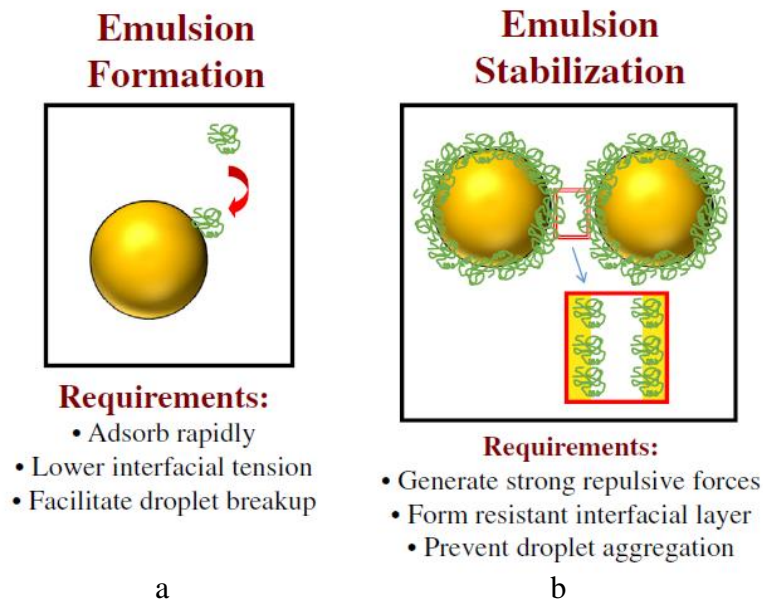


*Figure 1.3.* Stabilizing agents have two important key roles during commercial emulsion-based product formation: (a) they ease emulsion formation and (b) they enhance emulsion stability (McClements & Gumus, 2016)

Protein based agents as gelatin, egg protein, and caseinate are commonly used because of their surfactant and gelling properties in order to improve the stability and textural characteristics of an emulsion, whereas polysaccharide-based agents, like alginate, xanthan, gum arabic,  $\kappa$ -carrageenan are usually added for increasing the viscosity or achieving a gel-like product. Synthetic surfactants as Tweens are usually used for different targets, such as thickeners, stabilizers, texture modifiers, and gelling agents in the food industry (McClements & Gumus, 2016; Farahmandfar et al., 2017).

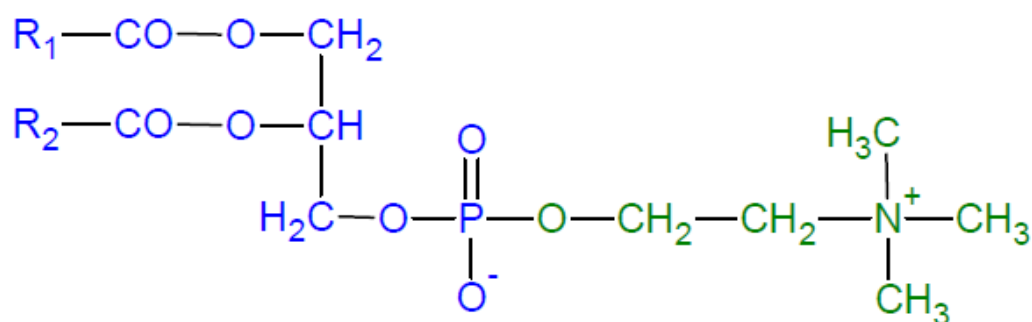
Preparation of the most of food products are obtained with the oil dispersion into water. The oil dispersion in water causes an increase in the contact area, so the interfacial tension between the two phases carries the system to a higher overall free energy state. According to thermodynamic laws, being in the minimum energy state is always preferable for all systems. By the way, the two phases of emulsions have a great tendency to separate and to minimize interfacial area. These thermodynamically unstable oil in water systems can be stabilized kinetically with the help of minimizing the separation rate. There are several methods for increasing the emulsion stability and

preventing this separation listed as (a) using a small surfactant and/or an adsorbing biopolymer which decreases interfacial tension of emulsion, (b) increasing viscoelastic behavior and thickness of the interfacial layer, and (c) using a non-adsorbing biopolymer as xanthan gum in order to increase the viscosity of the continuous phase and minimize particle collisions. (Kirtil & Oztop, 2016).

### 1.3.1. Natural Emulsifiers

#### 1.3.1.1. Phospholipids

Phospholipids are known as ionizable emulsifiers and they are used because of their ability for increasing colloidal stability and interfacial interactions between food components which are important factors for stability of emulsion and shelf life of foods (Moran-Valero, Ruiz-Henestrosa, & Pilosof, 2017). Commonly used natural phospholipids are known as phosphatidylcholine (PC), phosphatidylserine (PS), phosphatidylethanolamine (PE) and phosphatidylglycerol (PG). Phosphatidylcholine (PC) is an emulsifier known as the phospholipid-based functional ingredient, and it is called as lecithin whose chemical structure is shown in Figure 1.4. Lecithin can be obtained by isolation from different biological sources such as, eggs, milk, soybean, canola seed, cotton seed, and sunflower. Lecithin is typically a combination of different phospholipids and lipophilic materials such as sterols, triglycerides, and glycolipids (Guiotto, 2013).



**Phosphatidylcholine**

Figure 1.4. Chemical structure of phosphatidylcholine (lecithin).

Egg lecithin is usually produced with various combined extraction of ethanol and acetone. Because of producing processes and procedures, egg lecithins are expensive with respect to plant lecithins. On the other hand, commonly used lecithin is produced mainly from soybean that accounts 80% of worldwide production and small amounts is produced from sunflower and rapeseeds (Asomaning & Curtis, 2017).

Some lecithin ingredients are not effective about oil-in-water emulsion stabilization because of having low or intermediate hydrophilic-lipophilic-balance numbers that is directly related with emulsification property. In this situation, in order to obtain emulsion stability, ingredients of these lecithin can be combined with other natural emulsifiers (McClements & Gumus, 2016). Alternatively, natural lecithins are revised by chemically and/or enzymatically cleaving one of the fatty acid tails from the glycerol backbone in order to create more polar surfactants (lysolecithins). These are suitable for formation and stabilization of emulsions, especially when used in combination with other emulsifiers (Casado et al., 2012; Choi et al., 2011).

### **1.3.2. Protein Based Stabilizing Agents**

Proteins are biopolymers consisting of strings of amino acid units covalent linked by peptide bonds (Damodaran et al., 2007). Molecular, physicochemical, and functional properties of food proteins are determined with the help of the type, number, and position of amino acids. Most of the proteins contain a polar and non-polar amino acids mixture. Moreover, they are amphiphilic molecules that can attach to oil–water interfaces and provide stability of lipid droplets in emulsions. There are surface-active globular proteins that can be used as emulsifiers, such as whey, soy, egg, and plant proteins. Whey proteins and caseins from bovine milk are the most commonly used proteins as emulsifiers (McClements & Gumus, 2016).

In the most emulsions that stabilized with proteins, among the many colloid interactions present between droplets, the electrostatic interactions are often the most significant in influencing droplet aggregation (ultimately leading to coalescence).

Subsequently, the stability of protein- stabilised emulsions is susceptible to changes in ionic/ electrolyte concentration and pH (McClements, 1999). When the pH of this kind of emulsion is close to the isoelectric point (IEP) of the stabilising protein, droplet aggregation occurs. When the pH is far away from the IEP of protein, the charge on the emulsion droplet increases, raising stability against droplet aggregation (White et al., 2008).

### 1.3.2.1. Whey Protein

Whey protein is by product of cheese making process and contains a mixture of globular proteins mainly  $\beta$ -lactoglobulin,  $\alpha$ -lactalbumin as shown in Figure 1.5.

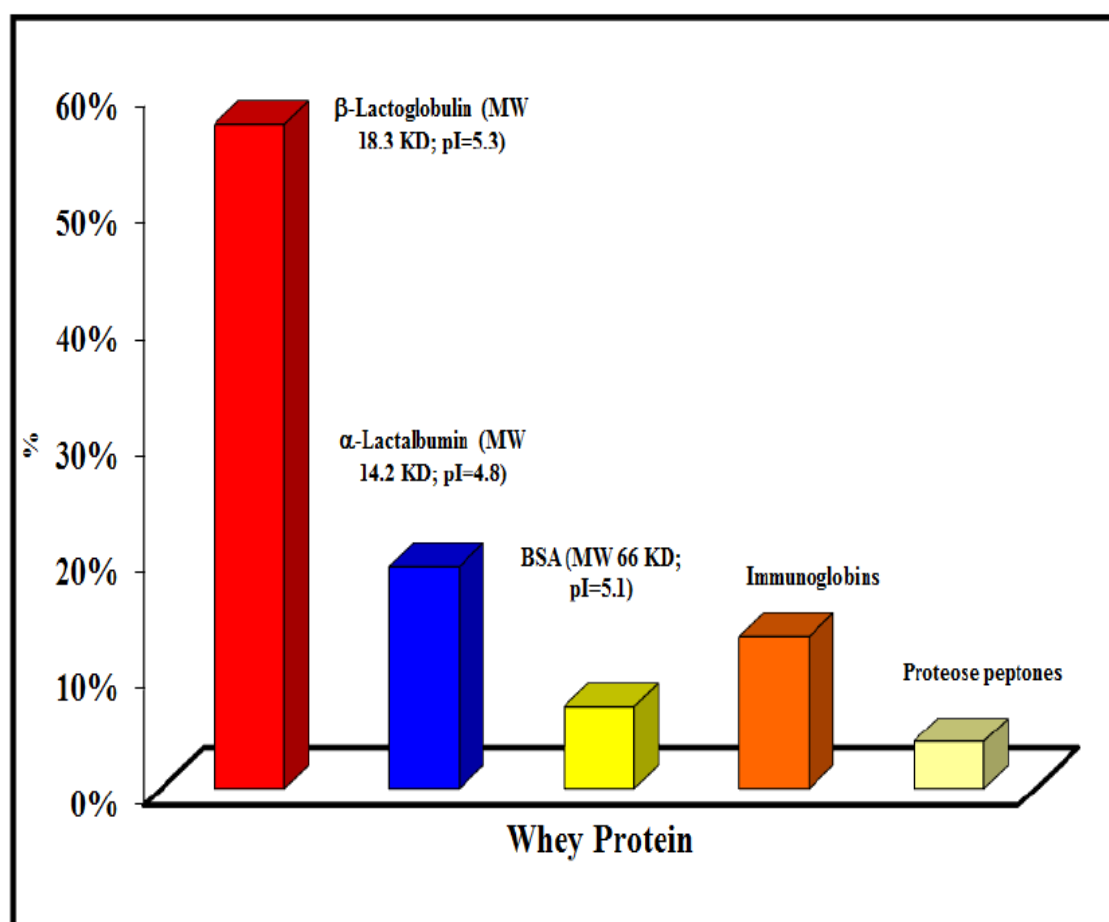


Figure 1.5. Composition of whey protein (Oztop, 2012).

Whey proteins provide functional properties such as gelation, water binding, solubility, foaming, viscosity and emulsification for foods. Emulsification property is directly related with its surface-active protein nature that adsorb on the oil droplets' surfaces and prevent the droplets from coming close enough to aggregate. They increase the repulsive colloidal interactions between droplets and it causes to observe an increase on the stability of formed droplets (Oztop, 2012; Kumar, Khouryieh, Williams, & Conte, 2016).

### **1.3.2.2. Casein**

Sodium caseinate is a widely used emulsifying agent that is the main protein component of mammalian milk, and a mixture of four caseins ( $\alpha_{s1}$ ,  $\alpha_{s2}$ ,  $\beta$ , and  $\kappa$  - casein). It effects the stability of emulsion with steric and electrostatic combination (Vázquez-Solorio, Vega-Méndez, Sosa-Herrera, & Martínez-Padilla, 2011). The  $\alpha_{s1}$ , and  $\beta$  are extremely effective emulsifying agents of casein. Decreasing the interfacial tension during emulsification, and protecting newly formed fine droplets against flocculation and coalescence with electrostatic and steric repulsion combination are directly related with these two casein components (Bouyer, Mekhloufi, Rosilio, & Grossiord, 2012). On the other hand, adsorbed  $\beta$ -casein layers at the air–water interface display a viscoelastic behavior (Bantchev and Schwartz, 2003).

### **1.3.3. Synthetic Surfactans**

#### **1.3.3.1. Tween 80**

Tween 80/polysorbate 80 is a synthetic non-ionic surfactant used in food and polymer industries (Figure 1.6). The stabilization mechanism relies on the surfactant ability for reducing the interfacial tension for short periods. Emulsion stability is achieved when the surfactant molecules cover the entire oil/water interface, enhancing interfacial rheology, contributing in this way to hinder droplet coalescence and aggregation by

the effects of steric repulsion. An interesting issue is to reliably determine the minimum amount of surfactant required for achieving maximum emulsion stability, as it impacts the cost of emulsion manufacture, without necessarily improving stability. (Roldan-cruz, Vernon-carter, & Alvarez-ramirez, 2016).

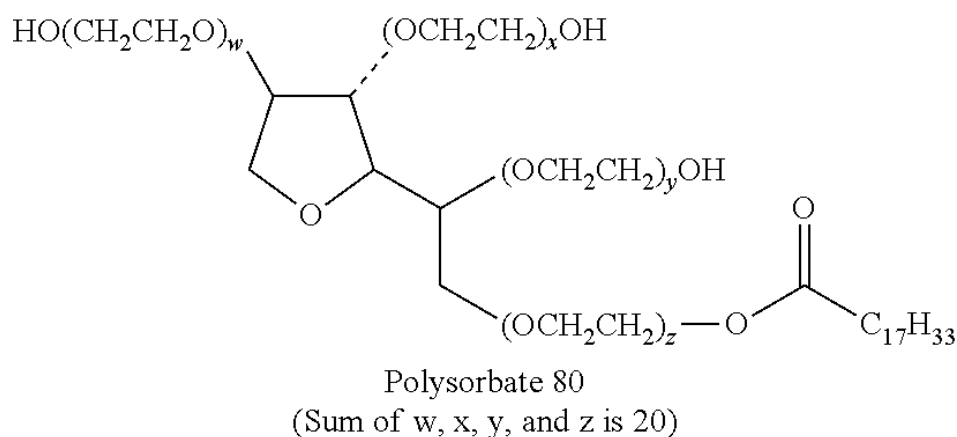


Figure 1.6. Chemical structure of Tween 80.

#### 1.3.4. Polysaccharide Based Stabilizing Agents

Polysaccharides are natural polymers contains one or more types of monosaccharide linked each other by glycosidic bonds (Brady, 2013). Because of their hydrophilic character and high molecular weight, polysaccharides are known with their water-holding and thickening properties (Bouyer et al., 2012). They can be classified in two categories with respect to their use in stabilizing emulsions droplets: non-adsorbing polysaccharides, and adsorbing polysaccharides. Non-adsorbing polysaccharides have no or limited surface activity and effect the emulsion stability by gelling or viscosity modifying of the aqueous continuous phase that causes the slowing down of droplet movement and encounters (Paraskevopoulou et al., 2004). The most common examples for non-adsorbing polysaccharides are xanthan gum, alginates, carrageenans, and chitosan. On the other hand, some other polysaccharides known as adsorbing polysaccharides display surface/interfacial activity that are gum-arabic,

hydroxypropylmethylcellulose (HPMC), chemically modified starch, galactomannans (guar gum, fenugreek gum), and pectin (Bouyer et al., 2012; Dickinson, 2003). They stabilize emulsions by adsorption at the oil droplet surface and then, prevent droplet flocculation and coalescence with electrostatic and/or steric repulsive forces.

Nowadays, the most commonly used natural polysaccharide emulsifier/stabilizer in the food industry is gum arabic (Williams & Phillips, 2009; Nie et al., 2013). Because of its non-polar polypeptide backbone with a number of polar polysaccharide chains attached, gum arabic is known as an amphiphilic. After adsorption to oil droplet surfaces, the polypeptide chain protrudes into the oil phase, whereas the polysaccharide chains swing into the water. This causes a relatively thick hydrophilic coating formation around oil droplets. This coating gives droplets good stability against aggregation with strong steric repulsion (McClements & Gumus, 2016).

Pectin is a well-known hydrocolloid that is commonly used in food industry to gel, to stabilize oil-in-water emulsions and to texturize food products (McClements & Gumus, 2016; Schmidt et al., 2015). Pectin fractions are extracted from various sources such as, cell walls of apple and/or citrus, sugar beet and grapefruit. The common use of pectin is related with its ability to form gels with sugar (and sometimes calcium ions) under acidic conditions and to stabilize dairy proteins like caseins (Schmidt et al., 2015).

Chitosan is another cationic polysaccharide used for facilitating emulsion formation and stability, and it is obtained from crustacean shells (Klinkesorn, 2013).

#### **1.3.4.1. Alginate**

Alginate is one of the major naturally occurring polysaccharide commonly used as a main emulsion stabilizer component for drug delivery systems (Figure 1.7). This linear polysaccharide is isolated from many strains of marine brown seaweed and algae, and is commercially available as alginate sodium salt and/or salts of alginic acid. This hydrophilic colloidal carbohydrate polymer is composed of unbranched binary copolymers of 1-4-linked  $\beta$ -D-mannuronic and  $\alpha$ -L-guluronic acid residues of

widely varying in composition. Alginic acid includes carboxyl groups in each residue that gives the ability to interact with polyvalent metal cations to form strong gels or insoluble polymers (Ozel, Uguz, Kilercioglu, Grunin, Oztop, 2016). Therefore, it is obvious that alginate is a powerful thickening, stabilizing, and gel-forming agent that utilized in a variety of foods. This anionic polysaccharide forms strong, flexible gels with calcium cations leading to microspheres with crosslink formation (Patel, 1995).

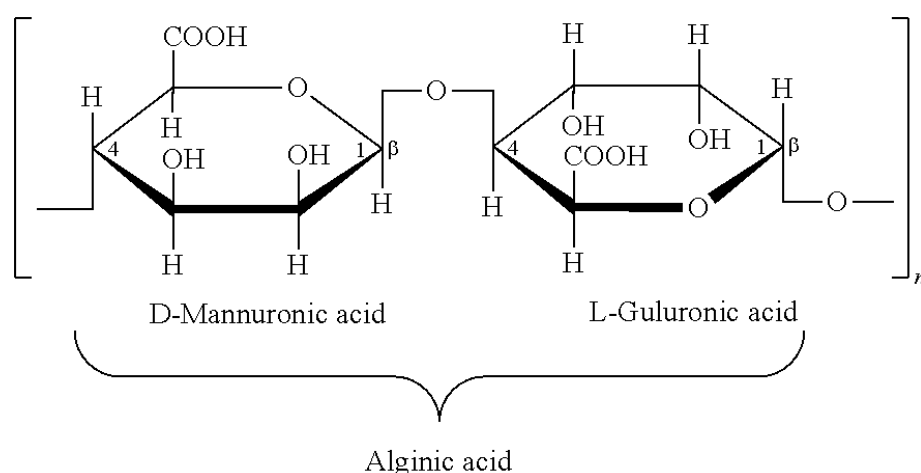


Figure 1.7. Chemical structure of alginate.

### 1.3.4.2. Xanthan

Xanthan gum is a hetero-polysaccharide produced by *Xanthomonas campestris*. Its main chain is constituted of glucose units. The side chain is a trisaccharide, consisting of alpha-D-mannose, which contains an acetyl group, beta-D-glucuronic acid, and a terminal beta-D-mannose unit linked with a pyruvate group as shown in Figure 1.8. Xanthan gum is a non-adsorbing polysaccharide which does not adsorb on the oil/water interface when used in emulsions (Kirtil & Oztop, 2016). It is one of the most preferred polysaccharides used to thicken and stabilize the emulsions by decreasing the rate of flocculation, creaming, and sedimentation and increasing the

physical stability and/or viscosity of the aqueous phase (Bouyer et al., 2012; Ozturk et al., 2015; Kumar, Khouryieh, Williams, & Conte, 2016).

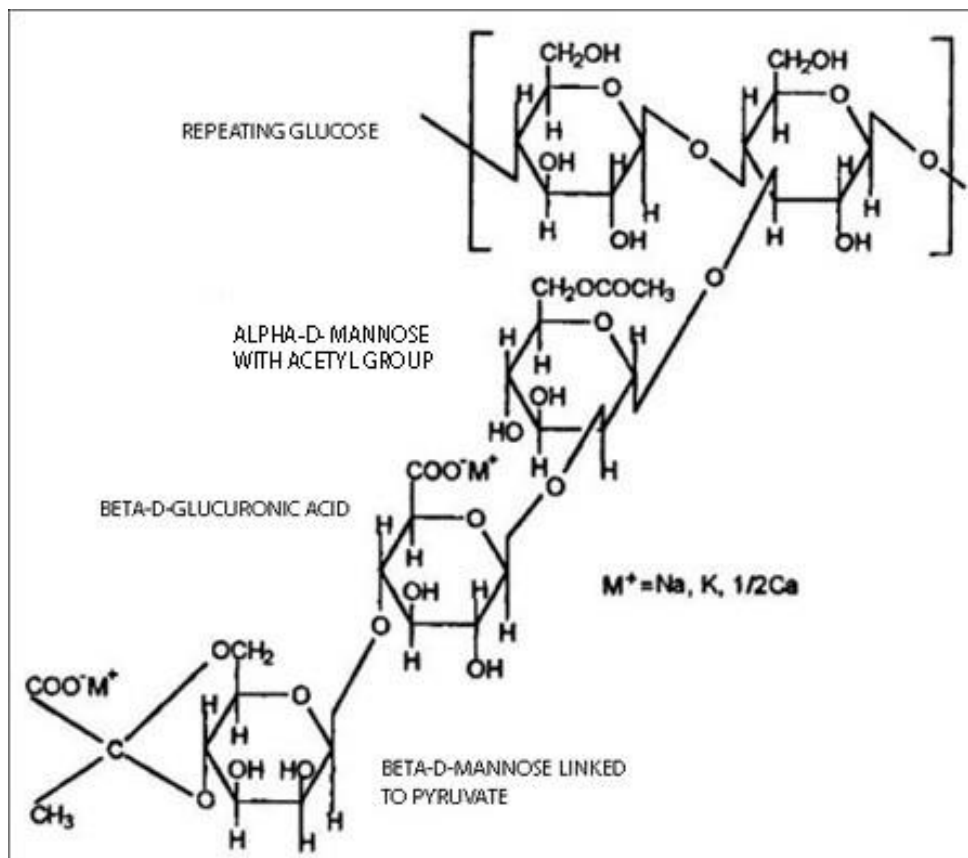


Figure 1.8. Chemical structure of xanthan gum.

The particular structure of xanthan gives the gum its unusual thickening properties, with a yield stress, shear-thinning and thixotropic behaviors, and because of these unique rheological properties, xanthan gum is recognized as an excellent emulsion stabilizer (Benmouffok-Benbelkacem et al., 2010; Hennock et al., 1984; Sun et al., 2007). Xanthan gum has not only the ability of thickening, dispersion, emulsification and suspension, but also is stable to acid, alkali, salts and temperature. Therefore, xanthan gum is widely used in food, oil recovery, pharmaceutical, cosmetic, textile and other industries (Wang, Wu, Zhu, & Zhan, 2017).

### **1.3.5. Quince Seed Powder: As a New Source of Stabilizing Agent**

Quince is the yellow-colored, woolly-haired, apple-shaped fruit of the botanical species of tree known as *Cydonia oblonga Miller*, and commonly cultivated in Caucasus regions, Syria, Afghanistan, Iran, Dagestan and Antalya. Each of these fruits contains six to fifteen seeds arranged in two rows of the fruit center (Silva, et al., 2005). Though the seeds have been used in Turkish culinary for gelling for years, they have recently attracted researchers' attention, which caused an increase in the amount of research on the subject.

The seeds are brown in color and contain various amino acids as well as phenolic compounds and antioxidants such as citric, ascorbic, malic acid (Silva, et al., 2005). On the other hand, seeds contain whitish Mucilaginous epithelium gives the fruit its primary value by adsorbing water quickly when soaked in water and produce a sticky and tasteless liquid (Figure 1.9). Quince seed mucilage is a complex mixture of a cellulosic fraction with more readily hydrolyzed polysaccharides and amino acids known as glutamic acid, aspartic acid, and asparagine (Panda, 2010; Kirtil & Oztop, 2016). Studies revealed that, basic components of quince seed mucilage are cellulose and water soluble polysaccharides are separated into glucans, galacto-glucans, manno-glucans or galacto-manno-glucans and acidic arabinoxylans with the major component is partially O-acetylated (4-O-methyl-D-glucurono)-D-xylan and high proportions of glucuronic acid residues (Lindberg, et al., 1990; Vignon & Gey, 1998). With respect to the recent studies, 46% of the total polysaccharides are water soluble hemicelluloses and celluloses by weight of dry mucilage, with the rest yielding 45% glucose residues when analyzed after enzymatic hydrolysis (Kirtil & Oztop, 2016). Considering its unique colloidal properties, low production cost, and easy extraction techniques with respect to most of the other polymers, this polysaccharide is of interest as a potential stabilizer, film or coating component.

In a recent study, the mucilage was shown a great gelling capacity and it revealed an improved viscosity and shear thinning behavior on solutions (Abbastabar et al., 2015).

Although the protein content of the quince seed extract had been known for years, the emulsifying properties of quince seed gum have been extensively studied in the new studies (Ritzoulis et al., 2014). On the other hand, quince seed mucilage is shown to be an adsorbing polymer (Kirtil & Oztop, 2016).

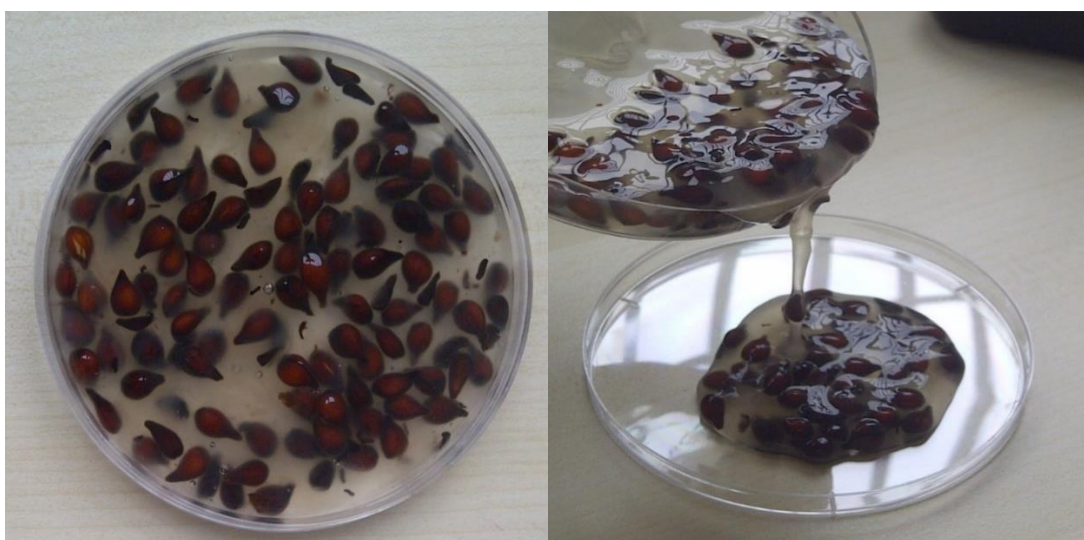


*Figure 1.9.* Gelation effect of quince seed mucilage when seeds are put into water.

#### **1.4. Food Gels**

The term “gel” is directly related with colloidal science and it is defined in the Polymer Dictionary as “polymers and their swollen matters with three-dimensional network structures that are insoluble in any solvent.” (Nazir, Asghar, & Maan, 2017). And more simplified definition of gel can be as “a form of matter intermediate between a solid and a liquid with both elastic/solid and viscous/liquid characteristics.” (Nazir, Asghar, & Maan, 2017; Oztop, 2012). A gel has flexible behavior as solid, and it gets distorted with pressure. However, if stress is removed, it turns to its initial shape because distortion has left the bonds between the particles integral. On the other hand, a gel has liquid behaviors, and its deformation cannot be recovered after the stress is removed. Therefore, the gel flows as a liquid because of its bonds are broken and new

bonds are formed (Nazir et al., 2017). Different types of interactions in gels can be observed as hydrogen bonding, hydrophobic interactions, ionic bonds, and covalent chemical bonds. With respect to the physical structure of the biopolymer network, polymer gels can be classified as strong, weak, or pseudo gels (Ross-Murphy, 1995). And chemically crosslinked polymer gels are known as strong gels, because crosslinks are permanent and cannot be reformed if broken. However, weak gels contain crosslinks which can be broken and reformed such as colloidal gels and some biopolymer gels (Richter, 2007; Solomon and Spicer, 2010). Different polysaccharides and proteins obtained from various plants, animals, or microorganisms can be used as gelling agents in addition to their thickening agent properties. (Einhorn-Stoll and Drusch, 2015). Natural gums, agar, carrageenan, alginate, glucomannan, starches, and pectin are the most commonly used polysaccharide based gelling agents while gelatin, casein, whey protein, soy protein, egg protein, and zein are most commonly used protein-based ones.

#### **1.4.1. Gel types**

##### **1.4.1.1. Polysaccharide Gels**

There are some polysaccharides that have the gelling ability at a certain concentration of the gelling agent, usually termed the critical concentration. At the end of hydration completion of the polysaccharides, the polymer strands start interacting in other words, crosslinking with each other to form junction zones. At critical polymer concentration and at a certain degree of crosslinking, the polymer solution (dispersion) ultimately turns into a gel comprising a firm network structure. Different types of junction zones can be possible with respect to the polysaccharide type and the gel-forming conditions, as shown in Fig. 1.10.

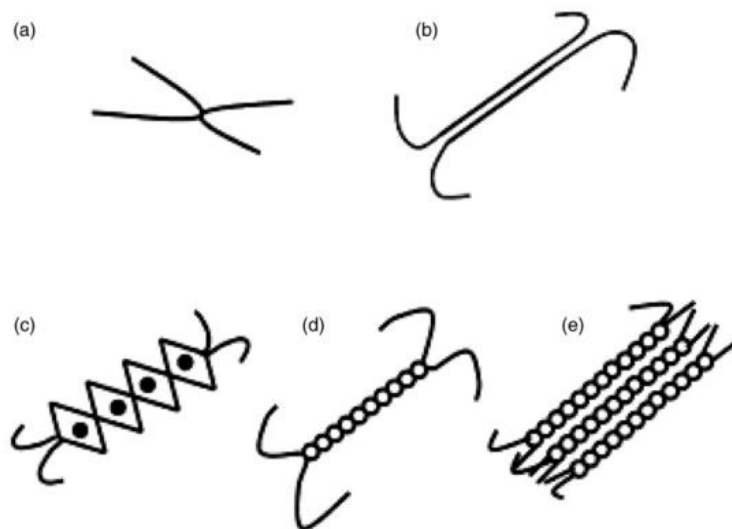


*Figure 1.10.* Idealized junction zones in polysaccharide gels. (a) Point crosslink, (b) extended block-like junction zone, (c) egg-box model for the junction zones in alginate and pectin gels [the calcium ions (eggs) link the blocks of the polysaccharide chains (egg-boxes) together], (d) double-helical junction zone, and (e) junction zone formed by aggregation of helical segments of the polysaccharide chains (Morris, 2007).

The most commonly used polysaccharide gels are mentioned in the subsequent sections.

#### **1.4.1.1.1. Agar**

Agar consists of fractions of agarose and agarpectin. The network formation and gelation in agar occur when heated solutions are cooled to below 40°C.

#### **1.4.1.1.2. Alginate**

Alginate as food grade polymers have been used for active agents owing to their biodegradability, biocompatibility and nontoxicity features. Moreover, the combination of protein and polysaccharides is used for development of novel gel systems since different polysaccharides interact variously with the protein network, giving control over manipulating release rates of such gels (Ozel et al., 2017).

Alginate gels are formed in the presence of divalent cations and the type of the used cation gives information about the strength of obtained gels.  $\text{Ca}^{2+}$ -induced gelation is the most important alginate-cation gelation example.  $\text{Ca}^{2+}$  ions and electronegative alginate molecules are located together like eggs in an egg-box that is known as the ‘egg-box’ model. Usage purpose of this combination is reducing the dissolution of alginate matrix for different applications. Alginate gels are generally heat stable and irreversible (Baimark & Srisuwan, 2014; Nazir et al., 2017).

#### **1.4.1.1.3. Pectin**

Pectin is a galacturonic acid units containing polymer which may be either free or methyl esterified. Gelation mechanism is related with the degree of esterification. According to this degree, pectins are classified as high methoxyl (HMP with >50% esterification) and low methoxyl pectin (LMP with < 50% esterification). In HMP, polymer chains are linked with the hydrogen bonding and hydrophobic interactions. And HMP gelation mechanism is promoted by the sugars and/or low pH conditions. However, LMP resembles alginates and its gelation is related with the presence of  $\text{Ca}^{2+}$  ions and egg box structures.

#### **1.4.1.1.4. Carrageenan**

Carrageenan forms strong gels at very low concentrations (around 1% w/w). There are different types of carrageenan known as  $\kappa$ ,  $\iota$ , and  $\lambda$ , and only  $\kappa$  and  $\iota$  can form gel while  $\lambda$ -carrageenan is used as a thickener. Because of anionic nature of polymer cations, especially  $\text{Ca}^{2+}$  and  $\text{K}^+$  are used to reduce electrostatic repulsion of polymer chains and induce linkages.  $\kappa$ -carrageenan forms strong gels in the presence of  $\text{K}^+$  while  $\iota$ -carrageenan forms soft gels in the presence of  $\text{Ca}^{2+}$  (Nazir, Asghar, & Maan, 2017).

### 1.4.1.2. Protein Gels

Protein gels have been extensively used in biomedical and food applications because of their renewable nature, superior nutritional value, inherent biocompatibility, and biodegradability. In recent years, applications of animal protein based gels (collagen, gelatin, albumin, whey protein, etc.) as wound dressings, scaffolds for cell growth in tissue engineering, and nutraceutical delivery systems have been widely studied (Yang, Wang, & Chen, 2017). According to researches, the gelation mechanism of proteins is related with the structure of the protein macromolecules. The proteins used for food gel preparation are globular and fibrous proteins. The globular proteins have coiled-shaped structures with hydrophobic groups pointed toward interior and hydrophilic groups being exposed outside of the molecule, and they are usually water soluble. And the fibrous proteins commonly contain long chain polypeptides running parallel to each other, linked by disulfide (—S—S—) cross bridges. And because of this molecular orientation, fibrous protein containing gels are generally water insoluble and have strong stability and strength. On the other hand, some proteins like casein are in micelles form that is different from globular and fibrous proteins (Nazir et al., 2017). The gelation requires the protein structure denaturation or destabilization to increase the intermolecular interactions. This protein denaturation may be carried out because of different effects such as heat, pressure, enzymes, and some chemical denaturants (Nishinari et al., 2000). When the protein structure is opened, a group of intermolecular interactions which are specific for the protein type, gel forming conditions, and having covalent/noncovalent nature will take place. The covalent interactions are irreversible, and they usually contain sulfhydryl (—SH)/disulfide (S—S) interchange reactions (Wijayanti et al., 2014). On the other hand, the noncovalent interactions are reversible and usually contain hydrogen bonding, hydrophobic interactions, and electrostatic interactions. All these intermolecular interactions cause protein aggregation, which finally end up into a three-dimensional organized network responsible for viscoelastic properties of gels. The gelation process is directly related with gel forming conditions and requires number of physical (i.e., temperature,

pressure) and chemical (i.e., pH, ionic strength, enzymes) parameters in order to end up in a gel form (Nazir et al., 2017).

Commonly used proteins gels are discussed in the subsequent sections.

#### **1.4.1.2.1. Gelatin**

Gelatin is one of the most commonly used biopolymers, and it is obtained through a hydrolytic reaction of the most abundant mammalian protein called collagen (Pocan, Ilhan, Oztop, 2019). Gelatin forms gel structure at the concentration of 0.5–1% w/w, and these gels melt at the temperature between 27 and 34°C. Gelatin forms two types of gels known as physical gels and chemical gels. Transition of coil to triple helices during cooling causes the physical gel formation, and this mechanism causes to obtain transparent, elastic, and thermos-reversible gels. On the other hand, chemical gel is formed with crosslinking of polymer chains, and this crosslinking results in stiff gels with improved thermostability.

Gelatin gels are mostly used for confectionary products could be considered as complex gel systems in food industry. For example, gelatin is commonly used in the production of jelly candies because the final product reveals desirable transparency and hardness that are accepted as the two vital characteristics affecting consumers' preference. And the structure of gummy jellies is supported by a soft colloidal system consisting of sugars, water, gelling agents, and other components, and gel formation occurs with the aid of the plasticizer effect of water (Pocan, Ilhan, Oztop, 2019).

#### **1.4.1.2.2. Whey Protein**

Whey protein (WP) is one of the most commonly used food proteins for gel formulation (Ozel et al., 2017). WP has the potential for forming heat-set gel matrixes and has the ability to absorb large amounts of water and entrap active agents for delivery (Oztop, McCarthy, McCarthy, & Rosenberg, 2012). WP mainly consists of

globular proteins known as  $\beta$ -lactoglobulin ( $\beta$ -Lg, ~65% w/w) and  $\alpha$ -lactalbumin ( $\alpha$ -La, ~25% w/w), which are responsible for gelling, emulsifying, foaming properties (Ozel et al., 2017).

WP gelling is mainly achieved by conventional heating above its thermal denaturation temperature (McClements, 2017). Because of the protein aggregation in the form of strings or clusters, whey proteins form irreversible particle gels with heating. The gelation occurs as a result of a number of transitions including denaturation and aggregation of molecules, strand formation and association of strands into a network (Nazir et al., 2017; Oztop, 2012).

#### **1.4.1.2.3. Egg Albumin**

Egg albumin can be defined as a system with plentiful globular proteins in the aqueous solution. Gelation of egg albumin occurs in three steps which are partial unfolding of molecules with heating, the sulfhydryl disulfide interchange, and sulfhydryl oxidation within and between the aggregates forming a network. In the sulfhydryl oxidation step multiple hydrogen bonding occurs during cooling. Egg albumin gelation process is affected pH, ionic strength, and the presence of salts/sugars.

#### **1.4.1.2.4. Casein**

Casein in milk proteins exists in the micelles form. Irreversible gelation takes place when micelles are destabilized through acidification and aggregation of casein micelles. And the aggregated micelles form clusters and chains to form a three-dimensional network.

#### **1.4.1.3. Binary, Mixed, or Composite Gels**

In recent years, different hydrogels obtained from proteins and polysaccharides like alginate, chitosan and pectin as food grade polymers have been used as delivery matrices for active agents because of their biodegradability, biocompatibility and nontoxicity features. Moreover, usage of protein and polysaccharide combinations is of high interest for development of novel gel systems since different polysaccharides interact variously with the protein network, giving control over manipulating release rates of such gels (Ozel et al., 2017).

Some gels contain more than one polymer and they are called as binary or mixed gels. The common combinations are known as polysaccharide–polysaccharide and polysaccharide-protein. To illustrate, a lot of polysaccharides have gelation behavior when they are used in combinations, although individual components are nongelling (Sandolo et al., 2010). Xanthan gum and locust bean gum are good examples for this situation because they are not gelling agents when used alone, but they form good gels when used with other polysaccharides (Pedersen, 1980). It is known that the presence of more than one polymer creates more effective three-dimensional network systems through extended interactions. These multiple interactions are attractive commercially and may be used to generate new functionality or to manipulate texture and rheology (Cairns et al., 1987).

An emulsion with a gel-like network structure and solid-like mechanical properties is called as an emulsion gel (Dickinson, 2013). Emulsion gels are used in food, pharmaceutical, and cosmetic industries, since they can provide stability and a solid-like functionality to fat-containing products, as well as used as carriers of lipophilic compounds. An oil-in-water (O/W) emulsion gel essentially involves producing emulsion using emulsifying agents and incorporating a gelling agent such as a hydrocolloid or other ingredients with gelling capacity in order to convert the emulsion into an emulsion gel by two methods known as aggregation of emulsion droplets and/or gelling of the continuous phase. Some emulsion gels have been

developed as oil structuring for providing desirable functionality, texture and palatability to food products (Jiang et al., 2019).

Composite emulsion gels are obtained by mixing polymer solutions with lipids. Composite emulsion gels consist of at least two phases known as continuous matrix and dispersed phase. The continuous network of the gel containing polymers that interact with lipids and three-dimensional junction zones are formed. Therefore, two constituent phases of the composite are physically connected (Ozel, Uguz, Kilercioglu, Grunin, Oztop, 2016).

#### **1.4.2. Gelation Mechanism**

An emulsion gel can be defined as an emulsion with a gel-like network structure and solid-like mechanical properties (Pintado, Ruiz-capillas, Jiménez-colmenero, Carmona, & Herrero, 2015). Emulsion gels can be defined in different ways. Heat-set protein-based emulsion gels, acid-induced emulsion gels and enzyme-induced emulsion gels are the most commonly used ones (Dickinson, 2012). An alternative to these emulsion gels could be the using of cold gelling agents based on polysaccharides and proteins that establish polymer interactions, creating a continuous network responsible for the functional properties of emulsion gels (Lam & Nickerson, 2013).

##### **1.4.2.1. Heat Gelation**

When dissolved proteins are placed at high temperatures, most of the proteins are immediately unfolded because of the disruption of weak interactions that include ionic effects, hydrogen bonds, and hydrophobic interactions (Noritomi, 2013). In other words, when protein load above the its critical concentration, undenaturated form of emulsions and solutions of whey proteins have the ability for forming rigid irreversible gels when heated above 75°C (Nguyen, Nicolai, Chassenieux, Schmitt, & Bovetto, 2016; Oztop, 2012). Heat induced whey protein gelation occurs in four steps:

denaturation of native proteins, aggregation of unfolded molecules, strand formation from aggregates, and association of strand into a network as shown in Figure 1.11 (Aguilera, 1995; Oztop, 2012).

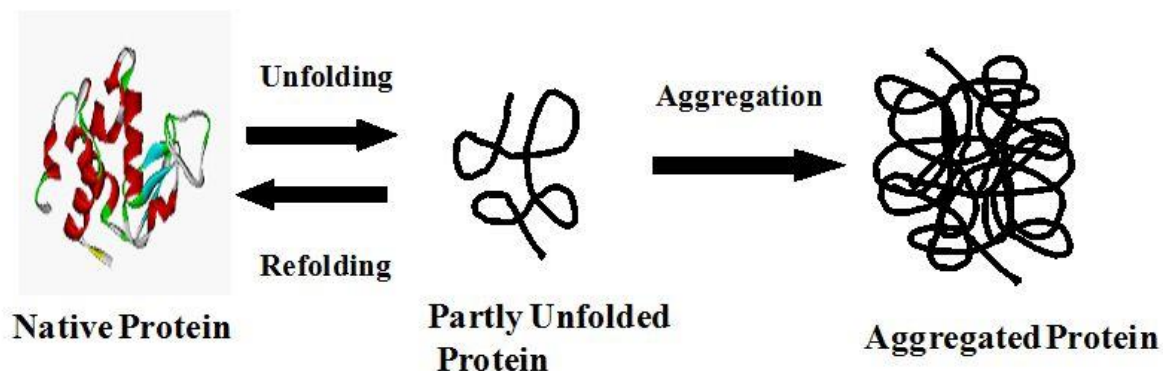


*Figure 1.11.* Schematic illustration of thermal denaturation of proteins (Noritomi, 2013).

Gelatinization is mainly achieved by conventional heating that provides direct heating of medium with conductive heat transfer. In addition to conventional heating, microwave heating which depends on the alternating electricity and magnetic field of the microwave radiation. With respect to the changes on the orientation of dipoles, gelation is observed. Polar molecules have fast rotation and it results in friction, collision, vibration and heat generation. By the way, a rapid increase in temperature is achieved in the medium, and it causes gelation (Ozel, Dag, Kilercioglu, Sumnu, Oztop, 2017).

#### **1.4.2.2. Cold Gelation**

Although the most common way to gel an emulsion is heating, cold gelation is a more suitable gelation technique for heat-sensitive ingredients, such as oils, volatile compounds, etc. (Morales, Martinez, Pilosof, 2019).

The protein particles are freely dispersed in the aqueous solution only if the electrostatic repulsion is sufficiently strong. When the electrostatic repulsion is reduced, they aggregate either by reducing the net charge density of the proteins by lowering the pH towards the isoelectric point or by adding salt and gels are formed. This gelation process does not require heating contrary to gelation of native globular protein solutions, and is therefore known as cold gelation (Gonzalez-Jordan, Benyahia & Nicolai, 2017).

As mentioned in section 1.4.1.1.2, alginate gels are formed in the presence of divalent cations and the type of the used cation gives information about the strength of obtained gels.  $\text{Ca}^{2+}$ -induced gelation is the most important alginate-cation and cold gelation example.  $\text{Ca}^{2+}$  ions and electronegative alginate molecules are located together like eggs in an egg-box that is known as the 'egg-box' model. Usage purpose of this combination is reducing the dissolution of alginate matrix for different applications. Alginate gels are generally heat stable and irreversible (Baimark & Srisuwan, 2014; Nazir et al., 2017).

Pectin is another representative polyuronate widely used in the food industry. Cold-set gelation is typical for gels of high-methoxylated pectins but it takes place, to a lower extent, also in all other pectin gels. The possible mechanism of pectin is known as *cold-set gelation* and takes place during cooling (Einhorn-Stoll, 2018).

## 1.5. Nuclear Magnetic Resonance Relaxometry

The first use of the low field nuclear magnetic resonance (NMR) spectrometers for food industry, especially for emulsions was limited to only the determination of water and fat content measurement (Mariette, 2009). However, nowadays, studies with low-field NMR about emulsions have reached a higher level. The main advantage of this non-destructive technique is that the entire sample is considered, and it gives accurate results for both transparent and opaque samples. NMR is routinely used to measure the water content of crude oil samples (Opedal, Sørland, & Sjöblom, 2010). In relaxometry, the transverse relaxation times ( $T_2$ ) are measured and these are related to the mobility of water molecules, and the mobility is affected by the interaction of water with macromolecules (Granizo, Reuhs, Stroshine, & Mauer, 2007).

This technique is based on the nuclear magnetism. Nuclear magnetism emerges from the spins of nucleons, namely, protons or neutrons. To obtain a net nuclear magnetization moment, the nucleus should have an odd number of nucleons. During experiments, any element containing an odd number of nucleons can be used. Because of having odd number of nucleons, presence of hydrogen in water and oil, and having high magnetic resonance sensitivity, mostly hydrogen is preferred (Konez, 2011). As shown in Figure 1.12, in order to acquire a signal from the sample, it is placed into a large static magnetic field called as  $B_0$ .

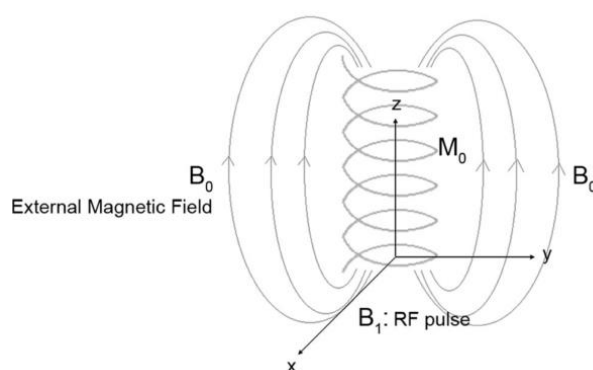


Figure 1.12. Schematic of magnetization occurred by placing a sample into an external magnetic field in z direction,  $B_0$ .

To obtain this large magnetic field, magnets (i.e., permanent, superconductive) with field strengths of 0.2 Tesla to 7.0 Tesla can be employed (Hashemi, Bradley, & Lisanti, 2010). When sample is placed into the magnetic field, the protons within the sample align themselves with this external magnetic field in z direction as in Figure 1.13.

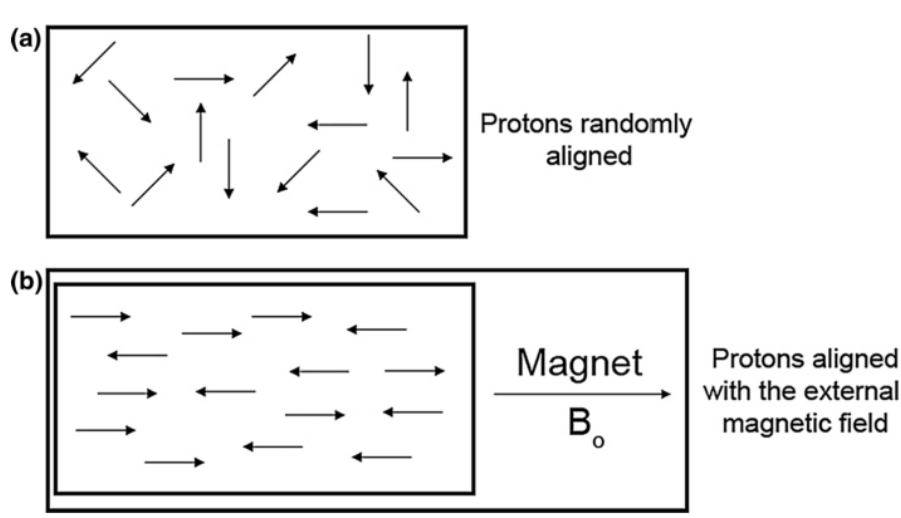


Figure 1.13. Schematic showing the direction the protons are facing in samples (a) without the presence of an external magnetic field. (b) under the influence of an external magnetic field of  $B_0$ .

As mentioned in Figure 1.14, when a  $90^\circ$  RF pulse is applied from the z-axis to the xy plane, owing to this RF pulse, some protons align themselves opposite to  $B_0$  and this causes a decline in longitudinal magnetization, and also precessional movement of protons get in-phase with each other giving rise to a transverse magnetization. And then, when RF pulse is removed, the protons will turn back to their previous states. This process is called as relaxation. The relaxation of longitudinal and transverse magnetization is measured to attain information on the sample (Kirtil & Oztop, 2016).

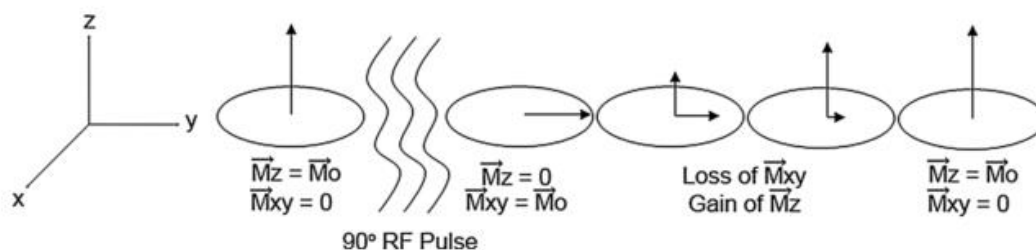


Figure 1.14. Relaxation of transverse ( $M_{xy}$ ), and longitudinal ( $M_z$ ) magnetization after application of a  $90^\circ$  RF pulse (Hashemi, Bradley, & Lisanti, 2010).

There are two important terms that are directly related with NMR results of used samples known as longitudinal relaxation time, and transverse relaxation time as mentioned in Figure 1.15. Longitudinal relaxation time, also referred to as spin-lattice relaxation time that is known as  $T_1$ , refers to the time that it takes for the spins to realign themselves along the axis of the external magnetic field.  $T_1$  indicates the effectiveness of the magnetic energy transfer between spinning  $^1\text{H}$  protons and the surrounding lattice. While pure bulk water has a very long  $T_1$  time, oil has much shorter  $T_1$  time. The alteration of the oil and water state can influence  $T_1$  times, as well as interaction of oil and water with the surrounding macromolecules. On the other hand, transverse relaxation time, also referred to as spin-spin relaxation time known as  $T_2$  refers to the time that it takes for the transverse magnetization, to decay to the equilibrium value of zero, and it is a measure of the effectiveness of energy transfer between neighboring spins. It is expected that,  $T_2$  data of closer proximity between molecules should be shorter. So that,  $T_2$  data is shortest in solids, followed by oil and water.  $T_2$  relaxometry measurements, coupled with  $T_2$  relaxation spectra, are known to yield information on water content, physical properties of water and interaction of water with the surrounding macromolecules (Kirtil & Oztop, 2016).

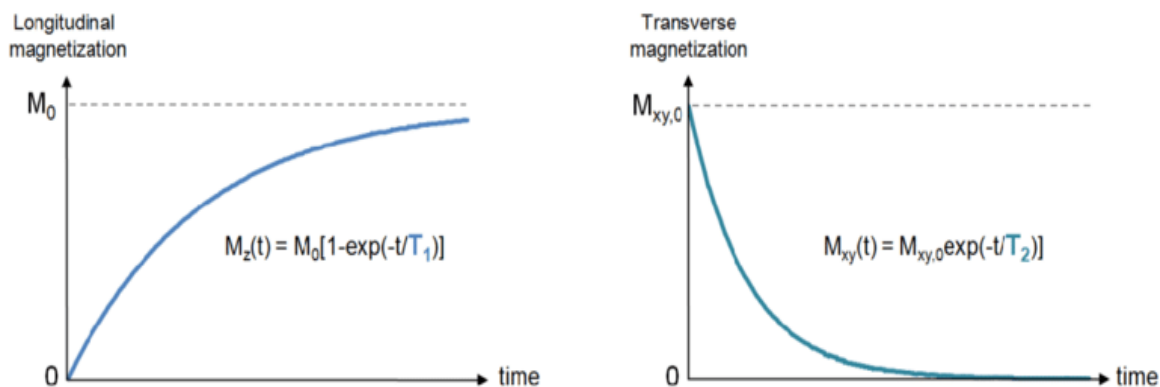


Figure 1.15. Representative curves of longitudinal magnetization,  $T_1$ , and transverse magnetization,  $T_2$ .

Among the different experimental methods, NMR techniques are effectively used to characterise emulsion systems, particularly to determine droplet size distribution. For example, NMR pulse field gradient (PFG) emulsion droplet sizing technique overcomes many problems being also readily applicable to suspended drops. It can be effectively used to study opaque and concentrated systems and results are not affected by possible contaminants, such as gas bubble or suspended solids. In addition, an interesting application of NMR analysis is analyzing the material behaviour in flow conditions giving relevant information on the structural changes induced by flow (Gabriele et al., 2009).

By using NMR techniques, relaxation spectrum analysis makes it possible to understand the water distribution within the hydrogels and further investigate the polymer-water, polymer-polymer, and polymer-oil interactions. (Ozel, Uguz, Kilercioglu, Grunin, Oztop, 2016).

Nondestructive NMR tool can be used to investigate the interior composition of food systems (Greiffet al., 2014) and is applicable to study emulsions due to its rapidity, accuracy, and convenience. The emulsions could be analyzed and measured without pretreatment and dilution during using this technique. The NMR indicates the performance of substances that possess proton peaks; further, the linewidth of the peak

changes according to the environment. Functional groups of the substances would be easily indicated by the form of signal peaks at characteristic chemical shift values. Moreover, the arrangement of the emulsifier at the oil-water interface would be displayed by the signal intensity of distinctive functional groups by  $^1\text{H}$  NMR (Sun, Liu, Feng, Xu, Zhou, 2019).

### 1.6. Magnetic Resonance Imaging

Magnetic resonance imaging (MRI) is also a non-invasive technique that has been commonly used in medical applications to investigate the internal structures of human tissues. Nevertheless, especially in recent years MRI has proven to be a strong analytical tool for engineering research as well, and nowadays, MRI can be used to characterize the many biological and non-biological systems (d'Avila et al., 2005), such as food samples as vegetables, fruits, chocolates, some packaged products as shown in Figure 1.16, and emulsions, and gels as shown in Figure 1.17.

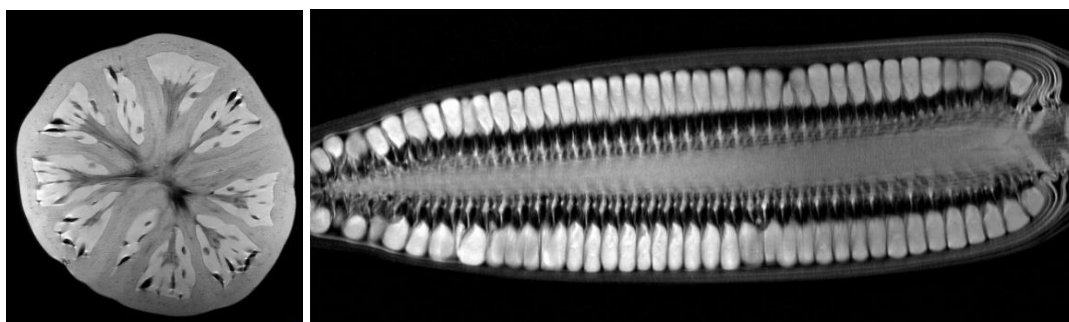


*Figure 1.16.* Tomato and corn images obtained using MRI.

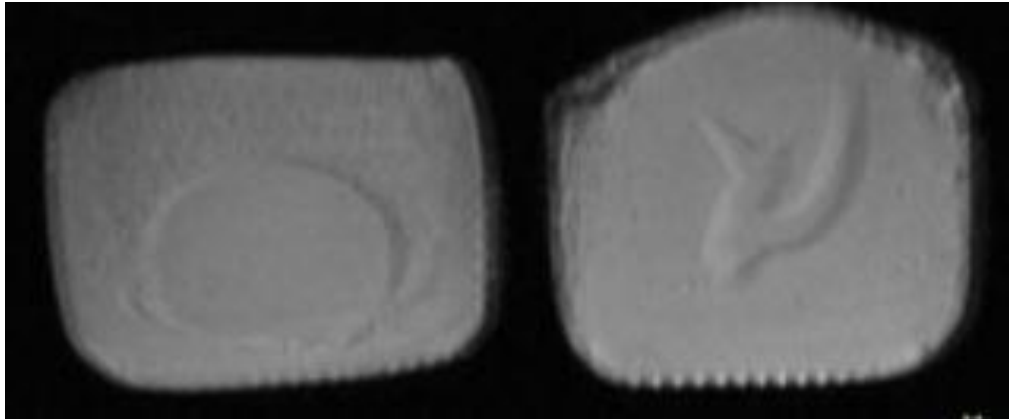


*Figure 1.17.* Gel system images obtained using MRI that are prepared with using different emulsifiers.

Magnetic resonance imaging (MRI) experiment is performed with an NMR instrument equipped with magnetic gradient coils that can spatially gather the data. Therefore, creating two-dimensional and three-dimensional images that display areas having different physico-chemical properties (e.g., water content) with different contrasts (d'Avila et al., 2005; Hashami, Bradley, & Lisanti, 2010). In other words, MRI provides spatial distribution of the signal due to presence of gradient in three axes. On the other hand, NMR relaxometry experiments do not require gradients. It uses the radio frequency (RF) pulse. In contrast to MRI, for an NMR relaxometry experiment, the signal attained comes from the whole sample and spatial information is not obtained. However, it is possible to differentiate signal coming from compartments with varying proton environments (e.g., cellular organelles, water compartments with different mobilities in hydrogels).

## 1.7. Objectives of Study

Quince seed powder forms mucilage in a solution and due to its composition it has been shown to act as an emulsifier. Alginate is a polymer that has perfect gelling ability without the need of heat, thus can be used to create gels entrapping hydrophobic and volatile active agents. However, since alginate is lacking emulsifying ability, to create a gel system capable of entrapping hydrophilic constituents it needs an additional polymer. In this study quince seed powder was used as an aiding agent to create model emulsion gels from alginate. Since emulsions gels are obtained from emulsions it was also aimed to understand the formation of a coarse emulsion from alginate and the effect of quince seed powder as an emulsifier.

In the current literature, there is not enough comprehensive studies regarding the use of quince seed powder for stabilizing emulsions, and gels. Thus, objectives of this study could be listed as follows

- To observe effect of quince seed powder on emulsion and on an emulsion gel system and interpret the polymer interactions in these systems by using Time Domain NMR Relaxometry accompanied with other techniques such as rheological, particle size and Scanning Electron Microscopy experiments
- To compare the emulsion and gel stabilizing performance of quince seed powder with respect to the most commonly used stabilizer, xanthan gum.

To obtain information on the structure of gels by using Magnetic Resonance Imaging experiments.

## CHAPTER 2

### MATERIALS AND METHODS

#### 2.1. Materials

Whey Protein Isolate (WPI) containing 88% protein content determined by Kjeldahl method was supplied by Bipro, Hardline Nutrition, Kavi Gıda San.Ltd.Şti (İstanbul, Turkey).

Sodium alginate, calcium chloride dihydrate ( $\text{CaCl}_2 \cdot 2\text{H}_2\text{O}$ ), and xanthan gum were supplied from Sigma-Aldrich Chemical Co. (St. Louis, MO, USA).

Sunflower oil (Yudum Gıda San. Tic A.Ş., Ayvalık, Balıkesir) used during emulsion preparation was purchased from a local grocery store.

Quince seed powder was prepared by using the seeds of quinces purchased from a local supermarket in Ankara.

#### 2.2. Methods

##### 2.2.1. Preparation of Quince Seed Powder

Quince seeds were separated from the fruits and frozen, and dried using a freeze drier (Christ, Alpha 2-4 LD plus, Germany) for 48 hours at  $-50^{\circ}\text{C}$  at 0.019 mbar. At the end of drying, samples were grinded by using a coffee grinder (MC23200, Siemens, Germany) into powder form.

### 2.2.2. Emulsion Capacity Determination

The method of Obatolu et al. (2001) was modified and 0.5 g weighted sample was dissolved in 25 ml distilled water and mixed with 25 ml refined sunflower oil for emulsion capacity experiments. Prepared emulsion was homogenized at 15,000 rpm for 1 min, and then centrifuged at  $3700 \times g$  for 30 min. Finally, using the length and volume of emulsified layer and whole layer, EC of samples were determined by using the following equation:

$$EC (\%) = \frac{\text{height or volume of emulsified layer} \times 100}{\text{height or volume of whole layer}}$$

### 2.2.3. Emulsion Preparation

During emulsion preparation 2% whey protein isolate (WPI), 2% alginate, and 10% (w/w) refined sunflower oil were dispersed in distilled water by using a high-speed homogenizer (WiseTis Homogenizer, Witeg Labortechnik GmbH, Germany) at 14,000 rpm for 4 min. To observe the effect of xanthan gum (XG) and quince seed powder (QSP) on emulsions, 0.5% (w/w) of the hydrocolloid was added to the mixture. During the preparation of quince seed powder containing emulsion, after all raw materials were homogenized for 1 min, emulsions were centrifuged at  $10,000 \times g$  for 2 min to remove the solid particles of seed powder. Then, centrifuged emulsion was re-homogenized at 14,000 rpm for 3 min. Figure 2.1 also shows the emulsion preparation in detail.

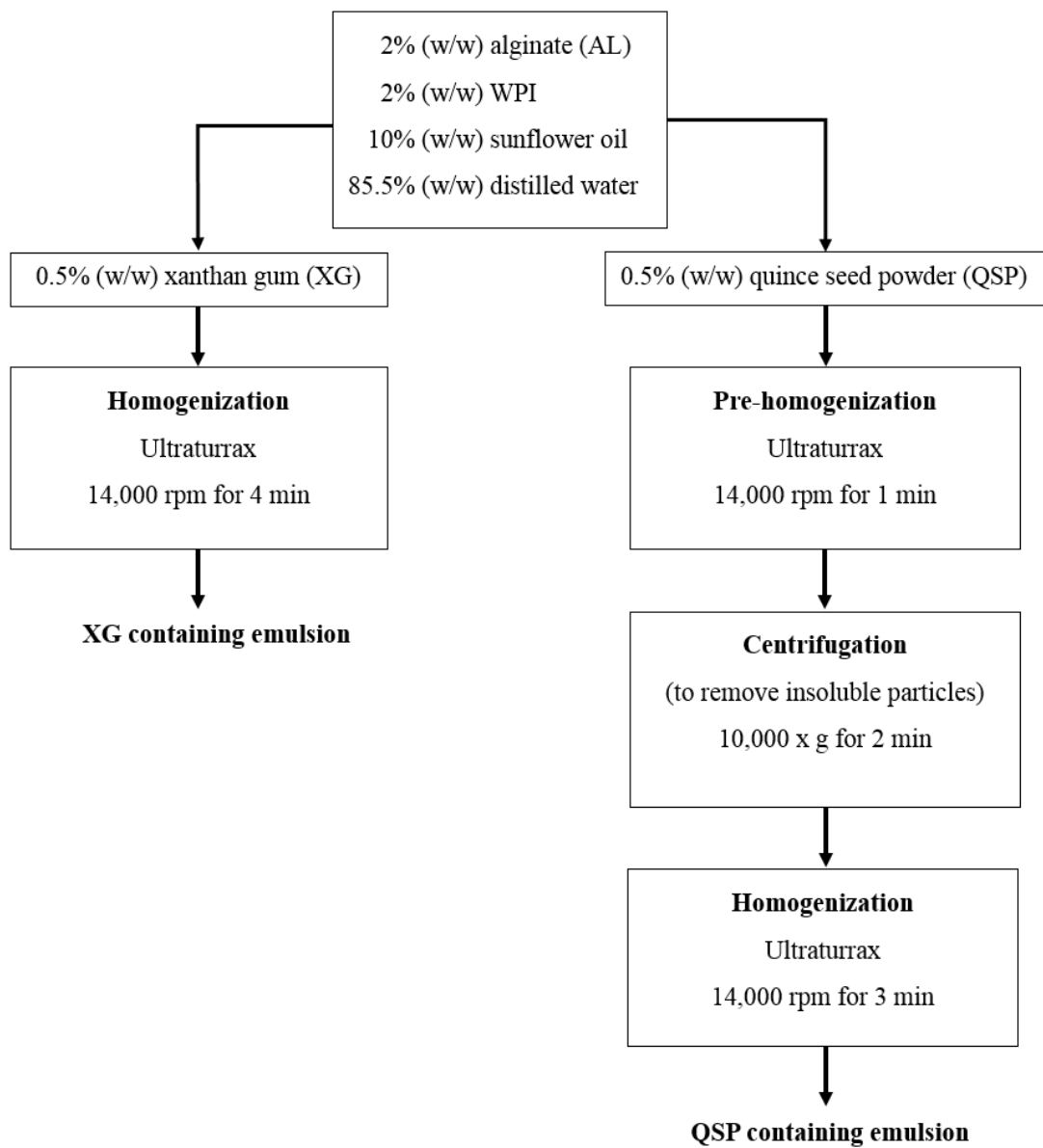


Figure 2.1. Flow chart of emulsion preparation.

#### 2.2.4. Cold Set Gel Preparation

In order to obtain cold set hydrogels, 50 mL of prepared emulsions without gum mentioned on part 2.2.3 were put into 0.25 M  $\text{CaCl}_2 \cdot 2\text{H}_2\text{O}$  solution at the ratio of 1:3 by the help of plastic mesh baskets shown in Figure 2.2 to enable isotropic diffusion and kept for 18 h to complete gelation. 18 h gelation time was confirmed after thickness change of the gels with respect to time was recorded. Photos of the hydrogel sample at the end of gelation time, and a cross-sectional view of a hydrogel sample without any hydrocolloid are also given in Figure 2.3. Photos of all hydrogels are also provided in Appendix C.



*Figure 2.2.* Plastic mesh baskets used during gelation.

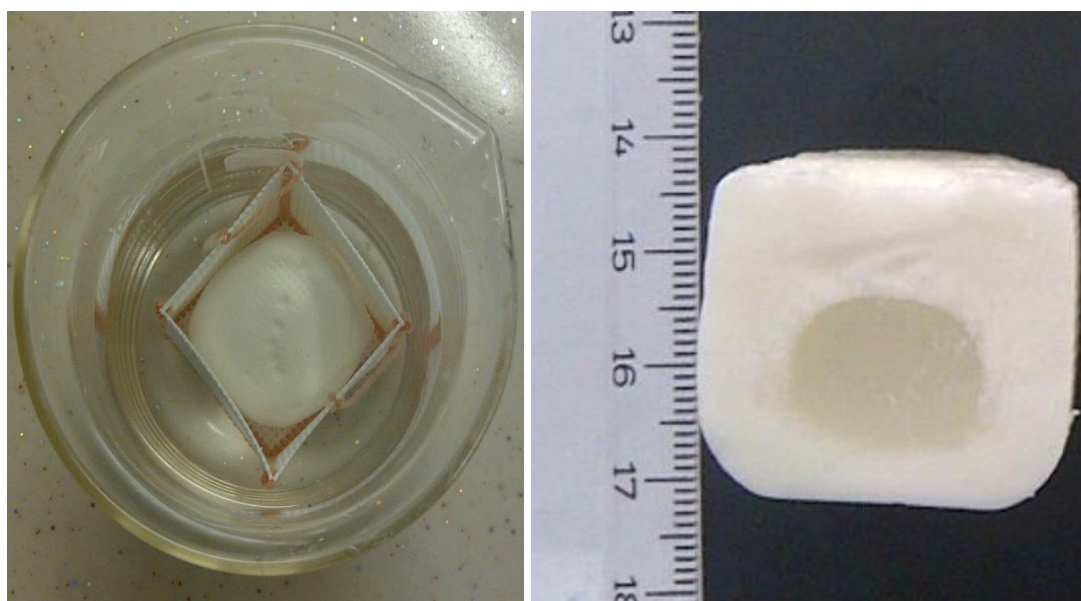


Figure 2.3. (a) A hydrogel sample in the 0.25M  $\text{CaCl}_2 \cdot 2\text{H}_2\text{O}$  solution at the end of gelation period, (b) A cross-sectional view of a hydrogel sample prepared without any hydrocolloid.

## 2.2.5. Emulsion and Hydrogel Characterization

### 2.2.5.1. Mean Particle Size Measurements

The mean particle sizes of emulsion samples were measured by using a light diffraction-based particle size analyzer (Mastersizer 3000, Malvern, Worcestershire, UK). Refractive index and absorption values were set to 1.56 and 0.001 as measurement parameters.

### 2.2.5.2. Scanning Electron Microscopy

Hydrogels were dried using freeze dryer (Christ, Alpha 2-4 LD plus, Germany) for 48 hours and then scanning electron microscopy experiments were performed using Jeol (JSM 6400, Tokyo, Japan) electron microscopy at 600 X magnification. Experiments were performed at METU Central Laboratory.

### **2.2.5.3. Determination of Rheological Properties**

Since cold set hydrogels will later be formulated using  $\text{CaCl}_2$  as the crosslinking agent, to understand the effect of calcium on the used hydrocolloids (QSP and XG), rheological properties were determined for 2% XG, and QSP containing solutions in 0.25 M  $\text{CaCl}_2 \cdot 2\text{H}_2\text{O}$  solution and in distilled water. Then, in order to observe rheological effects of quince seed powder and xanthan gum on the emulsions, emulsions were prepared as mentioned in the section 2.2.4. Then, rheological measurements were conducted for all formulations (Control (no hydrocolloid emulsions), QSP, XG) by using cone-and-plate (40 mm diameter,  $4^\circ$  cone angle, and 0.1425 mm gap) geometry probe of Malvern rheometer (Kinexus Dynamic Rheometer, Malvern, UK) at  $25 \pm 0.1^\circ\text{C}$ . Throughout the experiments, after determining yield stresses of samples, shear stress versus shear rate data were obtained. During shear rate ramp testing, shear stress values were recorded with respect to varying shear rates data from  $0.1 \text{ s}^{-1}$  to  $100 \text{ s}^{-1}$  with 20 sample points and 2 min total ramp time. The obtained data were fit to Power Law model.

### **2.2.5.4. Nuclear Magnetic Resonance (NMR) Relaxometry**

NMR relaxometry experiments, spin-spin relaxation ( $T_2$ ) measurements were conducted by using two different NMR spectrometers. 0.32 Tesla NMR spectrometer operating at 13.52 MHz for  $^1\text{H}$ -resonance frequency system (Spin-Vision, Resonance System, Russia) was used for emulsion characterization. A Carr-Purcell-Meiboom-Gill (CPMG) pulse sequence was used with an echo time (TE) of 1,000  $\mu\text{s}$ , repetition time (TR) of 1,000 ms, 16 acquisition points, and 64 scans to measure  $T_2$  values. With CPMG sequence a decay curve as shown in Figure 2.4.a was obtained. Since gel systems had shorter relaxation times, to have higher signal to noise ratios their relaxation times were acquired using 0.5 Tesla (22.40 MHz) NMR spectrometer system equipped with a 10mm coil (SpinCore Inc., Gainesville, U.S.A).  $T_2$  measurements with this instrument were also applied using CPMG sequence with a

TE of 1,000  $\mu$ s, TR of 3,000 ms and 32 scans.  $T_1$  spin lattice relaxation times as shown in Figure 2.4.b were also measured for gels and inversion recovery (IR) pulse sequence was used for these measurements. Inversion times changed between 1 and 10 ms and repetition delay of 3 s was used.

The samples for NMR experiments were prepared by loading 3 mL of solution sample into a 15 mm diameter cylindrical plexiglass tubes for SpinVision system and by loading 15 mm height of hydrogel sample into a 10 mm diameter cylindrical glass tubes for SpinCore system, and all NMR experiments were performed at room temperature (25°C).

$T_2$  measurements of each sample were replicated three times, and average  $T_2$  data with respect to mono-exponential fitting were analyzed by using MATLAB (Mathworks Inc, U.S.A). Multi-exponential fitting behavior of the decay curves were also analyzed using XPFit (Soft Scientific, Alango, Israel). Sample plots are shown in Figure 2.4.c.

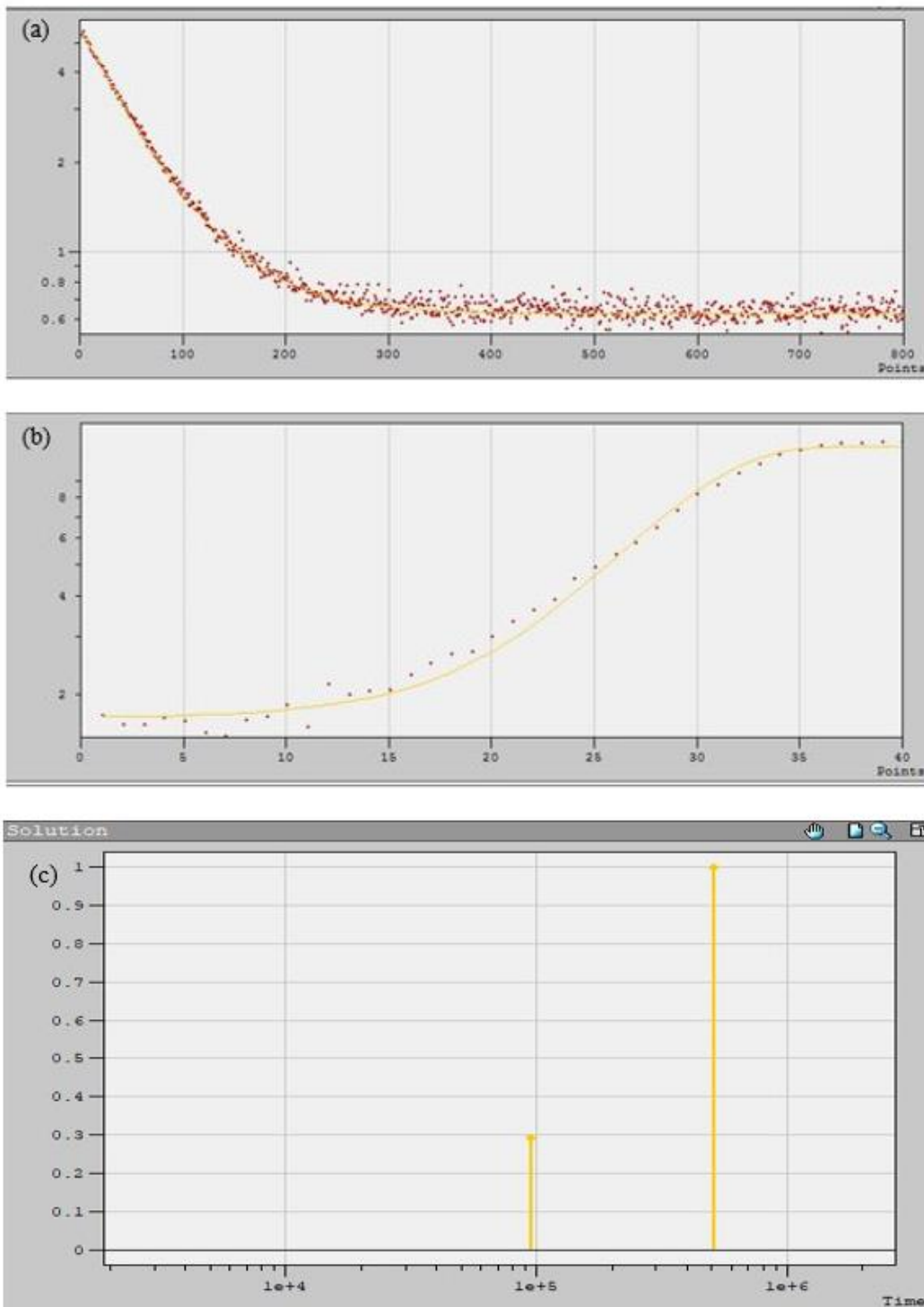


Figure 2.4. (a) Fitted decay curve of transverse relaxation,  $T_2$ , (b) Longitudinal relaxation,  $T_1$ , data fitted curve, (c) Multi-exponential distribution of the  $T_2$  decay curve.

### **2.2.5.5. Magnetic Resonance Imaging Experiments for Hydrogels**

In addition to relaxometry measurements, magnetic resonance images of gels were acquired using a clinical MR Scanner with a magnetic field of 3T at Bilkent University, National Magnetic Resonance Center (UMRAM) (SIEMENS, Germany). Knee coil with 160 mm diameter was used with the help of Multi Slice Multi Echo (MSME) sequence that based on Spin Echo (SE) sequence to obtain  $T_2$  maps of the gels. Repetition time (TR) of 3,150 ms, echo time (TE) of 13.8 ms was used with 32 echoes with 4 scans, constant field of view of  $150 \times 150 \text{ mm}^2$ , and constant matrix size of  $128 \times 128$ . Slice thickness was set to 3 mm and among the 7 slices were obtained, and the 4<sup>th</sup> slice (the middle one) was only used for the analysis (Appendix B). In each measurement 3 gels of the same hydrocolloid and a control sample was used. Oil in 10 mm tube and UV Cuvette were used as the correction samples to correct the hardware related signal intensity differences if needed. For each gel, 3 replicates were done and the mean of at most 9 images were reported for the results depending on the coefficient of variation (standard deviation/mean). Using the region of interest (ROI) tool in MATLAB, the gel region was selected, and images were analyzed accordingly. In addition to mean  $T_2$  values of the gels,  $T_2$  relaxation maps were also obtained. Figure 2.5-2.8 shows a representative MR image, echo images of the slice # 4,  $T_2$  decay fitting of the selected ROI (region of interest) and also the  $T_2$  maps of the selected region for different hydrocolloids and control hydrogels. A  $T_2$  map gives the spatial distribution of  $T_2$  values in the gel. In other words, each voxel corresponds to a different  $T_2$  value. Thus, the standard deviation of a  $T_2$  map image could give idea about the homogeneity of the sample. In addition to  $T_2$  maps,  $T_2$  CPMG decay curves were further analyzed with XPFit to show the presence of different compartments.

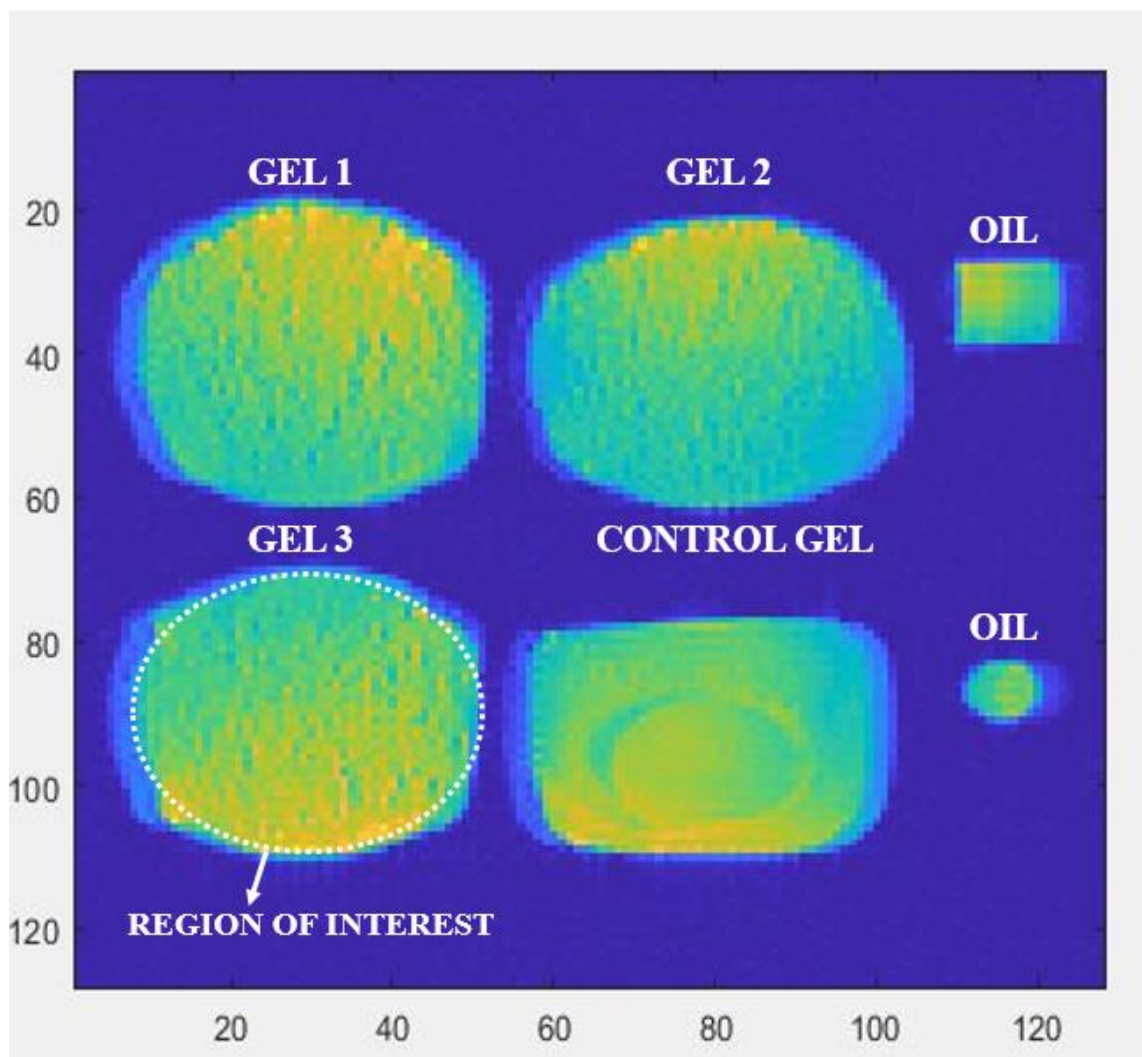


Figure 2.5. Representative Spin Echo MR images of the hydrogels containing quince seed gum acquired using an echo time 12ms, TR of 3s.

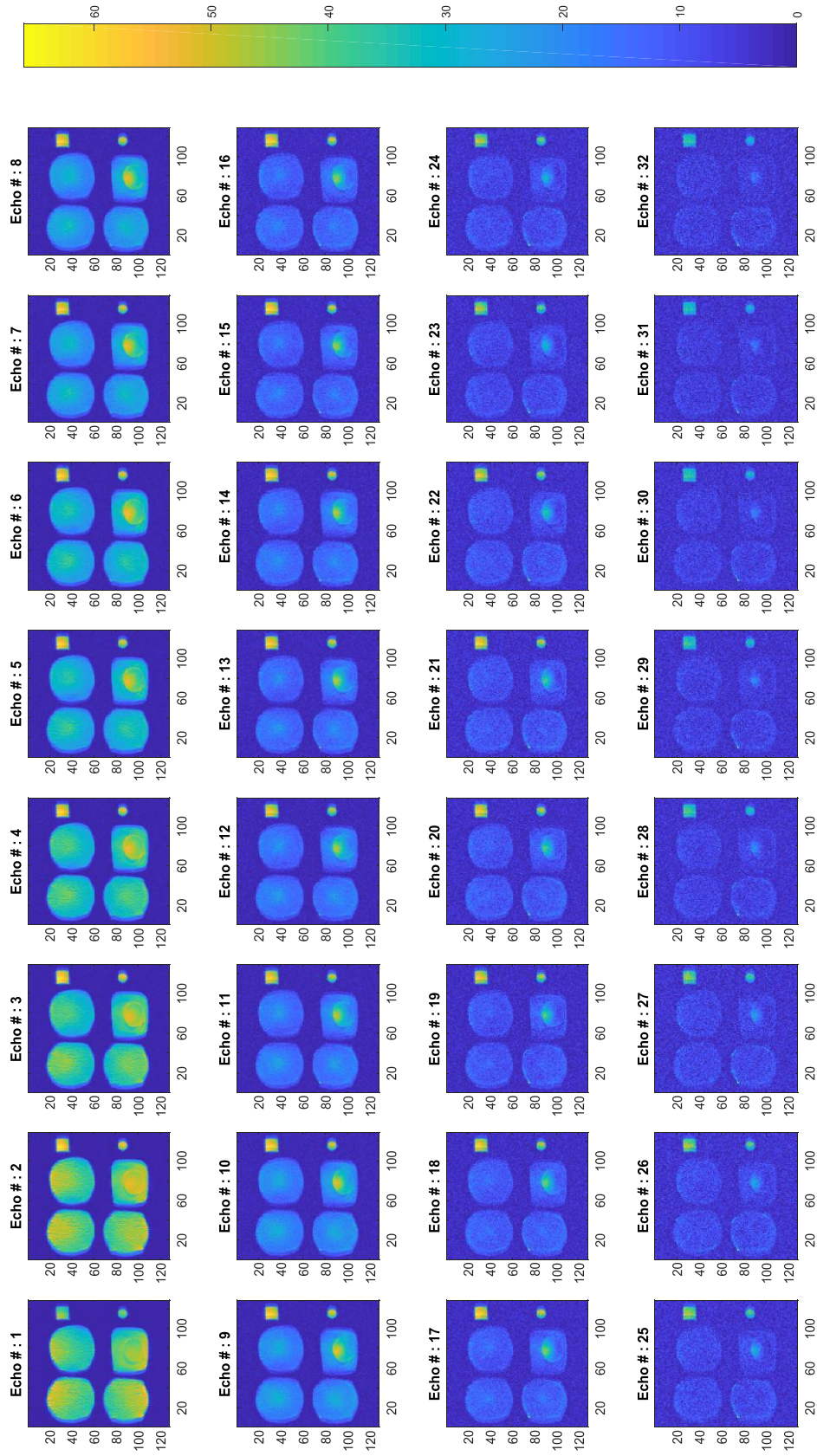
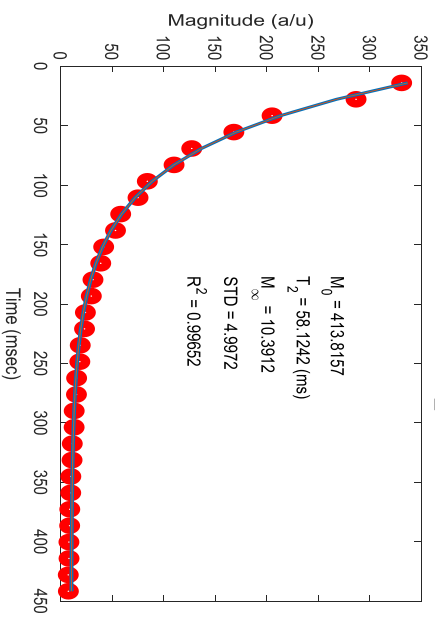


Figure 2.6. Multi-echo images of the quince seed containing hydrogels for Slice # 4.

### MonoExponential $T_2$ Analysis



### BiExponential $T_2$ Analysis

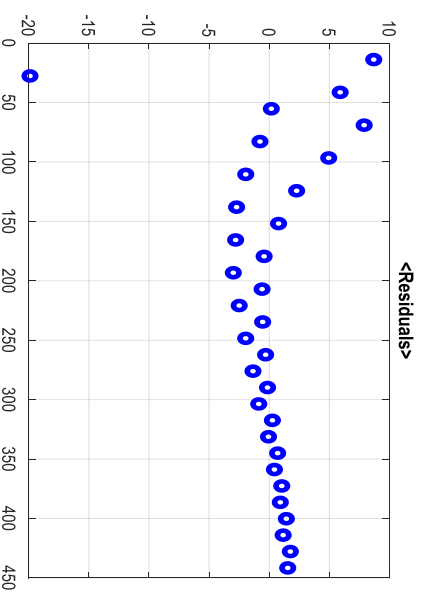
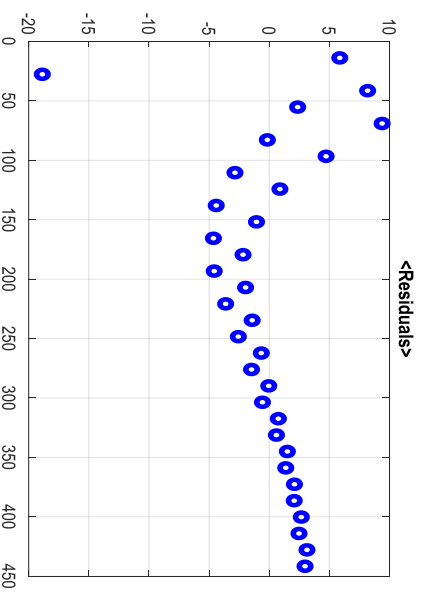
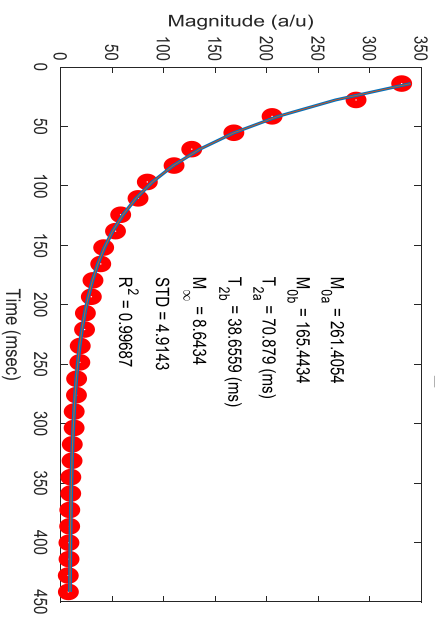


Figure 2.7. Representative CPMG decay of the hydrogels containing quince seed gum from the selected region of interest using an echo time 13.8 ms, TR of 3,150 ms.

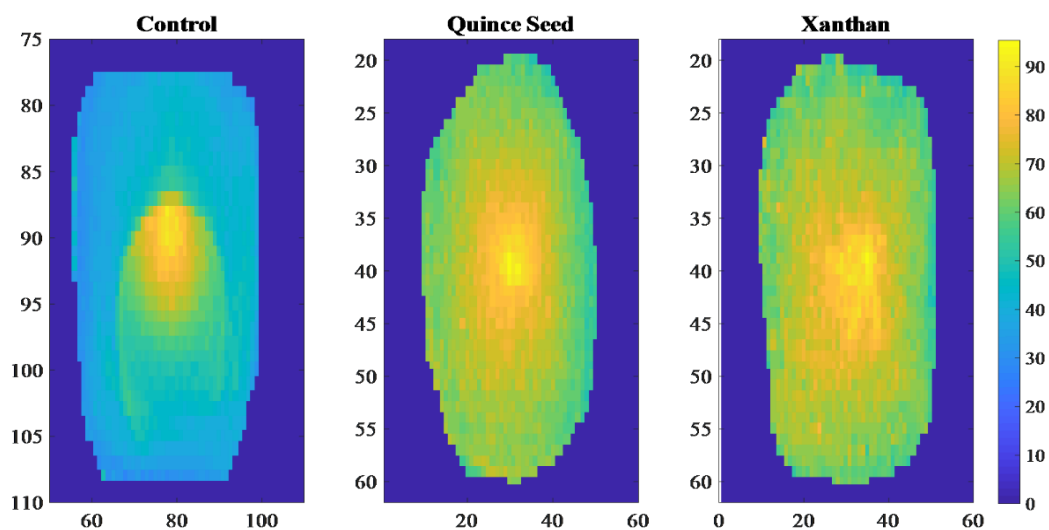


Figure 2.8.  $T_2$  Maps of hydrogels. Each voxel corresponds to a different relaxation time.

### 2.3. Statistical Analysis

For statistical analysis, MINITAB (Version 16.2.0.0, Minitab Inc., State College, Penn, USA) software was used. All experimental results were analyzed by Analysis of Variance (ANOVA) using the general linear model option and Tukey's test at 5% significance level ( $p \leq 0.05$ ) was performed as the comparison test to observe the effect of xanthan gum and quince seed powder on results. Assumptions of ANOVA (Normality and Test of Equal Variances) were checked and Box-Cox transformation was applied when necessary. All measurements were performed in three independent replicates.



## CHAPTER 3

### RESULTS AND DISCUSSION

#### 3.1. Gelation Time Determination

18 h gelation time was confirmed after thickness change of composite gel structure with respect to time was recorded for every 30 min for 24 h as results shown in Figure 3.1. Final form of the one of the hydrogels was also shown in the previous section. As seen in Figure 3.1, it was clear that gelation occurred from outside to inside. Gel layer completion took 18 hours as seen in Figure 3.2.



*Figure 3.1.* Image of thickness change of gels with respect to time for 30 min time periods for 5 h.

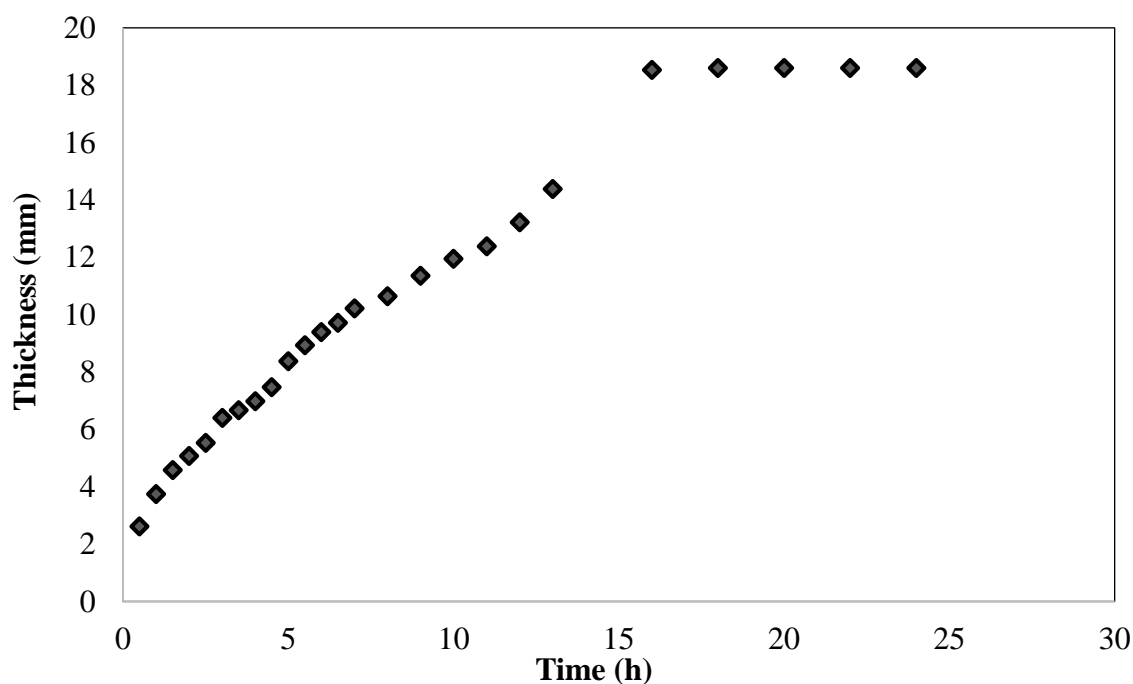


Figure 3.2. Thickness change (mm) of hydrogels with respect to time (h) for 24 h.

### 3.2. Determination of Emulsion Capacity

When the sample of quince seed powder was analyzed with the method mentioned in part 2.2.2, its emulsion capacity was determined as  $42.99 \pm 0.80$  % with respect to height and  $53.00 \pm 0.06$  % with respect to volume. So, the results showed reasonable values in terms of emulsification ability and these were further confirmed by NMR Relaxometry and MR Imaging experiments.

### 3.3. Particle Size Measurements

Physicochemical stability and texture properties of emulsions could be modified by combinations of proteins and polysaccharides (Sun et al., 2007). As a surface active agent, WPI can adsorb onto the oil droplet surfaces and form a monolayer (Cayot & Loriant, 1997). XG produces high viscosity solutions at low shear rates but due to its

strong shear-thinning character, gives lower viscosity at higher shear rates making it easy to mix, pour and swallow (Sun et al., 2007). In contrast to WPI, XG is a non-adsorbing polymer. When in combination with WPI, WPI adsorbs on the droplet surfaces but XG cannot bind to WPI stabilized oil droplet surfaces (Radford & Dickinson, 2004). By this way, XG provides a high viscosity in inter particle region hence a resistance against droplet coalescence. Kinetic stability of oil in water emulsions strongly depends on electrostatic effects such as repulsion of droplets due to their surface charges etc. Additionally, steric effects promoted by thick stabilizing barrier layer are among the factors contributing to stability of these emulsions. Therefore, combination of WPI and polysaccharides may produce a system both with high surface activity and high bulk viscosity forming gel-like and thick adsorbed layers (Sun et al., 2007). Although Krstonosic et al. (2015) reported a decrease in the particle size of XG and starch containing o/w emulsions as XG concentration increased from 0.01 to 0.2 % (w/w), XG stabilized emulsion systems through its non-adsorbing characteristics (Krstonošić, Dokić, Nikolić, & Milanović, 2015). Droplet size decreasing effect of XG with increasing concentration was also observed in some studies using different proteins as the main emulsifiers (Papalamprou, Makri, Kiosseoglou, & Doxastakis, 2005). Since XG is a non-adsorbing polymer, emulsions containing XG as the main stabilizing agent at a constant concentration generally do not attain lower particle size values (Moschakis, Murray, & Dickinson, 2005). However, XG emulsion also having AL and WPI as additional polymers, attained the lowest particle size values with respect to Control and QSP emulsions with the same AL and WPI composition as shown in Fig. 3.3 ( $p < 0.05$ ).

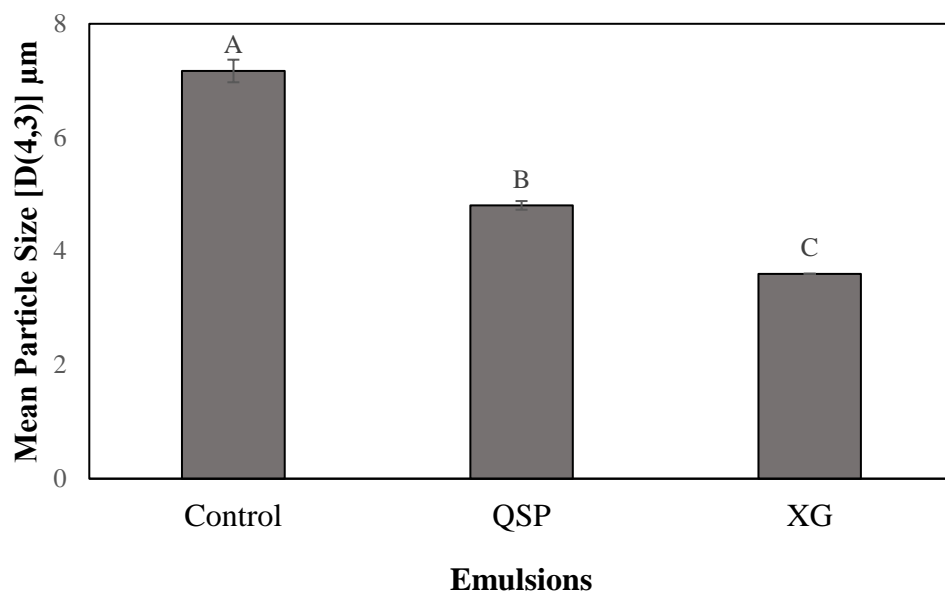


Figure 3.3. Mean particle size [D (4, 3)] values of emulsions ( $p < 0.05$ ). Control, QSP and XG emulsions represent the formulations; AL-WPI-Oil-Water, QSP-AL-WPI-Oil-Water, XG-AL-WPI-Oil-Water, respectively. Error bars are represented as standard errors.

The main reason behind this phenomenon was the viscosity increasing effect of XG on the continuous phase. WPI molecules adsorbed onto the oil droplet surfaces and lowered the interfacial tension of these droplets. Subsequently, these droplets fractured giving smaller diameter droplets. Later, small droplets could not coalesce again due to presence of XG and AL in the continuous phase. Thickener effect of XG and high hydrophilicity of AL molecules created a barrier for these droplets to come together thus, XG emulsions possessed the lower particle size distribution ( $p < 0.05$ ). At 0.5 % (w/w) concentration, XG concentration was high enough to immobilize the oil droplets (Sun et al., 2007). On the other hand, presence of only QSP could not retard oil droplet coalescence since QSP has a dominant interfacial activity rather than thickening effect. Both WPI and QSP provided similar activity on droplets and this did not cause a synergistic effect on lowering the mean particle size of the emulsions. Here, importance of the type of the combined polymer was justified. Control emulsions with no XG or QSP presence, had the highest droplet size as expected ( $p < 0.05$ ).

### 3.4. Rheological Measurements

#### 3.4.1. Polysaccharide Solution Rheology

Emulsion gels were obtained by introducing CaCl<sub>2</sub> to XG and QSP emulsions thus, understanding the effect of Ca<sup>2+</sup> cations on the molecular structures of these polysaccharides was at utmost importance. For this purpose, only XG or QSP containing solutions were prepared in 0.25 M CaCl<sub>2</sub> and the effect was analyzed via rheological measurements (Table 3.1).

*Table 3.1. Rheological constants of polysaccharide solutions prepared by distilled water and 0.25 M calcium chloride solution. Different letters in each column mean solution type differed significantly ( $p < 0.05$ ). Errors are represented as standard deviations.*

<b>Solution</b>	<b>k (Pa.s<sup>n</sup>)</b>	<b>n</b>	<b>R<sup>2</sup></b>
<b>XG-H<sub>2</sub>O</b>	20.41 ± 0.26 <sup>b</sup>	0.14 ± 0.01 <sup>d</sup>	0.989
<b>QSP-H<sub>2</sub>O</b>	0.72 ± 0.11 <sup>d</sup>	0.35 ± 0.02 <sup>a</sup>	0.979
<b>XG-CaCl<sub>2</sub></b>	63.44 ± 2.32 <sup>a</sup>	0.19 ± 0.01 <sup>c</sup>	0.965
<b>QSP-CaCl<sub>2</sub></b>	1.04 ± 0.03 <sup>c</sup>	0.24 ± 0.01 <sup>b</sup>	0.989

Generally, neutral polymers are not affected from salt (ion) addition but polymers having ions are more susceptible to salt addition. Added ions change the intrinsic viscosity of the charged polymers via electrostatic attraction or repulsion mechanisms. Based on the type of induced interaction, polymer molecules can experience contraction or expansion (Abbastabar, Azizi, Adnani, & Abbasi, 2015; Xu, Liu, & Zhang, 2006). Therefore, QSP and XG responded differently to CaCl<sub>2</sub> addition. Firstly, addition of CaCl<sub>2</sub> to XG solutions in distilled water increased the k value ( $p < 0.05$ ). Ca<sup>2+</sup> ions also induced higher k values for QSP solutions. However, effect was not as high as in Xanthan. Presence of calcium was more effective on XG due to the anionic and highly branched side chains of XG molecule. Crosslinking density within the XG molecules increased with CaCl<sub>2</sub> addition. During further crosslinking, new

interaction sites for XG molecules to interact with water were also created, thus a higher viscosity was achieved (Brunchi, Avadanei, Bercea, & Morariu, 2019). QSP, on the other hand, possesses a more linear structural and this reduced the susceptibility of QSP molecules to  $\text{Ca}^{2+}$  action. Although QSP is also an anionic polysaccharide, most charges could have accumulated on the main backbone of the molecule. Even after crosslinking with the added ion, conformation of the QSP molecules might have not changed sufficiently to alter the consistency index values. When the flow behavior indexes were observed, QSP solutions experienced a more shear-thinning character after  $\text{CaCl}_2$  addition ( $p < 0.05$ ). On the other hand, XG containing samples possessed a more Newtonian flow character in 0.25 M  $\text{CaCl}_2$  solution with respect to their correspondent solutions in distilled water ( $p < 0.05$ ). The reason was the contraction of the XG molecule because of the interactions between the side chains and the main cellulosic backbone.  $\text{Ca}^{+2}$  ions promoted crosslinking between side chains of XG but also induced collapse of some side chains on the main XG cellulosic backbone (Vega, Vásquez, Diaz, & Masuelli, 2015). Decrease of the hydrodynamic volume of the individual XG molecules ended up with a higher  $n$  value ( $p < 0.05$ ) (Hemmatzadeh, Hojjatoleslami, & Eivazzadeh, 2011). QSP with less branched structure compared to XG, was more prone to exert a shear-thinning flow character with increasing shear rates. Intermolecular crosslinking effect of  $\text{Ca}^{2+}$  ions made it possible for QSP molecules to align in the direction of applied shear and produced lower  $n$  values ( $p < 0.05$ ). Besides the effect of  $\text{Ca}^{+2}$  ions on molecular conformations, XG and QSP solutions showed a consistent trend in rheological measurements. XG solutions always had higher viscosity and a more pseudoplastic flow behavior with respect to QSP solutions, whether solutions contained  $\text{CaCl}_2$  or not ( $p < 0.05$ ). This consistency proved the characteristic differences of the respective polymers in terms of molecular conformation in solutions. Consequently, consistency and flow behavior index results of XG and QSP polymers in the presence and absence of a cation demonstrated that each polymer had distinct flow characteristics.

### 3.4.2. Emulsion Rheology

Sun et al. (2007) reported that when no or low amount of XG (0 – 0.02 w/w, %) was added to 2 % (w/w) WPI containing emulsions, these systems possessed Newtonian flow characteristics. At relatively higher XG concentrations ( $\geq 0.05$  w/w, %) samples exhibited a shear-thinning flow behavior. As seen in Figure 3.4, all emulsion formulations (Control emulsion, XG containing emulsion and QSP containing emulsion) show a Power Law Flow behavior. At higher shear rates, samples also experienced a shear thinning effect. The reason was the alignment of the emulsion droplets more ordered along the flow direction at higher shear rates. XG emulsions attained  $n$  values less than unity and showed a decreasing trend with increasing XG concentration, suggesting a more pronounced shear-thinning behavior (Sun et al., 2007).

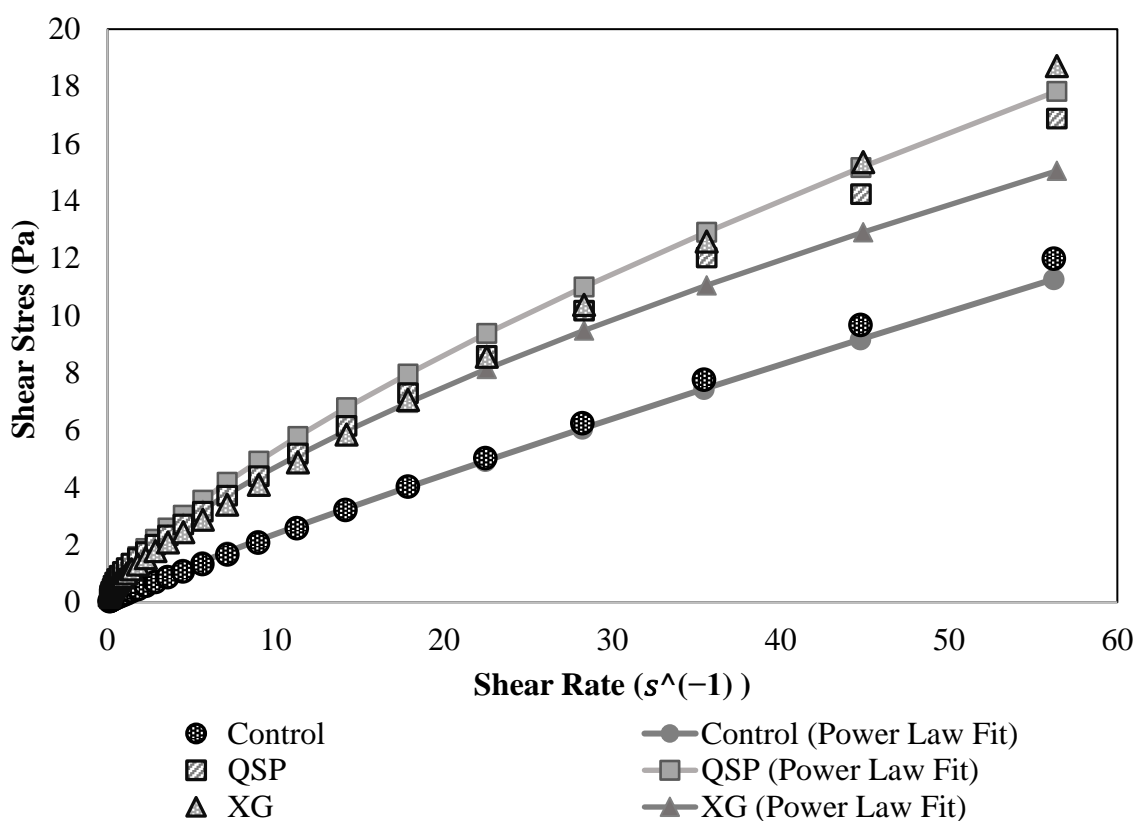


Figure 3.4. Shear stress vs shear rate measurements and power law fitting curves of Control, QSP and XG emulsions.

Table 3.2. Rheological constants of emulsions. Control, QSP and XG emulsions represent the formulations; AL-WPI-Oil-Water, QSP-AL-WPI-Oil-Water, XG-AL-WPI-Oil-Water, respectively. Different letters in each column mean emulsion type differed significantly ( $p < 0.05$ ). Errors are represented as standard deviations.

<b>Emulsion</b>	<b>k (Pa.s<sup>n</sup>)</b>	<b>n</b>	<b>R<sup>2</sup></b>
<b>Control</b>	$0.31 \pm 0.04^b$	$0.88 \pm 0.03^a$	0.999
<b>QSP</b>	$1.04 \pm 0.05^a$	$0.68 \pm 0.02^b$	0.997
<b>XG</b>	$0.99 \pm 0.02^a$	$0.68 \pm 0.02^b$	0.993

Therefore, the n value of XG emulsions in our study was consistent with the previous results (Table 3.2). Compared to Control emulsions both XG and QSP emulsions attained lower n values ( $p < 0.05$ ). XG or QSP addition also increased the k values of the emulsions demonstrating the higher viscosity of the gum added emulsions ( $p < 0.05$ ). Emulsion rheology results showed that addition of gum altered the rheology of the emulsions and the effects were similar. Although both XG and QSP emulsions attained similar k and n values, their stabilizing effects were different from each other. Bryant and McClements (2000) stated that 8.5 % WPI and 0.2 % XG (w/w) were thermodynamically compatible since their mixture solutions at pH 7.0 did not show any phase separation over a 72 h period (Bryant & McClements, 2000). They also suggested that XG dominated the rheological behaviors of these solutions. WPI – XG containing solutions were reported to achieve a much higher viscosity than only WPI or XG containing solutions. This synergistic effect was attributed to conformation of WPI and XG molecules in the solution. The free volume available to XG molecules decreased by the presence of WPI molecules and this increased the effective volume fraction of the XG in the aqueous solution (Sanchez, Schmitt, Babak, & Hardy, 1997). Therefore, increasing viscosity effect of XG was more consistent and XG produced thick non-adsorbing layers in contrast to QSP emulsions which was justified by the particle size measurements. QSP has shear thinning property like XG and it also has

a high intrinsic viscosity leading to high hydrodynamic volume in solutions. This shows the gelling capacity of QSP (Abbastabar et al., 2015). However, higher surface activity of QSP than XG resulted in less permanent viscosity increasing effect for QSP in the emulsions.

### 3.5. NMR Relaxometry Measurements

#### 3.5.1. Transverse Relaxation Times ( $T_2$ ) of Solutions and Emulsions

Transverse relaxation which is also known as spin – spin relaxation measures the relaxation rate of the  $^1\text{H}$  protons in the transverse plane and depends on the efficiency of energy transfer between neighboring spins (Kirtil & Oztop, 2016a).  $T_2$  measurements of the emulsions (Fig. 3.5) showed that generally QSP containing samples attained longer  $T_2$  compared to XG containing samples except for WPI added gum solutions ( $p < 0.05$ ).

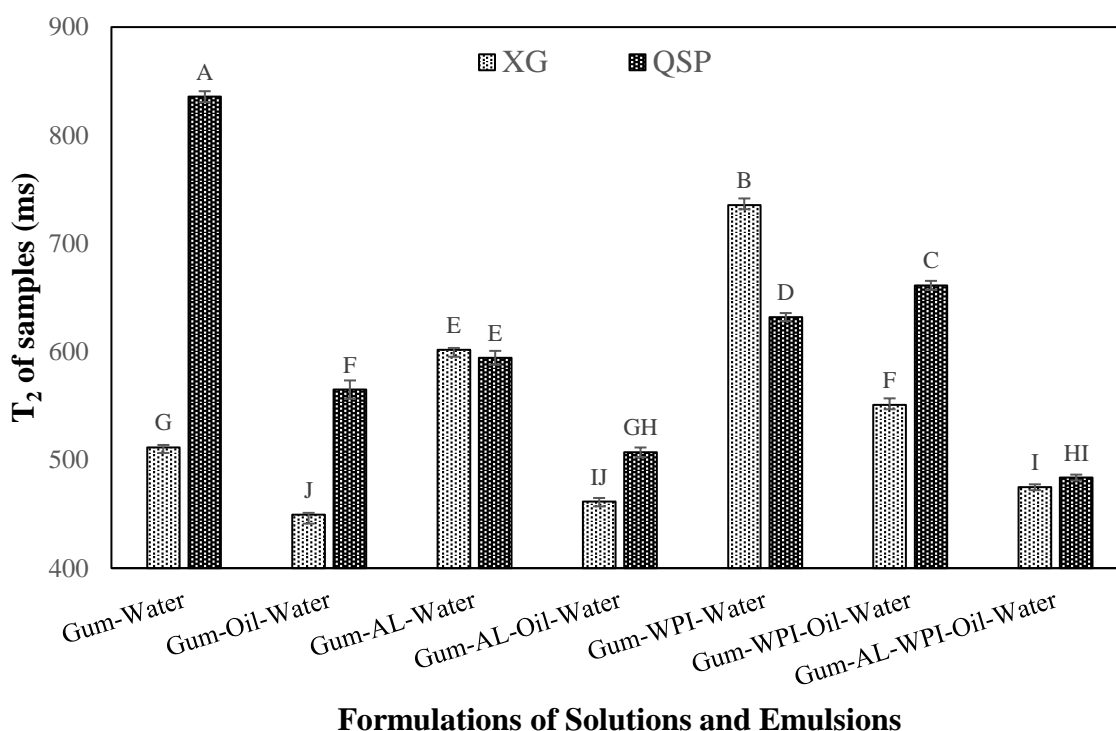


Figure 3.5. Transverse relaxation profiles of all formulations ( $p < 0.05$ ). Gums represent either XG or QSP. Error bars are represented as standard errors.

Another trend was the shorter  $T_2$  of samples including oil which was an expected case since oil protons possess a higher rate of energy exchange rate compared to water protons (Hashemi, Bradley, & Lisanti, 2010; Kirtil & Oztop, 2016b). Transverse relaxation times of oil containing samples were biexponential whereas other non-oil bearing samples had a monoexponential behaviour. Accordingly, these overall  $T_2$  values were dominated by oil and water phases in the emulsions.

Longer QSP-water  $T_2$  compared to XG-water solution was mainly due to the big and complex structure of XG molecules. Side chains of XG interacted more intensely with the surrounding water molecules giving shorter  $T_2$  (Mariette, 2009). Particular viscosity increasing effect of XG molecule originating from its helical conformation in water also decreased the mobility of water and shortened the overall  $T_2$ . Amphiphilic character, less branched and smaller molecular size of QSP resulted in a longer  $T_2$  ( $p < 0.05$ ). Oil addition to these gum solutions decreased the  $T_2$  of both samples as expected but the longer  $T_2$  trend for QSP including samples continued. QSP also interacted with oil particles to some extent but XG molecules continued to interact extensively with the water phase. In contrast to these results, longer  $T_2$  trend of QSP containing gum solutions was reversed in the presence of WPI. WPI decreased the  $T_2$  values of the gum solutions but this time XG-WPI-water samples attained longer  $T_2$  ( $p < 0.05$ ). Electrostatic interactions between the positive patches of WPI and anionic XG side chains provided a reduction in the polysaccharide – water interactions. Consequently, these samples had longer  $T_2$  times ( $p < 0.05$ ). When oil was incorporated into the gum-WPI-water systems, the general  $T_2$  trend for QSP containing samples was observed again. Surface active properties of both WPI and QSP enabled them to interact on the interface but only the hydrophilic fraction of WPI interacted with water in the aqueous phase. Steric incompatibility between the WPI and XG molecules, on the other hand, promoted a higher amount of protein adsorption on oil droplets (Papalamprou et al., 2005). Energy exchange rate at the emulsion interface increased and XG restricted the mobility of the water molecules in the continuous phase. Thus, inevitably, XG-WPI-oil-water emulsions attained shorter  $T_2$

( $p < 0.05$ ). Lastly, AL was added to the emulsion formulations. AL predominated the transverse relaxation process of water in the gum solutions since QSP-AL-Water and XG-AL-Water solutions had similar  $T_2$ . XG and AL are both classified as non-adsorbing polysaccharides (Bouyer et al., 2012). Therefore, XG and AL together, interacted strongly with the water in the aqueous phase. In addition, close  $T_2$  of QSP-AL-Water system indicated the dominant hydrophilic behavior of AL. As a supportive observation for that claim, AL decreased the  $T_2$  of the gum solutions more effectively compared to WPI ( $p < 0.05$ ). Presence of oil in the same AL containing systems resulted in shorter  $T_2$  for both emulsions but QSP-AL-Oil-Water samples had longer  $T_2$  with respect to its XG containing correspondents ( $p < 0.05$ ). This result was also related to the amphiphilic character of QSP. Finally, QSP-AL-WPI-Oil-Water and XG-AL-WPI-Oil-Water emulsions, from which  $Ca^{2+}$  induced gels obtained, were prepared. These QSP and XG emulsions were found to have similar  $T_2$  probably due to the presence of all emulsifiers at the same time within the emulsions. Conformational arrangements of globular proteins like WPI constituents and rigid anionic polysaccharides played a crucial role in their interactions since all their charged groups could not contact efficiently due to the conformational limitations (Tolstoguzov, 2003). But, AL molecules carry negative charge over a wide pH range and this enabled electrostatic interactions between WPI and AL leading to stable emulsions (Albano, Cavallieri, & Nicoletti, 2019). In this case, the dominant factor for emulsion stabilization was the viscosity of the continuous phase. The lower mean particle size of XG emulsions was in agreement with this claim (Fig. 3.3). Lower particle size values are generally associated with more stable systems (Albano et al., 2019). Although both emulsion systems provided emulsification and lower  $T_2$  values, XG emulsions achieved more preferable properties compared to QSP emulsions. High water holding and emulsion capacity results of XG molecules also supported this claim.

When oil was introduced to the system and emulsions were formed relaxation behavior changed. Table 3.3 summarizes the relaxation spectrum of oil containing

emulsions. These samples had two distinct proton populations with their respective peak time and area values (Mariette, 2009). First peaks having shorter peak times and lower areas are attributed to the contribution of dispersed oil phase to the relaxation since oil protons have much lower  $T_2$  than water protons (Marigheto et al., 2007).

Table 3.3. Transverse relaxation spectrum analysis of all emulsion formulations. Different letters in each column mean emulsion type differed significantly ( $p < 0.05$ ). Errors are represented as standard deviations.

Emulsion	Peak 1 (ms)	Area 1 (%)	Peak 2 (ms)	Area 2 (%)
<b>QSP-oil-water</b>	81.00 ± 3.46 <sup>a</sup>	13.61 ± 0.99 <sup>a</sup>	626.67 ± 23.09 <sup>b</sup>	86.39 ± 0.99 <sup>e</sup>
<b>QSP-WPI-oil-water</b>	66.33 ± 4.04 <sup>b</sup>	13.15 ± 0.77 <sup>ab</sup>	693.33 ± 40.41 <sup>a</sup>	86.85 ± 0.77 <sup>de</sup>
<b>QSP-AL-oil-water</b>	56.00 ± 1.73 <sup>c</sup>	10.31 ± 0.91 <sup>cd</sup>	550.00 ± 17.32 <sup>c</sup>	89.69 ± 0.91 <sup>bc</sup>
<b>QSP-AL-WPI-oil-water</b>	37.67 ± 2.31 <sup>d</sup>	6.09 ± 0.19 <sup>e</sup>	490.00 ± 0.00 <sup>d</sup>	93.91 ± 0.19 <sup>a</sup>
<b>XG-oil-water</b>	62.33 ± 2.31 <sup>bc</sup>	8.63 ± 0.39 <sup>d</sup>	460.00 ± 0.00 <sup>d</sup>	91.37 ± 0.39 <sup>b</sup>
<b>XG-WPI-oil-water</b>	54.67 ± 2.89 <sup>c</sup>	12.05 ± 0.73 <sup>abc</sup>	600.00 ± 0.00 <sup>b</sup>	87.95 ± 0.73 <sup>cde</sup>
<b>XG-AL-oil-water</b>	57.00 ± 0.00 <sup>c</sup>	11.46 ± 0.23 <sup>bc</sup>	490.00 ± 0.00 <sup>d</sup>	88.54 ± 0.23 <sup>cd</sup>
<b>XG-AL-WPI-oil-water</b>	32.00 ± 3.00 <sup>d</sup>	8.98 ± 0.70 <sup>d</sup>	490.00 ± 0.00 <sup>d</sup>	91.02 ± 0.70 <sup>b</sup>

QSP-Oil-Water and QSP-WPI-Oil-Water formulations had longer  $T_2$  in peak 1 than correspondent XG formulations indicating the emulsifier effect of QSP ( $p < 0.05$ ). A longer peak 1 time exhibited that water in the continuous aqueous phase was able to participate in the interactions on the interface giving longer  $T_2$  for this peak. XG interacted mostly in the continuous phase and did not show any surface activity. Therefore, XG-Oil-Water and XG-WPI-Oil-Water samples had shorter peak times ( $p < 0.05$ ). Moreover, addition of AL to Gum-Oil-Water and Gum-WPI-Oil-Water systems resulted in a shorter peak 1  $T_2$  ( $p < 0.05$ ) compared to non-AL bearing systems and similar peak times were obtained for QSP and XG systems. Hydrophilic character of AL dominated the continuous phase of the emulsions and abundance of interactions

between the water phase and oil phase was replaced by AL – water interactions. QSP solutions were more susceptible to WPI and AL addition in terms of shorter peak 1 times which was mainly due to surface active property of QSP rather than viscosity increasing effect in the bulk phase. When AL and WPI were present in the emulsions at the same time, continuous phase viscosity properties determined the peak 1 time values.

Areas of peak 1 (Table 3.3) suggested that QSP and WPI were surface active polymers which was in agreement with the literature findings (Dickinson, 2010; Ritzoulis et al., 2014). WPI molecules were reported to act as emulsifiers and during homogenization they migrate to oil-water interfaces. Hydrophobic adsorption sites of WPI anchor on the oil droplet surface. After covering the droplet surface, WPI molecules starts forming a viscoelastic film contributing to steric stabilization of the system (Albano et al., 2019). WPI adsorb on the droplet surfaces layer by layer. The first layer behaves as the substrate for the further adsorption of WPI molecules (Tcholakova, Denkov, Ivanov, & Campbell, 2002). Moreover, Sun et al. (2009) reported that WPI was effective on determining the surface charge of oil droplets (Sun & Gunasekaran, 2009). On the other hand, Ritzoulis et al. (2014) stated that quince seed extracts that they analyzed contained substantial amounts of protein ranging from 10% to 25 %. Presence of protein in the quince seeds played a crucial role in adsorbing of QSP molecules on the particles (Ritzoulis et al., 2014). Protein fraction of the QSP caused electrostatic repulsion at the interface and stabilized the systems (Ritzoulis et al., 2014; Tcholakova, Denkov, Sidzhakova, Ivanov, & Campbell, 2005). Peak 1 area values as shown in Table 3.3 were compatible with these claims. Firstly, QSP-Oil-Water system had higher peak 1 area than XG-Oil-Water system emphasizing the surface activity of QSP ( $p < 0.05$ ). A higher area for the first peak suggests a higher rate of interaction taking place in this proton population. When WPI was put into the Gum-Oil-Water emulsions, relative peak areas of QSP and XG added samples attained similar values ( $p < 0.05$ ). This indicated that WPI was more dominant than QSP molecules in terms of providing surface activity on the interphase. AL addition also revealed statistically

same peak 1 areas. Predominant effect of WPI was also observed in Gum-AL-WPI-Oil-Water combinations since XG containing emulsions had higher peak 1 area with respect to relative peak area of QSP emulsions ( $p < 0.05$ ). WPI – AL biopolymeric interface acted as an anchor between the oil droplet surface and the aqueous continuous phase (Leon et al., 2018). This result was quite opposite to the area values belonging to Gum-Oil-Water formulations. WPI with its bigger molecular size and amphiphilic patches predominated the interactions on the oil droplets independent from the gum type added to the formulation.

Peak 2 was associated with the interactions mainly taking place in the aqueous phase of the emulsions and revealed considerably longer  $T_2$  than peak 1 (Table 3.3) (Vermeir, Balcaen, Sabatino, Dewettinck, & Van der Meeren, 2014). Most of the emulsion combinations including QSP attained longer  $T_2$  than XG bearing formulations for the second peak ( $p < 0.05$ ). Only Gum-AL-WPI-Oil-Water combinations attained statistically same peak times ( $p > 0.05$ ). Shorter peak times of XG blended samples proved the enhanced interaction of XG molecules with the surrounding water molecules in the aqueous phase. Simultaneous presence of WPI and AL in the emulsions predominated the physicochemical properties in the continuous phase and similar  $T_2$ 's at peak 2 were observed. Peak 2 areas were substantially higher than peak 1 areas representing the importance of the continuous phase contribution to stabilize the emulsion systems ( $p < 0.05$ ) (Kirtil & Oztop, 2016b). WPI and AL containing emulsions generally promoted more interactions within the systems giving higher relative areas ( $p < 0.05$ ). XG-Oil-Water emulsions possessed a higher relative peak area compared to QSP-Oil-Water emulsions as expected ( $p < 0.05$ ). However, peak 2 area of QSP-AL-WPI-Oil-Water formulations attained higher area values with respect to correspondent XG emulsions ( $p < 0.05$ ). This reverse correlation between the peak 2 areas for the aforementioned formulations indicated that WPI and AL affected the continuous phase properties substantially. Although XG is the predominant component for the regulation of the aqueous phase rheological properties, interactions in this phase also depended strongly on WPI and

AL actions. Generally, proton relaxation compartment described by peak 2 simulated the overall monoexponential  $T_2$  results of the emulsions. Similar overall  $T_2$  for QSP and XG emulsions for the final formulations supported these findings.

### 3.5.2. NMR Relaxometry for Hydrogels

As hydrogels being solid systems, in addition to  $T_2$  relaxation times  $T_1$  longitudinal relaxation times were also measured. Longitudinal or spin – lattice relaxation time,  $T_1$ , represents the energy exchange rate of  $^1\text{H}$  protons with the surrounding lattice (Hashemi et al., 2010). Figure 3.6 shows the  $T_1$  times of  $\text{Ca}^{+2}$  induced emulsion gels having gum (QSP or XG), AL, WPI, oil and water. XG gels had the longest  $T_1$  ( $p < 0.05$ ). Local water populations not interacting with the surrounding polymer lattice relaxed slowly in XG gels.

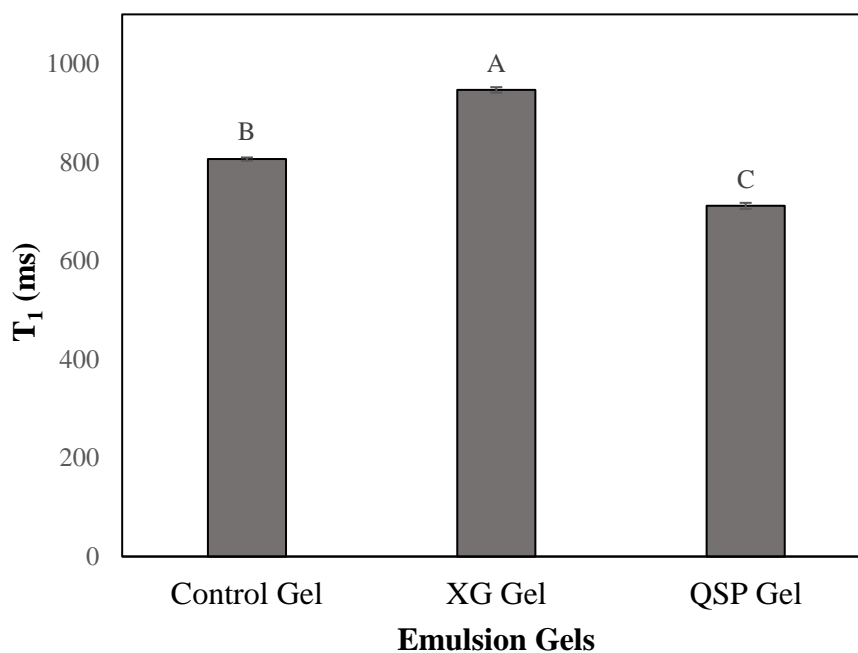


Figure 3.6. Longitudinal relaxation profiles of gels ( $p < 0.05$ ). Control, XG and QSP gels represent the formulations; AL-WPI-Oil-Water, XG-AL-WPI-Oil-Water, QSP-AL-WPI-Oil-Water, respectively. Error bars are represented as standard errors.

In addition, XG molecules with no or negligible surface activity did not commit energy exchange with the oil droplets. These exchanges were only carried out by WPI molecules which was not sufficient to attain high energy exchange rates that would reduce the  $T_1$  of XG gels. QSP gels had the shortest  $T_1$  and main reason was the interfacial activity of QSP molecules on the oil droplets ( $p < 0.05$ ). QSP molecules adsorbed on the oil-water interface experienced intense proton exchange rate with the surrounding molecules thus longitudinal relaxation process was faster for these samples (Le Botlan, Wennington, & Cheftel, 2000). Control gels attained a moderate  $T_1$  which was consistent with the emulsification capabilities of the added XG and QSP polymers.  $T_2$  results of hydrogels showed a mono exponential behavior. XPFit analysis also resulted in the presence of one proton compartment. Magnetic field strength being low (0.5 T); gelation having an effect on restricting the mobility of water might have brought the relaxation time of water close to oil thus a merging on the compartment could have been observed. 2D  $T_1$ - $T_2$  analysis might be needed to see the presence of different compartments in this system. However, as will be discussed later, multi echo MR images obtained at a 3T system provided that info and 2 compartments were identified. Anyway, results of the monoexponential fitting of the hydrogels obtained at the 0.5 T showed that XG gels had the longest  $T_2$  while QSP and Control ones had same but shorter  $T_2$  values ( $p < 0.05$ ) (Figure 3.7).

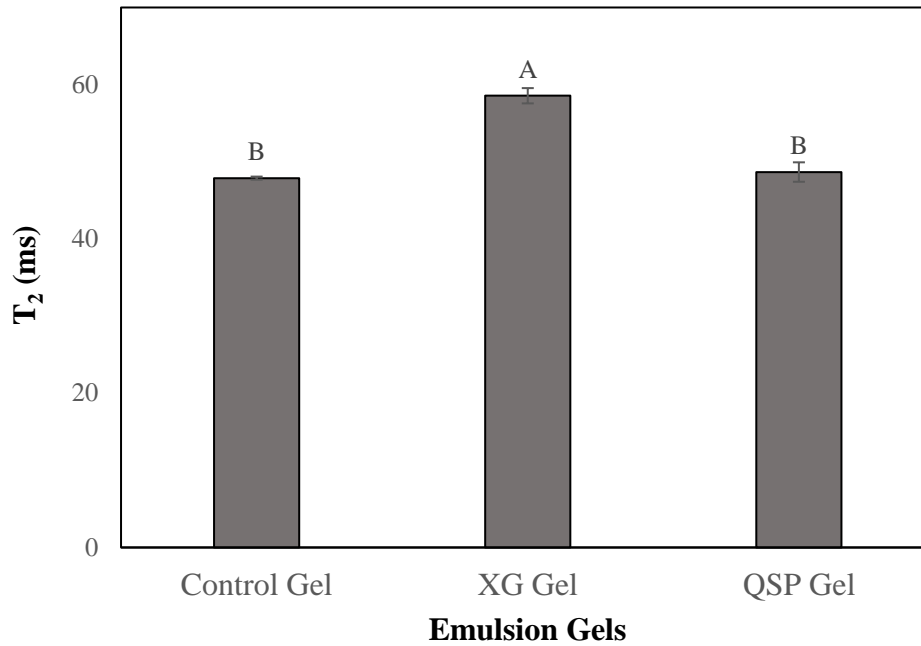


Figure 3.7. Transverse relaxation profiles of gels ( $p < 0.05$ ). Control, XG and QSP gels represent the formulations; AL-WPI-Oil-Water, XG-AL-WPI-Oil-Water, QSP-AL-WPI-Oil-Water, respectively.

Error bars are represented as standard errors.

During gelling, QSP, XG and Control emulsions were subjected to 0.25 M  $\text{CaCl}_2$  solution with the ionic strength of 0.75. Interactions between the WPI and the added polysaccharides in the continuous phase was modified by the ions present in the emulsion. Association of the WPI molecules highly depended on the ion concentration in the system (Grinberg & Tolstoguzov, 1997). Anionic side chains of XG interacted extensively with  $\text{Ca}^{2+}$  ions during gelling and a stiff conformation of XG was established. Therefore, XG gels created distinct water pools within its structure and immobilized water in these compartments leading to longer  $T_2$  (Ozel, Uguz, Kilercioglu, Grunin, & Oztop, 2017). Presence of QSP could not produce such compartments due to its lower association with  $\text{Ca}^{+2}$  with respect to XG molecules. Extracts of quince seeds contain cellulose, hemicellulose, lignin and water soluble polysaccharides such as glucan, galacto-glucan and arabino-xylan fractions (Hakala et al., 2014; Ritzoulis et al., 2014). QSP also possesses a high dietary fiber content and

gum constituents. These fibers and gums have a good water-binding capacity leading to higher viscosities in the QSP containing solutions (Kurt & Atalar, 2018; Wang et al., 2018). QSP were reported to have both thickening and amphiphilic properties (Kirtil & Oztop, 2016b; Kurt & Atalar, 2018). The amphiphilic characteristics of QSP originates from its protein fraction and sugar based hydrophobic methylene groups (Ritzoulis et al., 2014). These fractions enable QSP molecules to adsorb onto the hydrophobic oil droplet surfaces and form a strong interfacial layer (Kurt & Atalar, 2018). On the other hand, high molecular weight polysaccharides of QSP provide emulsion stabilization and give QSP a gelation behavior in the solutions (Jouki, Mortazavi, Yazdi, & Koocheki, 2014). All these properties of QSP provided a shorter  $T_2$  for its gels ( $p < 0.05$ ). Presence of WPI and AL contributed to gelation of Control samples in the absence of QSP or XG. Divalent cations interacted with glucuronate blocks of AL to form egg-box model gel like structures (Lee & Mooney, 2012). By this way, junction zones between the adjacent chains were created giving a three-dimensional weak gel network (Bajpai & Tankhiwale, 2006). AL molecules located in the aqueous phase of the emulsions could interact with surfactants adsorbed on the oil droplets through electrostatic repulsion and steric interactions (Artiga-Artigas, Acevedo-Fani, & Martín-Belloso, 2017). Depending of the pH of the solution, globular proteins were reported to form soluble or insoluble complexes with AL molecules in the aqueous phase (Sosa-Herrera, Lozano-Esquivel, Ponce de León-Ramírez, & Martínez-Padilla, 2012). Therefore, Control emulsions were also able to gel under the same conditions with XG and QSP emulsions and they had gelling characteristics closer to QSP gels.  $T_2$  values of the hydrogels including quince seed and alginate being similar could be a reflection of various overlapping effects; exchange between the compartments; emulsification activity of the quince seed making the  $T_2$  of oil component close to water.

### **3.5.3. NMR Relaxometry for the Hydrogels Using MR Imaging**

As explained in the materials and methods section, MR images of the hydrogels were also acquired to obtain  $T_2$  values of the gels and also to obtain a  $T_2$  relaxation map. Example images are given in Chapter 2.  $T_2$  results obtained from MR Images were different than the results found in the low field system. Although the SNR values were quite high in the low field systems, the field being not homogenous enough and the fast exchange rate at low field might have prevented the detection of 2 compartments thus 1 component was observed, and results were interpreted accordingly. However, MR images showed the presence of 2 compartments as seen in Figure 3.8.b. 1<sup>st</sup> component's  $T_2$  changed between 50-55 ms whereas for the 2<sup>nd</sup> component  $T_2$  values were in the range of 100-130 ms. Results for different hydrogels and the contribution of each peak to the overall signal is given in Table 3.4.

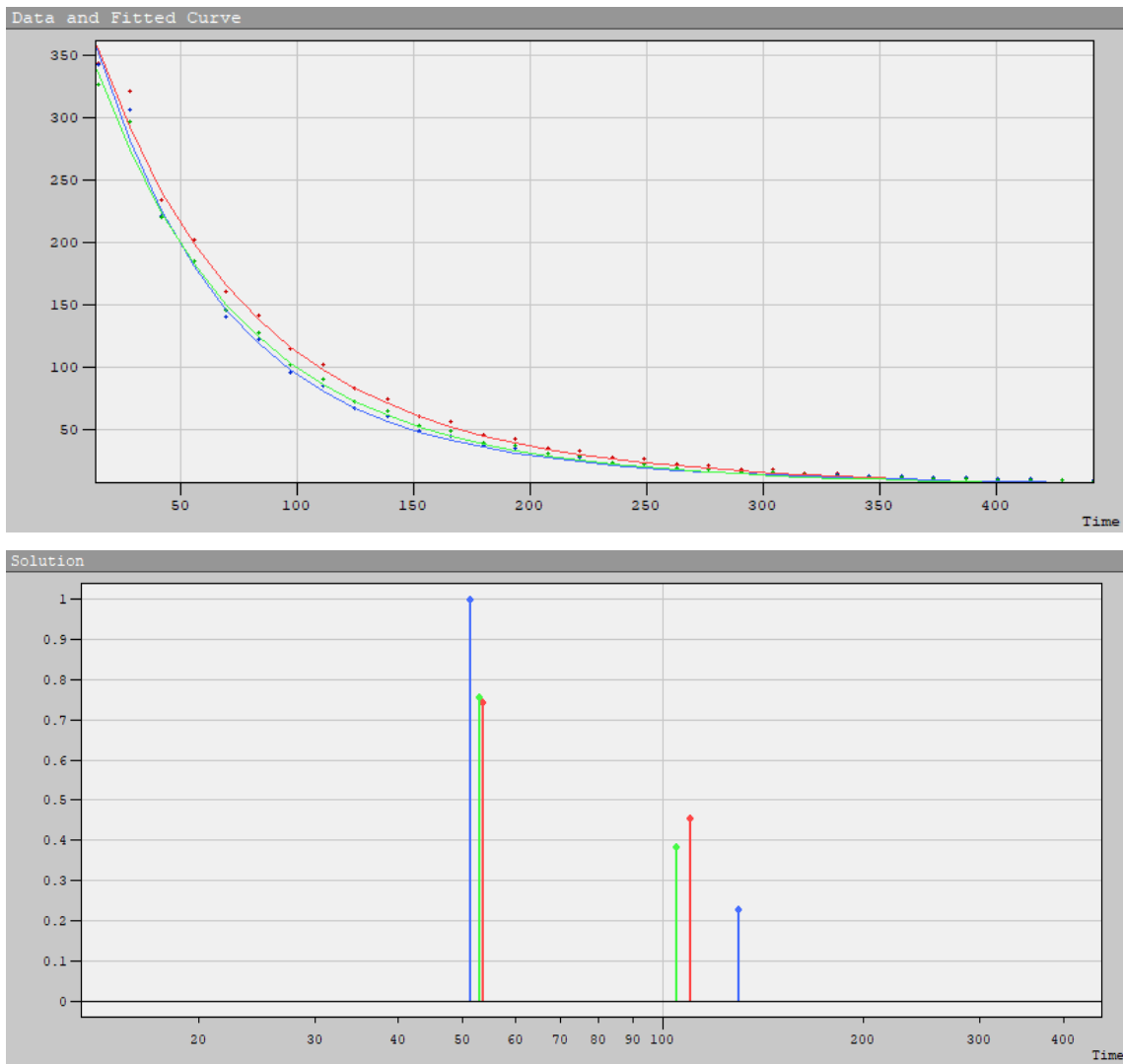


Figure 3.8. (a) CPMG decay curve of samples, (b)  $T_2$  compartments obtained using XPFit from the MR images (Control, QSP, and XG).

Table 3.4. XPFit  $T_2$  results obtained from the MR images.

	$T_{21}$ (ms)	$T_{22}$ (ms)	$RA_1^*$	$RA_2$
<b>Control</b>	$52.28 \pm 0.99^{ab}$	$108.93 \pm 2.27^b$	$60.90 \pm 1.31^c$	$39.10 \pm 1.31^c$
<b>QSP</b>	$50.38 \pm 0.40^b$	$127.57 \pm 1.62^a$	$81.5 \pm 0.44^a$	$18.50 \pm 0.44^a$
<b>XG</b>	$53.59 \pm 0.83^a$	$103.53 \pm 2.57^b$	$64.43 \pm 2.85^b$	$35.57 \pm 2.85^b$

(\*RA denotes the contribution of that peak to the signal)

Since it is known that oil has a relaxation time that could change between 90-120 ms, 2<sup>nd</sup> compartment was associated with protons coming from the oil present in the gels whereas 1<sup>st</sup> component denoted the protons that were strongly interacting with the polymer matrix. For the 1<sup>st</sup> component xanthan and quince hydrogels were significantly different from each other ( $p < 0.05$ ) indicating that polymer water interaction was stronger in the gels. But since quince has also emulsifying ability contribution of oil could have also decreased the relaxation times. The difference was also obvious in the 2<sup>nd</sup> component as 2<sup>nd</sup> component had the longest  $T_2$  which was indicative of the good emulsifying ability of QSP as it was helping to disperse oil much better in the continuous phase and also having exchanging proton contributions from the water phase. The high contribution of the 1<sup>st</sup> component was also a good indication showing that QSP gels were more homogenous and emulsified much better as the contribution was significantly higher compared to control and xanthan samples. This was also consistent with the fact that QSP hydrogels had the shortest  $T_2$  for the 1<sup>st</sup> component indicating a strong gel network with oil.

In addition to relaxation times,  $T_2$  maps were also evaluated. As seen in Figure 3.9.a, there was oil accumulation in the center. This was also clearly seen on the  $T_2$  profile drawn on the axis shown in Fig 3.9.b. Accumulation of the oil phase in the center indicated the instability. There is a significant signal intensity difference between the center and the edges. This was quantified by calculating the standard deviation on the  $T_2$  maps as seen in the Fig. For control samples standard deviation was quite high and when ANOVA was conducted between xanthan and quince samples it was seen that QSP hydrogels significantly have lower deviations than the xanthan hydrogels.

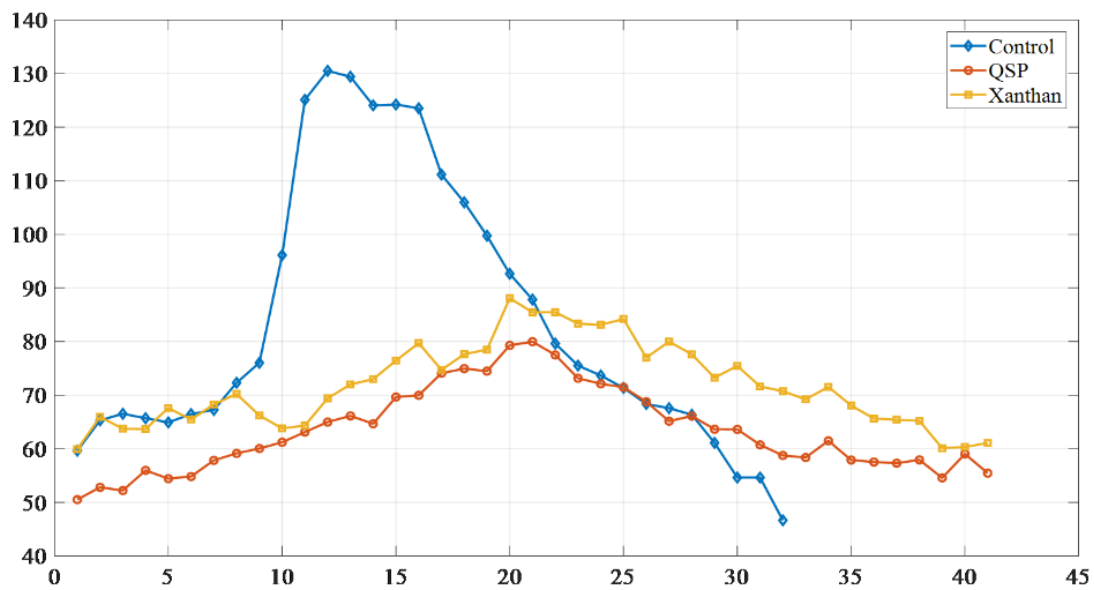
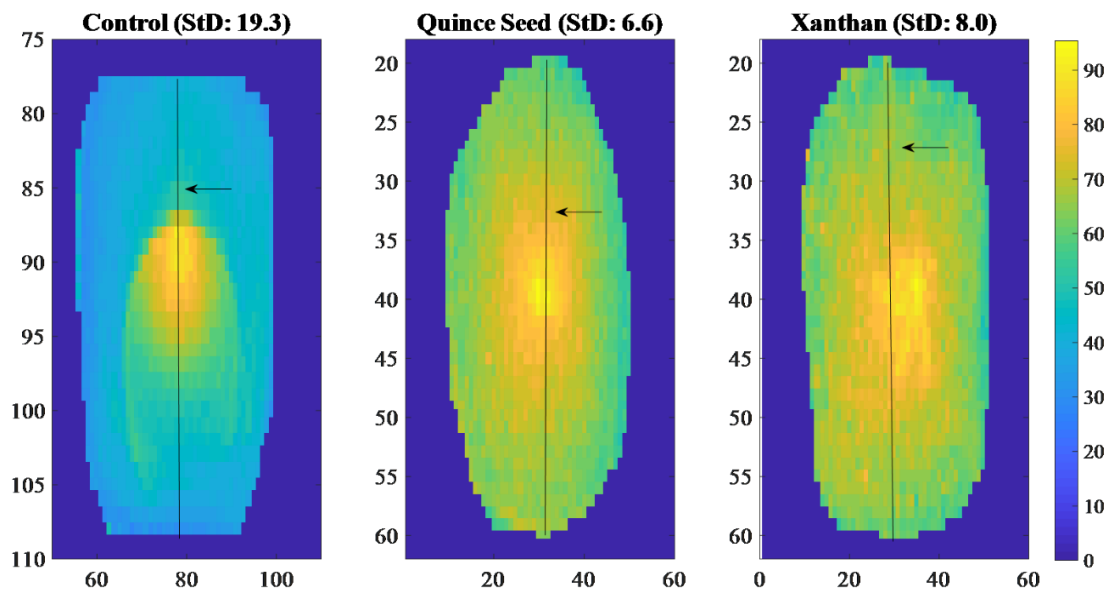
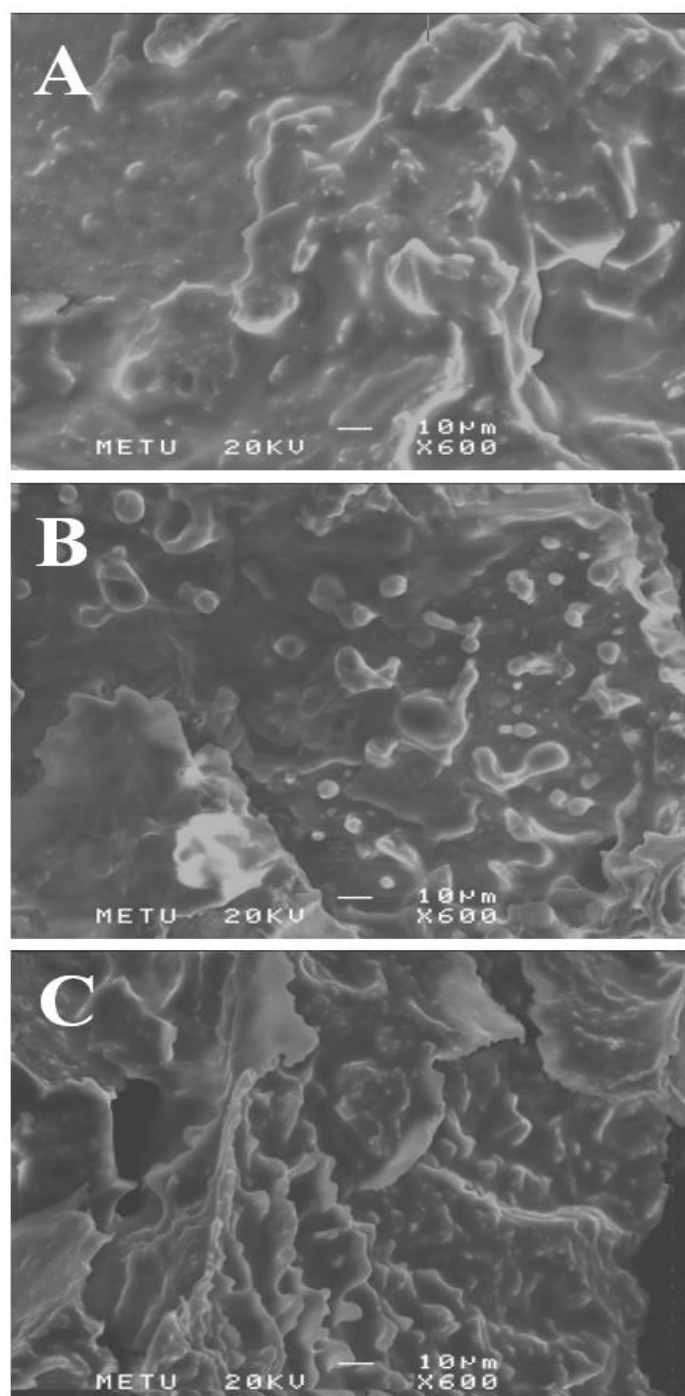


Figure 3.9. (a) Oil accumulation presentation, T<sub>2</sub> maps of taken MR images (b) T<sub>2</sub> profile of samples.

### 3.6. Scanning Electron Microscopy (SEM) Experiments



*Figure 3.10.* SEM images of gels: A, Control; B, QSP; C, XG. Control, QSP and XG gels represent the formulations; AL-WPI-Oil-Water, QSP-AL-WPI-Oil-Water, XG-AL-WPI-Oil-Water, respectively.

Control gels had a smooth structure in the absence of QSP or XG, as shown in the SEM image (Fig. 3.10.a). These gels possessed large clumps on the relatively plain background. Figure 3.10.b shows the QSP gel image having random sized droplet structures on the surface. QSP as an adsorbing polymer probably coated the droplets to some extent with WPI contribution. The nonhomogeneous size distribution of the clumpy structures was due to the insufficient continuous phase viscosity of the QSP emulsions and during gelling this caused a random distribution of the coated droplets. XG gel (Fig. 3.10.c) exerted a filamentous and fragmented structure with denser and smaller clumps (Krstonošić et al., 2015). These structures could be attributed to the branched network of XG and the resulting intense interactions with the added  $\text{Ca}^{+2}$  ions during gelation (Wang et al., 2018). The abundance and complexity of anionic side chains led to a more distorted texture for XG gels with respect to Control and QSP gels.

## CHAPTER 4

### CONCLUSION

QSP and XG blended emulsion formulations were characterized mainly by NMR relaxometry transverse and longitudinal relaxation parameters. A detailed relaxation spectrum analysis of biexponential samples was also conducted. NMR results were discussed with particle size, rheology and SEM image analyses. Consequently, XG based emulsions produced lower particle size systems with respect to QSP based samples, in the presence of WPI and AL as additional polymers. It was demonstrated that the interactions of non-adsorbing XG and adsorbing QSP molecules within the o/w emulsions could be monitored by  $T_2$  measurements. The longest  $T_1$  and  $T_2$  results of XG emulsion gels agreed with the lower particle size distribution of respective XG emulsions ( $p < 0.05$ ).  $T_1$  and  $T_2$  decreasing effect of oil lumps were compensated by smaller and more homogenous oil droplet distribution within the XG gels. However, MR images provided more info on the relaxation time of hydrogels. Relaxation spectrum analysis denoted the presence of 2 compartment and the high contribution and long relaxation time of the 1<sup>st</sup> peak confirmed the emulsification ability of QSP in hydrogels. Moreover,  $T_2$  maps revealed that hydrocolloids definitely improved the stability of the gels as observed on the deviations obtained from  $T_2$  maps.

In overall, it was shown that QSP would be a good alternative to be used in emulsions and hydrogel systems. To understand the mechanism better other techniques such FTIR, viscoelastic measurements could be performed. QSP hydrogels could also be recommended to be used for encapsulating hydrophilic and hydrophobic compounds.



## REFERENCES

- Abbastabar, B., Azizi, M. H., Adnani, A., & Abbasi, S. (2015). Determining and modeling rheological characteristics of quince seed gum. *Food Hydrocolloids*, *43*, 259–264. <https://doi.org/10.1016/j.foodhyd.2014.05.026>
- Albano, K. M., Cavallieri, Â. L. F., & Nicoletti, V. R. (2019). Electrostatic interaction between proteins and polysaccharides: Physicochemical aspects and applications in emulsion stabilization. *Food Reviews International*, *35*(1), 54–89. <https://doi.org/10.1080/87559129.2018.1467442>
- Artiga-Artigas, M., Acevedo-Fani, A., & Martín-Belloso, O. (2017). Effect of sodium alginate incorporation procedure on the physicochemical properties of nanoemulsions. *Food Hydrocolloids*, *70*, 191–200. <https://doi.org/10.1016/j.foodhyd.2017.04.006>
- Asomaning, J., & Curtis, J. M. (2017). Enzymatic modification of egg lecithin to improve properties. *Food Chemistry*, *220*, 385–392. <http://doi.org/10.1016/j.foodchem.2016.09.155>
- Baimark, Y., & Srisuwan, Y. (2014). Preparation of alginate microspheres by water-in-oil emulsion method for drug delivery: Effect of Ca<sup>2+</sup> post-cross-linking. *Advanced Powder Technology*, *25*(5), 1541–1546. <http://doi.org/10.1016/j.appt.2014.05.001>
- Bajpai, S. K., & Tankhiwale, R. (2006). Investigation of water uptake behavior and stability of calcium alginate/chitosan bi-polymeric beads: Part-1. *Reactive and Functional Polymers*, *66*(6), 645–658. <https://doi.org/10.1016/j.reactfunctpolym.2005.10.017>
- Bantchev, G.B., Schwartz, D.K., 2003. Surface shear rheology of  $\beta$ -casein layers at the air/ solution interface: formation of a two-dimensional physical gel.

Langmuir 19, 2673-2682.

Bouyer, E., Mekhloufi, G., Rosilio, V., Grossiord, J. L., & Agnely, F. (2012). Proteins, polysaccharides, and their complexes used as stabilizers for emulsions: Alternatives to synthetic surfactants in the pharmaceutical field? *International Journal of Pharmaceutics*, 436(1–2), 359–378. <https://doi.org/10.1016/j.ijpharm.2012.06.052>

Brady JW. Introductory food chemistry. Ithaca, N.Y.: Cornell University Press; 2013

Brunchi, C. E., Avadanei, M., Bercea, M., & Morariu, S. (2019). Chain conformation of xanthan in solution as influenced by temperature and salt addition. *Journal of Molecular Liquids*, 287, 111008. <https://doi.org/10.1016/j.molliq.2019.111008>

Bryant, C. M., & McClements, D. J. (2000). Influence of xanthan gum on physical characteristics of heat-denatured whey protein solutions and gels. *Food Hydrocolloids*, 14(4), 383–390. [https://doi.org/10.1016/S0268-005X\(00\)00018-7](https://doi.org/10.1016/S0268-005X(00)00018-7)

Cairns, P., Miles, M.J., Morris, V.J., Brownsey, G.J., 1987. X-ray fibre-diffraction studies of synergistic, binary polysaccharide gels. *Carbohydr. Res.* 160, 411–423.

Casado V, Martin D, Torres C, Reglero G. Phospholipases in food industry: a review. *Lipases phospholipases: methods and protocols*, 861; 2012 495–523.

Cayot, P., & Lorient, D. (1997). *Food proteins and their applications*. (S. Damodaran & A. Parf, Eds.). New York: Marcel Dekker.

Chau, C. F., & Cheung, P. C. K. (1998). Functional properties of flours prepared from three Chinese indigenous legume seeds. *Food Chemistry*, 61(4), 429–433. [https://doi.org/10.1016/S0308-8146\(97\)00091-5](https://doi.org/10.1016/S0308-8146(97)00091-5)

- Choi, S. J., Decker, E. A., Henson, L., Popplewell, L. M., Xiao, H., & McClements, D. J. (2011). Formulation and properties of model beverage emulsions stabilized by sucrose monopalmitate: Influence of pH and lyso-lecithin addition. *Food Research International*, 44(9), 3006–3012. <http://doi.org/10.1016/j.foodres.2011.07.007>
- Damodaran S, Parkin KL, Fennema OR. Fennema's food chemistry. 4th ed. Boca Raton, FL: CRC Press; 2007.
- Dickinson, E. (2003). Hydrocolloids at interfaces and the influence on the properties of dispersed systems. *Food Hydrocolloids*, 17, 25–39. Retrieved from [www.elsevier.com/locate/foodhyd](http://www.elsevier.com/locate/foodhyd)
- Dickinson, E. (2009). Hydrocolloids as emulsifiers and emulsion stabilizers. *Food Hydrocolloids*, 23(6), 1473–1482. <https://doi.org/10.1016/j.foodhyd.2008.08.005>
- Dickinson, E. (2010). Flocculation of protein-stabilized oil-in-water emulsions. *Colloids and Surfaces B: Biointerfaces*, 81(1), 130–140. <https://doi.org/10.1016/j.colsurfb.2010.06.033>
- Dickinson, E. (2013). Stabilising emulsion-based colloidal structures with mixed food ingredients. *Journal of the Science of Food and Agriculture*, 93(4), 710–721.
- Djordjevic, D., Kim, H. J., McClements, D. J., & Decker, E. A. (2004). Physical stability of whey protein-stabilized oil-in-water emulsions at pH 3: Potential omega-3 fatty acid delivery systems (Part A). *Journal of Food Science*, 69(5), C351-C355.
- Duval, F. P., Duynhoven, J. P. M. Van, & Bot, A. (2006). Practical Implications of the Phase-Compositional Assessment of Lipid-Based Food Products by Time-Domain NMR. *Journal of American Oil Chemists' Society*, 83(11), 905–912.

- Duynhoven, J. P. M. Van, Goudappel, G. J. W., Dalen, G. Van, Bruggen, P. C. Van, Blonk, J. C. G., & Eijkelenboom, A. P. A. M. (2002). Scope of droplet size measurements in food emulsions by pulsed field gradient NMR at low field. *Magnetic Resonance in Chemistry*, *40*, 51–59. <https://doi.org/10.1002/mrc.1115>
- Einhorn-Stoll, U., Drusch, S., 2015. Methods for investigation of diffusion processes and biopolymer physics in food gels. *Curr. Opin. Food Sci.* *3*, 118–124.
- Gabriele, D., Migliori, M., Di Sanzo, R., Rossi, C. O., Ruffolo, S. A., Cindio, B. (2009). Characterisation of dairy emulsions by NMR and rheological techniques. *Food Hydrocolloids* (*23*), 619-628.
- George, M., & Abraham, T. E. (2006). Polyionic hydrocolloids for the intestinal delivery of protein drugs: Alginate and chitosan - a review. *Journal of Controlled Release*, *114*(1), 1–14. <https://doi.org/10.1016/j.jconrel.2006.04.017>
- Gonzalez-Jordan, A., Benyahia, L., Nicolai, T. (2017). Cold gelation of water in water emulsions stabilized by protein particles. *Colloids and Surfaces A* (*532*), 332-341.
- Granizo, D. P., Reuhs, B. L., Stroshine, R., & Mauer, L. J. (2007). Evaluating the solubility of powdered food ingredients using dynamic nuclear magnetic resonance (NMR) relaxometry. *LWT - Food Science and Technology*, *40*(1), 36–42. <http://doi.org/10.1016/j.lwt.2005.08.012>
- Grinberg, V. Y., & Tolstoguzov, V. B. (1997). Thermodynamic incompatibility of proteins and polysaccharides in solutions. *Food Hydrocolloids*, *11*(2), 145–158. [https://doi.org/10.1016/S0268-005X\(97\)80022-7](https://doi.org/10.1016/S0268-005X(97)80022-7)
- Guiotto EN, Cabezas DM, Diehl BWK, Tomas MC. Characterization and emulsifying properties of different sunflower phosphatidylcholine enriched fractions. *Eur J Lipid Sci Technol* 2013;*115*:865–73.

- Hakala, T. J., Saikko, V., Arola, S., Ahlroos, T., Helle, A., Kuosmanen, P., Laaksonen, P. (2014). Structural characterization and tribological evaluation of quince seed mucilage. *Tribology International*, 77, 24–31. <https://doi.org/10.1016/j.triboint.2014.04.018>
- Hashemi, R. H., Bradley, W. G., & Lisanti, C. J. (2010). *MRI: The basics* (3rd ed.). Baltimore: Lippincott Williams and Wilkins.
- Hemar, Y., Tamehana, M., Munro, P. A., & Singh, H. (2001). Influence of xanthan gum on the formation and stability of sodium caseinate oil-in-water emulsions. *Food Hydrocolloids*, 15(4–6), 513–519. [https://doi.org/10.1016/S0268-005X\(01\)00075-3](https://doi.org/10.1016/S0268-005X(01)00075-3)
- Hemmatzadeh, S., Hojjatoleslami, M., & Eivazzadeh, O. (2011). Hemmatzadeh Effect of pH and calcium salt on rheological properties of XG carboxymethyl cellulose blends. *Annual Transactions of the Nordic Rheology Society*, 19.
- Huang, X., Kakuda, Y., & Cui, W. (2001). Hydrocolloids in emulsions: Particle size distribution and interfacial activity. *Food Hydrocolloids*, 15(4–6), 533–542. [https://doi.org/10.1016/S0268-005X\(01\)00091-1](https://doi.org/10.1016/S0268-005X(01)00091-1)
- Jiang, Y., Liu, L., Wang, B., Yang, X., Chen, Z., Zhong, Y., Zhang, L., Mao, Z., Xu, H., Sui, X. 2019. Polysaccharide-based edible emulsion gel stabilized by regenerated cellulose. *Food Hydrocolloids* (91), 232-237.
- Jouki, M., Mortazavi, S. A., Yazdi, F. T., & Koocheki, A. (2014). Optimization of extraction, antioxidant activity and functional properties of quince seed mucilage by RSM. *International Journal of Biological Macromolecules*, 66, 113–124. <https://doi.org/10.1016/j.ijbiomac.2014.02.026>
- Kirtil, E., & Oztop, M. H. (2016a). <sup>1</sup>H Nuclear Magnetic Resonance Relaxometry and Magnetic Resonance Imaging and Applications in Food Science and Processing. *Food Engineering Reviews*, 8(1), 1–22. <https://doi.org/10.1007/s12393-015-9118-y>

- Kirtil, E., & Oztop, M. H. (2016b). Characterization of emulsion stabilization properties of quince seed extract as a new source of hydrocolloid. *Food Research International*, *85*, 84–94. <https://doi.org/10.1016/j.foodres.2016.04.019>
- Krstonošić, V., Dokić, L., Nikolić, I., & Milanović, M. (2015). Influence of xanthan gum on oil-in-water emulsion characteristics stabilized by OSA starch. *Food Hydrocolloids*, *45*, 9–17. <https://doi.org/10.1016/j.foodhyd.2014.10.024>
- Kumar, P., Khouryieh, H., Williams, K., & Conte, E. (2016). Effect of xanthan / enzyme-modified guar gum mixtures on the stability of whey protein isolate stabilized fish oil-in-water emulsions. *Food Chemistry*, *212*, 332–340. <http://doi.org/10.1016/j.foodchem.2016.05.187>
- Kurt, A., & Atalar, I. (2018). Food Hydrocolloids Effects of quince seed on the rheological , structural and sensory characteristics of ice cream. *Food Hydrocolloids*, *82*, 186–195. <https://doi.org/10.1016/j.foodhyd.2018.04.011>
- Le Botlan, D., Wennington, J., & Cheftel, J. C. (2000). Study of the state of water and oil in frozen emulsions using time domain nmr. *Journal of Colloid and Interface Science*, *226*(1), 16–21. <https://doi.org/10.1006/jcis.2000.6785>
- Lee, K. Y., & Mooney, D. J. (2012). Alginate: Properties and biomedical applications. *Progress in Polymer Science (Oxford)*, *37*(1), 106–126. <https://doi.org/10.1016/j.progpolymsci.2011.06.003>
- Leon, A. M., Medina, W. T., Park, D. J., & Aguilera, J. M. (2018). Properties of microparticles from a whey protein isolate/alginate emulsion gel. *Food Science and Technology International*, *24*(5), 414–423. <https://doi.org/10.1177/1082013218762210>
- Liling, G., Di, Z., Jiachao, X., Xin, G., Xiaoting, F., & Qing, Z. (2016). Effects of ionic crosslinking on physical and mechanical properties of alginate mulching films. *Carbohydrate Polymers*, *136*, 259–265.

<https://doi.org/10.1016/j.carbpol.2015.09.034>

Mariette, F. (2009). Investigations of food colloids by NMR and MRI. *Current Opinion in Colloid and Interface Science*, 14(3), 203–211. <https://doi.org/10.1016/j.cocis.2008.10.006>

Marigheto, N., Venturi, L., Hibberd, D., Wright, K. M., Ferrante, G., & Hills, B. P. (2007). Methods for peak assignment in low-resolution multidimensional NMR cross-correlation relaxometry. *Journal of Magnetic Resonance*, 187(2), 327–342. <https://doi.org/10.1016/j.jmr.2007.04.016>

McClements, D. J., & Gumus, C. E. (2016). Natural emulsifiers — Biosurfactants, phospholipids, biopolymers, and colloidal particles: Molecular and physicochemical basis of functional performance. *Advances in Colloid and Interface Science*, 234, 3–26. <https://doi.org/10.1016/j.cis.2016.03.002>

McClements, D. J., & Gumus, C. E. (2016). colloidal particles: Molecular and physicochemical basis of functional performance. *Advances in Colloid and Interface Science*, 234, 3–26. <http://doi.org/10.1016/j.cis.2016.03.002>

McClements, D. J. (2017). Recent Progress In Hydrogel Delivery Systems For Improving Nutraceutical Bioavailability. *Food Hydrocolloids*, 68, 238-245.

Mohamed, A.I.A., Hussein, I.A., Sultan, A.S., Al-Muntasheri, G.A., (2018). Use of organoclay as a stabilizer for water-in-oil emulsions under high-temperature high-salinity conditions. *Journal of Petroleum Science and Engineering* 160, 302-312.

Molares, R., Martinez, M. J., Pilosof, A. M. J. (2019). pH-induced cold gelation of casein-glycomacropeptide emulsions. *Food Hydrocolloids* (87), 805-813.

Monahan, F. J., McClements, D. J., & Kinsella, J. E. (1993). Polymerization of Whey Proteins in Whey Protein-Stabilized Emulsions. *Journal of Agricultural and Food Chemistry*, 41(11), 1826–1829. <https://doi.org/10.1021/jf00035a004>

- Moran-Valero, M. I., Ruiz-Henestrosa, V. M. P., & Pilosof, A. M. R. (2017). Synergistic performance of lecithin and glycerol monostearate in oil/water emulsions. *Colloids and Surfaces B: Biointerfaces*, *151*, 68–75. <http://doi.org/10.1016/j.colsurfb.2016.12.015>
- Moschakis, T., Murray, B. S., & Dickinson, E. (2005). Microstructural evolution of viscoelastic emulsions stabilised by sodium caseinate and xanthan gum. *Journal of Colloid and Interface Science*, *284*(2), 714–728. <https://doi.org/10.1016/j.jcis.2004.10.036>
- Nakauma, M., Funami, T., Fang, Y., Nishinari, K., Draget, K. I., & Phillips, G. O. (2016). Calcium binding and calcium-induced gelation of sodium alginate modified by low molecular-weight polyuronate. *Food Hydrocolloids*, *55*, 65–76. <http://doi.org/10.1016/j.foodhyd.2015.10.021>
- Nazir, A., Asghar, A., & Maan, A. A. (2017). *Food Gels : Gelling Process and New Applications. Advances in Food Rheology and its Applications*. Elsevier Ltd. <http://doi.org/10.1016/B978-0-08-100431-9/00013-9>
- Nguyen, B. T., Nicolai, T., Chassenieux, C., Schmitt, C., & Bovetto, L. (2016). Heat-induced gelation of mixtures of whey protein isolate and sodium caseinate between pH 5.8 and pH 6.6. *Food Hydrocolloids*, *61*, 433–441. <http://doi.org/10.1016/j.foodhyd.2016.05.030>
- Nie, S. P., Wang, C., Cui, S. W., Wang, Q., Xie, M. Y., & Phillips, G. O. (2013). A further amendment to the classical core structure of gum arabic (*Acacia senegal*). *Food Hydrocolloids*, *31*(1), 42–48. <http://doi.org/10.1016/j.foodhyd.2012.09.014>
- Obatolu, V. A., & Cole, A. H. (2000). Functional property of complementary blends of soybean and cowpea with malted or unmalted maize. *Food Chemistry*, *70*(2), 147–153. [https://doi.org/10.1016/S0308-8146\(99\)00248-4](https://doi.org/10.1016/S0308-8146(99)00248-4)
- Opedal, N. V. D. T., Sørland, G., & Sjöblom, J. (2010). Emulsion Stability Studied by

- Nuclear Magnetic Resonance (NMR). *Energy & Fuels*, 24(6), 3628–3633.  
<http://doi.org/10.1021/ef100268x>
- Ozel, B., Uguz, S. S., Kilercioglu, M., Grunin, L., & Oztop, M. H. (2017). Effect of different polysaccharides on swelling of composite whey protein hydrogels: A low field (LF) NMR relaxometry study. *Journal of Food Process Engineering*, 40(3), 1–9. <https://doi.org/10.1111/jfpe.12465>
- Ozel, B., Cikrikci, S., Aydin, O., Oztop, M. H. (2017). Polysaccharide Blended Whey Protein Isolate-(WPI) Hydrogels: A Physicochemical and Controlled Release Study. *Food Hydrocolloids* 71, 35-46.
- Ozel B., Dag, D., Kilercioglu, M., Sumnu, S. G., Oztop, M. H.(2017). NMR relaxometry as a tool to understand the effect of microwave heating on starch-water interactions and gelatinization behavior. *LWT - Food Science and Technology* 83, 10-17.
- Oztop, M. H., McCarthy, K. L., McCarthy, M. J., & Rosenberg, M. (2012). Uptake of divalent ions (Mn  $\beta$ 2 and Ca  $\beta$ 2) by heat-set whey protein gels. *Journal of Food Science*, 77(2), 68-73.
- Panaras, G., Moatsou, G., Yanniotis, S., Mandala, I. (2011). The influence of functional properties of different whey protein concentrates on the rheological and emulsification capacity of blends with xanthan gum. *Carbohydrate Polymers* (86), 433-440.
- Papalamprou, E. M., Makri, E. A., Kiosseoglou, V. D., & Doxastakis, G. I. (2005). Effect of medium molecular weight xanthan gum in rheology and stability of oil-in-water emulsion stabilized with legume proteins. *Journal of the Science of Food and Agriculture*, 85(12), 1967–1973. <https://doi.org/10.1002/jsfa.2159>
- Pena, A. A., & Hirasaki, G. J. (2003). Enhanced characterization of oilfield emulsions via NMR diffusion and transverse relaxation experiments. *Advances in Colloid and Interface Science*, 105, 103–150. <https://doi.org/10.1016/S0001-8686>

- Pintado, T., Ruiz-capillas, C., Jiménez-colmenero, F., Carmona, P., & Herrero, A. M. (2015). Oil-in-water emulsion gels stabilized with chia ( *Salvia hispanica* L .) and cold gelling agents : Technological and infrared spectroscopic characterization. *FOOD CHEMISTRY*, *185*, 470–478. <http://doi.org/10.1016/j.foodchem.2015.04.024>
- Pocan P, Ilhan E, Oztop M. H. (2019). Effect of D-psicose substitution on gelatin based soft candies: A TD-NMR study. *Magn Reson Chem.* *2019*;1–13. <https://doi.org/10.1002/mrc.4847>
- Ptaszek, P., Basu, S., Tatar, B. C., Sumnu, G., & Sahin, S. (2017). *Advances in Food Rheology and its Applications. Advances in Food Rheology and its Applications.* Elsevier Ltd. <http://doi.org/10.1016/B978-0-08-100431-9.00017-6>
- Radford, S. J., & Dickinson, E. (2004). Depletion flocculation of caseinate-stabilised emulsions: What is the optimum size of the non-adsorbed protein nano-particles? *Colloids and Surfaces A: Physicochemical and Engineering Aspects*, *238*(1–3), 71–81. <https://doi.org/10.1016/j.colsurfa.2004.02.020>
- Ritzoulis, C., Marini, E., Aslanidou, A., Georgiadis, N., Karayannakidis, P. D., Koukiotis, C., ... Lousinian, S. (2014). Food Hydrocolloids Hydrocolloids from quince seed : Extraction , characterization , and study of their emulsifying / stabilizing capacity. *Food Hydrocolloids*, *42*, 178–186. <https://doi.org/10.1016/j.foodhyd.2014.03.031>
- Roldan-cruz, C., Vernon-carter, E. J., & Alvarez-ramirez, J. (2016). Colloids and Surfaces A : Physicochemical and Engineering Aspects Assessing the stability of Tween 80-based O / W emulsions with cyclic voltammetry and electrical impedance spectroscopy. *Colloids and Surfaces A: Physicochemical and Engineering Aspects*, *511*, 145–152. <http://doi.org/10.1016/j.colsurfa.2016.09.074>
- Sanchez, C., Schmitt, C., Babak, V. G., & Hardy, J. (1997). Rheology of whey protein

isolate-xanthan mixed solutions and gels. Effect of pH and xanthan concentration. *Nahrung - Food*, 41(6), 336–343. <https://doi.org/10.1002/food.19970410604>

Sandolo, C., Bulone, D., Mangione, M. R., Margheritelli, S., Di Meo, C., Alhaique, F., Coviello, T. (2010). Synergistic interaction of Locust Bean Gum and Xanthan investigated by rheology and light scattering. *Carbohydrate Polymers*, 82(3), 733–741. <http://doi.org/10.1016/j.carbpol.2010.05.044>

Schmelz, T., Lesmes, U., Weiss, J., & McClements, D. J. (2011). Modulation of physicochemical properties of lipid droplets using  $\beta$ -lactoglobulin and/or lactoferrin interfacial coatings. *Food Hydrocolloids*, 25(5), 1181–1189. <https://doi.org/10.1016/j.foodhyd.2010.11.005>

Schmidt, U. S., Schmidt, K., Kurz, T., Endreß, H. U., & Schuchmann, H. P. (2015). Pectins of different origin and their performance in forming and stabilizing oil-in-water-emulsions. *Food Hydrocolloids*, 46, 59–66. <http://doi.org/10.1016/j.foodhyd.2014.12.012>

Sosa-Herrera, M. G., Lozano-Esquivel, I. E., Ponce de León-Ramírez, Y. R., & Martínez-Padilla, L. P. (2012). Effect of added calcium chloride on the physicochemical and rheological properties of aqueous mixtures of sodium caseinate/sodium alginate and respective oil-in-water emulsions. *Food Hydrocolloids*, 29(1), 175–184. <https://doi.org/10.1016/j.foodhyd.2012.02.017>

Sun, C., & Gunasekaran, S. (2009). Effects of protein concentration and oil-phase volume fraction on the stability and rheology of menhaden oil-in-water emulsions stabilized by whey protein isolate with xanthan gum. *Food Hydrocolloids*, 23(1), 165–174. <https://doi.org/10.1016/j.foodhyd.2007.12.006>

Sun, C., Gunasekaran, S., & Richards, M. P. (2007). Effect of xanthan gum on physicochemical properties of whey protein isolate stabilized oil-in-water emulsions. *Food Hydrocolloids*, 21(4), 555–564.

<https://doi.org/10.1016/j.foodhyd.2006.06.003>

- Sun, J., Liu, W., Feng, M., Xu, X., Zhou, G. (2019). Characterization of olive oil emulsions stabilized by flaxseed gum. *Journal of Food Engineering* (247), 74-79.
- Tcholakova, S., Denkov, N. D., Ivanov, I. B., & Campbell, B. (2002). Coalescence in  $\beta$ -lactoglobulin-stabilized emulsions: Effects of protein adsorption and drop size. *Langmuir*, 18(23), 8960–8971. <https://doi.org/10.1021/la0258188>
- Tcholakova, S., Denkov, N. D., Sidzhakova, D., Ivanov, I. B., & Campbell, B. (2005). Effects of electrolyte concentration and pH on the coalescence stability of  $\beta$ -lactoglobulin emulsions: Experiment and interpretation. *Langmuir*, 21(11), 4842–4855. <https://doi.org/10.1021/la046891w>
- Tcholakova, S., Denkov, N. D., Ivanov, I. B., & Campbell, B. (2006). Coalescence stability of emulsions containing globular milk proteins, 126, 259–293. <http://doi.org/10.1016/j.cis.2006.05.021>
- Tolstoguzov, V. B. (2003). Some thermodynamic considerations in food formulation. *Food Hydrocolloids*, 17, 1.
- Vázquez-Solorio, S. C., Vega-Méndez, D. D., Sosa-Herrera, M. G., & Martínez-Padilla, L. P. (2011). Rheological properties of emulsions containing milk proteins mixed with xanthan gum. *Procedia Food Science*, 1, 335–339. <http://doi.org/10.1016/j.profoo.2011.09.052>
- Vega, E., Vásquez, E., Diaz, J., & Masuelli, M. (2015). Influence of the Ionic Strength in the Intrinsic Viscosity of Xanthan Gum. An Experimental Review. *Journal of Polymer and Biopolymer Physics Chemistry*, 3(1), 12–18. <https://doi.org/10.12691/jpbpc-3-1-3>
- Vermeir, L., Balcaen, M., Sabatino, P., Dewettinck, K., & Van der Meeren, P. (2014). Influence of molecular exchange on the enclosed water volume fraction of W/O/W double emulsions as determined by low-resolution NMR diffusometry

and T2-relaxometry. *Colloids and Surfaces A: Physicochemical and Engineering Aspects*, 456(1), 129–138. <https://doi.org/10.1016/j.colsurfa.2014.05.022>

Walstra P. *Physical Chemistry of Foods*, Marcel Decker, New York, NY, 2003.

Wang, L., Liu, H. M., Xie, A. J., Wang, X. De, Zhu, C. Y., & Qin, G. Y. (2018). Chinese quince (*Chaenomeles sinensis*) seed gum: Structural characterization. *Food Hydrocolloids*, 75, 237–245. <https://doi.org/10.1016/j.foodhyd.2017.08.001>

Wang, Z., Wu, J., Zhu, L., & Zhan, X. (2017). Characterization of xanthan gum produced from glycerol by a mutant strain *Xanthomonas campestris* CCTCC M2015714. *Carbohydrate Polymers*, 157, 521–526. <http://doi.org/10.1016/j.carbpol.2016.10.033>

White, D. A., Fisk, I. D., Mitchell, J. R., Wolf, B., Hill, S. E., & Gray, D. A. (2008). Sunflower-seed oil body emulsions: Rheology and stability assessment of a natural emulsion. *Food Hydrocolloids*, 22(7), 1224–1232.

Wijayanti, H.B., Bansal, N., Deeth, H.C., 2014. Stability of whey proteins during thermal processing: a review. *Compr. Rev. Food Sci. Food Saf.* 13, 1235–1251.

Williams PA, Phillips GO. Gum arabic. *Handbook of hydrocolloids*. 2nd ed; 2009. p. 252–73.

Yang, C., Wang, Y., & Chen, L. (2017). Fabrication, characterization and controlled release properties of oat protein gels with percolating structure induced by cold gelation. *Food Hydrocolloids*, 62, 21–34. <http://doi.org/10.1016/j.foodhyd.2016.07.023>

Xu, X., Liu, W., & Zhang, L. (2006). Rheological behavior of *Aeromonas* gum in aqueous solutions. *Food Hydrocolloids*, 20(5), 723–729. <https://doi.org/10.1016/j.foodhyd.2005.06.012>



## APPENDICES

### A. ANOVA TABLES

#### A.1. Mean particle size measurements

Source	DF	SS	MS	F	P
Sample	2	19,7545	9,8772	218,25	0,000
Error	6	0,2715	0,0453		
Total	8	20,0260			

S = 0,2127    R-Sq = 98,64%    R-Sq(adj) = 98,19%

Grouping Information Using Tukey Method

Sample	N	Mean	Grouping
Control	3	7,1700	A
QS	3	4,8067	B
XG	3	3,6033	C

#### A.2. Comparison of 'Span' Values

Source	DF	SS	MS	F	P
Sample	2	0,022710	0,011355	13,83	0,006
Error	6	0,004927	0,000821		
Total	8	0,027637			

S = 0,02866    R-Sq = 82,17%    R-Sq(adj) = 76,23%

Grouping Information Using Tukey Method

Sample	N	Mean	Grouping
XG	3	1,84667	A
Control	3	1,79367	A B
QS	3	1,72400	B

#### A.3. Consistency index 'k' values of the hydrocolloid solutions in the presence of CaCl<sub>2</sub>

Factor	Type	Levels	Values
Combination	fixed	4	QSP, QSP_CaCl <sub>2</sub> , XG, XG_CaCl <sub>2</sub>

Analysis of Variance for BC, using Adjusted SS for Tests

Source	DF	Seq SS	Adj SS	Adj MS	F	P
Combination	3	15.0689	15.0689	5.0230	5266.96	0.000
Error	8	0.0076	0.0076	0.0010		
Total	11	15.0765				

S = 0.0308816    R-Sq = 99.95%    R-Sq(adj) = 99.93%

Grouping Information Using Tukey Method and 95.0% Confidence

Combination	N	Mean	Grouping
XG_CaCl2	3	3.6	A
XG	3	2.5	B
QSP_CaCl2	3	1.0	C
QSP	3	0.9	D

#### A.4. Flow behavior index 'n' values of the hydrocolloid solutions (in the presence of CaCl<sub>2</sub>)

Factor	Type	Levels	Values
sample	fixed	2	Quince; Xanthan
solution type	fixed	2	CaCl <sub>2</sub> ; water

Analysis of Variance for n, using Adjusted SS for Tests

Source	DF	Seq SS	Adj SS	Adj MS	F	P
sample	1	0,049408	0,049408	0,049408	329,39	0,000
solution type	1	0,003008	0,003008	0,003008	20,06	0,002
sample*solution type	1	0,016875	0,016875	0,016875	112,50	0,000
Error	8	0,001200	0,001200	0,000150		
Total	11	0,070492				

S = 0,0122474 R-Sq = 98,30% R-Sq(adj) = 97,66%

Grouping Information Using Tukey Method and 95,0% Confidence

sample	N	Mean	Grouping
Quince	6	0,2933	A
Xanthan	6	0,1650	B

Grouping Information Using Tukey Method and 95,0% Confidence

solution type	N	Mean	Grouping
water	6	0,2450	A
CaCl <sub>2</sub>	6	0,2133	B

Grouping Information Using Tukey Method and 95,0% Confidence

sample	solution type	N	Mean	Grouping
Quince	water	3	0,3467	A
Quince	CaCl <sub>2</sub>	3	0,2400	B
Xanthan	CaCl <sub>2</sub>	3	0,1867	C
Xanthan	water	3	0,1433	D

### A.5. Consistency index 'k' values of the emulsions

Source	DF	SS	MS	F	P
Sample	2	0,98842	0,49421	300,53	0,000
Error	6	0,00987	0,00164		
Total	8	0,99829			

S = 0,04055    R-Sq = 99,01%    R-Sq(adj) = 98,68%

Grouping Information Using Tukey Method

Sample	N	Mean	Grouping
Quince	3	1,04000	A
Xanthan	3	0,99000	A
Control	3	0,31333	B

### A.6. Flow behavior index 'n' values of the emulsions

Source	DF	SS	MS	F	P
Sample	2	0,080000	0,040000	80,00	0,000
Error	6	0,003000	0,000500		
Total	8	0,083000			

S = 0,02236    R-Sq = 96,39%    R-Sq(adj) = 95,18%

Grouping Information Using Tukey Method

Sample	N	Mean	Grouping
Control	3	0,88333	A
Xanthan	3	0,68333	B
Quince	3	0,68333	B

### A.7. T<sub>2</sub> Relaxation Times of the Solutions and Emulsions

Factor	Type	Levels	Values
Sample	fixed	7	Gum + Alginate + Oil + Water; Gum + Alginate + Water;
			Gum + Alginate + WP + Oil + Water; Gum + Oil + Water;
			Gum + Water; Gum + WP + Oil + Water; Gum + WP + Water
Gum Type	fixed	2	QS; XG

Analysis of Variance for T<sub>2</sub>, using Adjusted SS for Tests

Source	DF	Seq SS	Adj SS	Adj MS	F	P
Sample	6	270221	270221	45037	704,20	0,000
Gum Type	1	52075	52075	52075	814,25	0,000
Sample*Gum Type	6	163233	163233	27205	425,39	0,000
Error	28	1791	1791	64		
Total	41	487319				

S = 7,99716    R-Sq = 99,63%    R-Sq(adj) = 99,46%

Grouping Information Using Tukey Method and 95,0% Confidence

Sample	N	Mean	Grouping
--------	---	------	----------



Sample	N	Mean	Grouping
Gum + Oil + Water	6	71,67	A
Gum + WP + Oil + Water	6	60,50	B
Gum + Alginate + Oil + Water	6	56,50	B
Gum + Alginate + WP + Oil + Water	6	34,83	C

Grouping Information Using Tukey Method and 95,0% Confidence

Gum Type	N	Mean	Grouping
QS	12	60,25	A
XG	12	51,50	B

Grouping Information Using Tukey Method and 95,0% Confidence

Sample	Gum Type	N	Mean	Grouping
Gum + Oil + Water	QS	3	81,00	A
Gum + WP + Oil + Water	QS	3	66,33	B
Gum + Oil + Water	XG	3	62,33	B C
Gum + Alginate + Oil + Water	XG	3	57,00	C
Gum + Alginate + Oil + Water	QS	3	56,00	C
Gum + WP + Oil + Water	XG	3	54,67	C
Gum + Alginate + WP + Oil + Water	QS	3	37,67	D
Gum + Alginate + WP + Oil + Water	XG	3	32,00	D

### A.9. T<sub>2</sub> peak areas of the 1<sup>st</sup> component in emulsions from XPFit

Factor	Type	Levels	Values
Sample	fixed	4	Gum + Alginate + Oil + Water; Gum + Alginate + WP + Oil + Water; Gum + Oil + Water; Gum + WP + Oil + Water
Gum Type	fixed	2	QS; XG

Analysis of Variance for Peak Area 1, using Adjusted SS for Tests

Source	DF	Seq SS	Adj SS	Adj MS	F	P
Sample	3	0,0082539	0,0082539	0,0027513	59,96	0,000
Gum Type	1	0,0001568	0,0001568	0,0001568	3,42	0,083
Sample*Gum Type	3	0,0052052	0,0052052	0,0017351	37,81	0,000
Error	16	0,0007342	0,0007342	0,0000459		
Total	23	0,0143502				

S = 0,00677400    R-Sq = 94,88%    R-Sq(adj) = 92,65%

Grouping Information Using Tukey Method and 95,0% Confidence

Sample	N	Mean	Grouping
Gum + WP + Oil + Water	6	0,12604	A
Gum + Oil + Water	6	0,11121	B
Gum + Alginate + Oil + Water	6	0,10882	B
Gum + Alginate + WP + Oil + Water	6	0,07533	C

Grouping Information Using Tukey Method and 95,0% Confidence

Gum Type	N	Mean	Grouping
QS	12	0,10791	A
XG	12	0,10279	A

Grouping Information Using Tukey Method and 95,0% Confidence

Sample	Gum Type	N	Mean	Grouping
Gum + Oil + Water	QS	3	0,13613	A
Gum + WP + Oil + Water	QS	3	0,13155	A B
Gum + WP + Oil + Water	XG	3	0,12053	A B C
Gum + Alginate + Oil + Water	XG	3	0,11457	B C
Gum + Alginate + Oil + Water	QS	3	0,10307	C D
Gum + Alginate + WP + Oil + Water	XG	3	0,08978	D
Gum + Oil + Water	XG	3	0,08628	D
Gum + Alginate + WP + Oil + Water	QS	3	0,06087	E

## A.10. T<sub>2</sub> results of the 2<sup>nd</sup> component in emulsions from XPfit

Factor	Type	Levels	Values
Sample	fixed	4	Gum + Alginate + Oil + Water; Gum + Alginate + WP + Oil + Water; Gum + Oil + Water; Gum + WP + Oil + Water
Gum Type	fixed	2	QS; XG

Analysis of Variance for Peak Time 2, using Adjusted SS for Tests

Source	DF	Seq SS	Adj SS	Adj MS	F	P
Sample	3	83333	83333	27778	90,09	0,000
Gum Type	1	38400	38400	38400	124,54	0,000
Sample*Gum Type	3	21733	21733	7244	23,50	0,000
Error	16	4933	4933	308		
Total	23	148400				

S = 17,5594 R-Sq = 96,68% R-Sq(adj) = 95,22%

Grouping Information Using Tukey Method and 95,0% Confidence

Sample	N	Mean	Grouping
Gum + WP + Oil + Water	6	646,7	A
Gum + Oil + Water	6	543,3	B
Gum + Alginate + Oil + Water	6	520,0	B
Gum + Alginate + WP + Oil + Water	6	490,0	C

Grouping Information Using Tukey Method and 95,0% Confidence

Gum	Type	N	Mean	Grouping
QS	12	590,0	A	
XG	12	510,0	B	

Grouping Information Using Tukey Method and 95,0% Confidence

Sample	Gum Type	N	Mean	Grouping
Gum + WP + Oil + Water	QS	3	693,3	A
Gum + Oil + Water	QS	3	626,7	B
Gum + WP + Oil + Water	XG	3	600,0	B
Gum + Alginate + Oil + Water	QS	3	550,0	C
Gum + Alginate + WP + Oil + Water	XG	3	490,0	D
Gum + Alginate + WP + Oil + Water	QS	3	490,0	D
Gum + Alginate + Oil + Water	XG	3	490,0	D
Gum + Oil + Water	XG	3	460,0	D

### A.11. T<sub>2</sub> peak areas of the 1<sup>st</sup> component in emulsions from XPFit

Factor	Type	Levels	Values
Sample	fixed	4	Gum + Alginate + Oil + Water; Gum + Alginate + WP + Oil + Water; Gum + Oil + Water; Gum + WP + Oil + Water
Gum Type	fixed	2	QS; XG

Analysis of Variance for Peak Area 2, using Adjusted SS for Tests

Source	DF	Seq SS	Adj SS	Adj MS	F	P
Sample	3	0,0082539	0,0082539	0,0027513	59,96	0,000
Gum Type	1	0,0001568	0,0001568	0,0001568	3,42	0,083
Sample*Gum Type	3	0,0052052	0,0052052	0,0017351	37,81	0,000
Error	16	0,0007342	0,0007342	0,0000459		
Total	23	0,0143502				

S = 0,00677400 R-Sq = 94,88% R-Sq(adj) = 92,65%

Grouping Information Using Tukey Method and 95,0% Confidence

Sample	N	Mean	Grouping
Gum + Alginate + WP + Oil + Water	6	0,9247	A
Gum + Alginate + Oil + Water	6	0,8912	B
Gum + Oil + Water	6	0,8888	B
Gum + WP + Oil + Water	6	0,8740	C

Grouping Information Using Tukey Method and 95,0% Confidence

Gum			
Type	N	Mean	Grouping
XG	12	0,8972	A
QS	12	0,8921	A

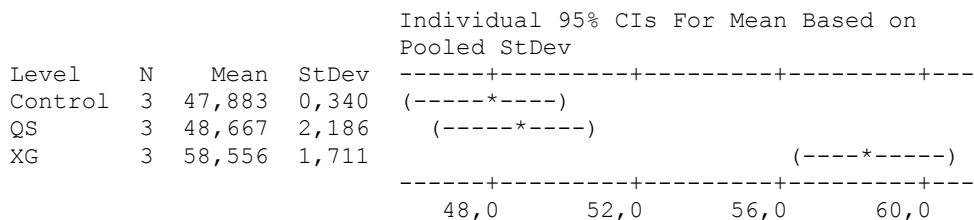
Grouping Information Using Tukey Method and 95,0% Confidence

Sample				Gum		
	Type	N	Mean	Grouping		
Gum + Alginate + WP + Oil + Water	QS	3	0,9391	A		
Gum + Oil + Water	XG	3	0,9137	B		
Gum + Alginate + WP + Oil + Water	XG	3	0,9102	B		
Gum + Alginate + Oil + Water	QS	3	0,8969	B C		
Gum + Alginate + Oil + Water	XG	3	0,8854	C D		
Gum + WP + Oil + Water	XG	3	0,8795	C D E		
Gum + WP + Oil + Water	QS	3	0,8685	D E		
Gum + Oil + Water	QS	3	0,8639	E		

## A.12. T<sub>2</sub> results of hydrogels

Source	DF	SS	MS	F	P
Sample	2	212,30	106,15	40,72	0,000
Error	6	15,64	2,61		
Total	8	227,94			

S = 1,614    R-Sq = 93,14%    R-Sq(adj) = 90,85%



Pooled StDev = 1,614

Grouping Information Using Tukey Method

Sample	N	Mean	Grouping
XG	3	58,556	A
QS	3	48,667	B
Control	3	47,883	B

Means that do not share a letter are significantly different.

### A.13. T<sub>1</sub> values of hydrogels

Source	DF	SS	MS	F	P
Sample	2	84081,2	42040,6	530,64	0,000
Error	6	475,4	79,2		
Total	8	84556,6			

S = 8,901    R-Sq = 99,44%    R-Sq(adj) = 99,25%

Grouping Information Using Tukey Method

Sample	N	Mean	Grouping
XG	3	946,77	A
Control	3	806,40	B
QS	3	711,47	C

### A.14. ANOVA Results for Data Obtained by MRI (Table 3.4)

#### A.14.1. T<sub>2</sub> results of the 1<sup>st</sup> component in hydrogels

Source	DF	Seq SS	Adj SS	Adj MS	F	P
Gum	2	10.9448	10.9448	5.4724	9.18	0.021
Error	5	2.9819	2.9819	0.5964		
Total	7	13.9267				

S = 0.772259    R-Sq = 78.59%    R-Sq(adj) = 70.02%

Grouping Information Using Tukey Method and 95.0% Confidence

Gum	N	Mean	Grouping
XG	2	53.3	A
Control	3	52.3	A B
QS	3	50.4	B

Means that do not share a letter are significantly different.

#### A.14.2. T<sub>2</sub> results of the 2<sup>nd</sup> component in hydrogels

Source	DF	Seq SS	Adj SS	Adj MS	F	P
Gum	2	786.14	786.14	393.07	117.84	0.000
Error	5	16.68	16.68	3.34		
Total	7	802.82				

S = 1.82638    R-Sq = 97.92%    R-Sq(adj) = 97.09%

Grouping Information Using Tukey Method and 95.0% Confidence

Gum	N	Mean	Grouping
QS	3	127.6	A
Control	3	108.9	B
XG	2	104.9	B

Means that do not share a letter are significantly different.

### A.14.3. T<sub>2</sub> peak areas of the 1<sup>st</sup> component in hydrogels

Source	DF	Seq SS	Adj SS	Adj MS	F	P
Gum	2	0.067632	0.067632	0.033816	382.10	0.000
Error	5	0.000443	0.000443	0.000089		
Total	7	0.068075				

S = 0.00940744    R-Sq = 99.35%    R-Sq(adj) = 99.09%

Grouping Information Using Tukey Method and 95.0% Confidence

Gum	N	Mean	Grouping
QS	3	0.8	A
XG	2	0.7	B
Control	3	0.6	C

Means that do not share a letter are significantly different.

### A.14.4. General Linear Model: StDeviation versus Gum

Factor	Type	Levels	Values
Gum	fixed	3	Control, QS, XG

### A.14.5. General Linear Model: StDeviation versus Gum

Factor	Type	Levels	Values
Gum	fixed	2	QS, XG

Analysis of Variance for StDeviation, using Adjusted SS for Tests

Source	DF	Seq SS	Adj SS	Adj MS	F	P
Gum	1	3.0104	3.0104	3.0104	8.67	0.042
Error	4	1.3887	1.3887	0.3472		
Total	5	4.3991				

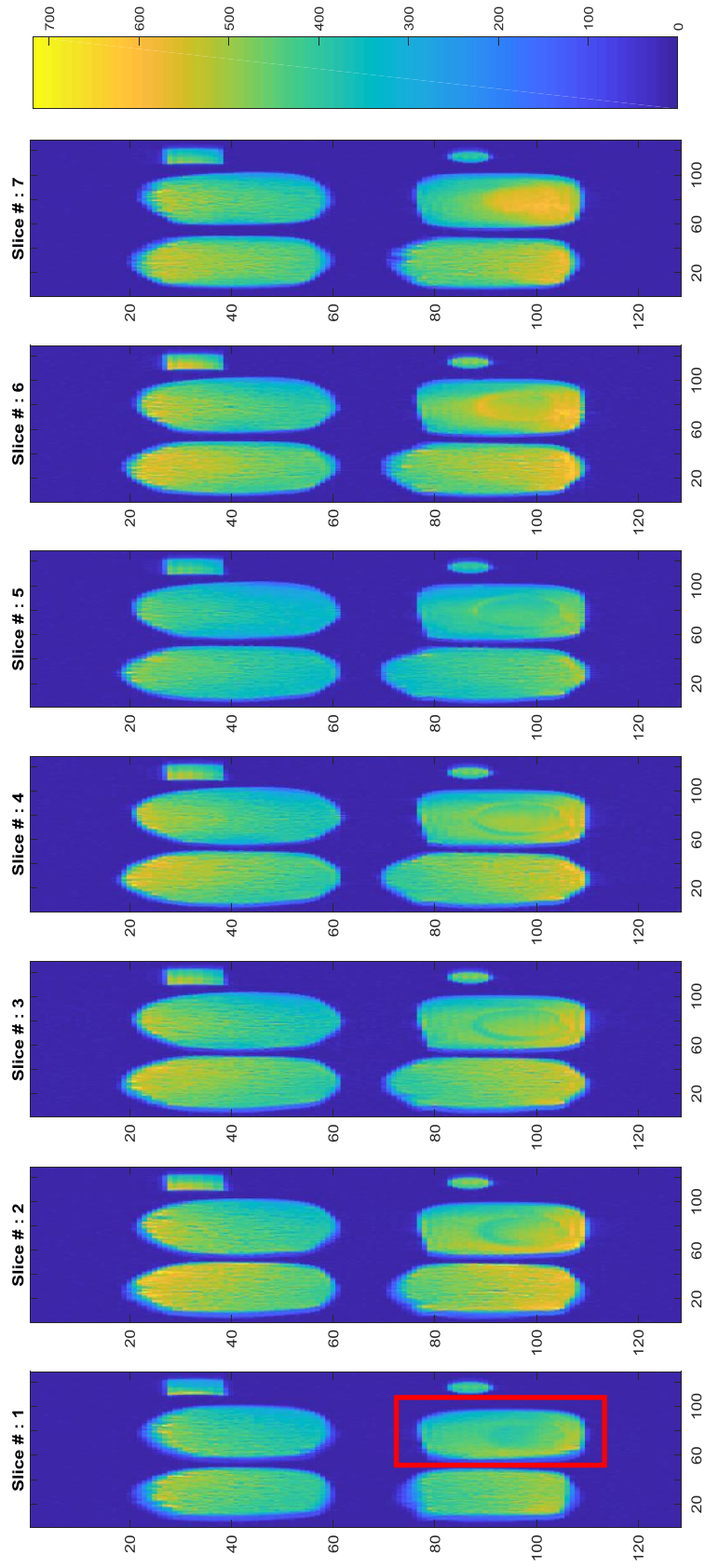
S = 0.589223    R-Sq = 68.43%    R-Sq(adj) = 60.54%

Grouping Information Using Tukey Method and 95.0% Confidence

Gum	N	Mean	Grouping
XG	3	8.0	A
QS	3	6.6	B

Means that do not share a letter are significantly different.

## B. SPIN ECHO MR IMAGES



Spin Echo MR images showing the all 7 slices for QSP including hydrogels.

(\* The bottom right gel in each slice shown in red rectangle corresponds to the 'Control Gel' (gel that does not include any hydrocolloids).)

**C. CROSS-SECTIONAL VISUAL OF HYDROGEL SAMPLES**

